

# **Die Pro-Form des Nervenwachstumsfaktors NGF: Biophysikalische Charakterisierung der Strukturbildung**



Dissertation  
zur Erlangung des akademischen Grads  
doctor rerum naturalium (Dr. rer. nat.)

vorgelegt der  
Naturwissenschaftlichen Fakultät I Biowissenschaften  
der Martin-Luther-Universität Halle-Wittenberg

von  
Marco Kliemannel  
geb. am 06. Nov. 1975 in Leipzig

Gutachter /in:

1. PD Dr. Elisabeth Schwarz
2. Prof. Dr. Ursula Jakob
3. Prof. Dr. Gunter Fischer

Halle (Saale), den 27. April 2007

**urn:nbn:de:gbv:3-000011827**

[<http://nbn-resolving.de/urn/resolver.pl?urn=nbn%3Ade%3Agbv%3A3-000011827>]

<b>1</b>	<b>Zusammenfassung .....</b>	<b>2</b>
<b>2</b>	<b>Einleitung &amp; Hintergrund .....</b>	<b>4</b>
2.1	Geschichte und Einordnung des Nervenwachstumsfaktors NGF.....	4
2.2	Struktur des Nervenwachstumsfaktors .....	5
2.3	Biologie des NGF .....	6
2.4	Rezeptoren und Signalwege von Neurotrophinen .....	8
2.5	Pro-Proteine und Pro-Peptide .....	11
2.6	Biotechnologie & Herstellung von NGF und ProNGF.....	14
2.7	Biophysikalische Charakterisierung von NGF und ProNGF.....	15
2.8	Problemstellung und Ziele der Arbeit.....	18
<b>3</b>	<b>Ergebnisse.....</b>	<b>19</b>
3.1	Untersuchungen der langsamen Entfaltung der Pro-Form des Nervenwachstumsfaktors sprechen gegen die "loop-threading"-Hypothese bei NGF .....	19
3.2	Die native NGF-Domäne induziert die Struktur des Pro-Peptids im ProNGF.....	25
3.3	Das Pro-Peptid des ProNGF: Strukturbildung und intramolekulare Assoziation mit NGF .....	28
3.4	Sortilin ist essentiell für den ProNGF induzierten neuronalen Zelltod .....	34
<b>4</b>	<b>Veröffentlichungen .....</b>	<b>35</b>
<b>Anhang.....</b>		<b>64</b>
	Literaturverzeichnis .....	64
	Abkürzungen.....	77
	Danksagung.....	78

# 1 Zusammenfassung

Der Nervenwachstumsfaktor NGF reguliert und stimuliert Wachstum, Differenzierung und Überleben von neuronalen Zellen. NGF wird als Prä-Pro-Protein synthetisiert und posttranslational zu reifem NGF prozessiert. In vielen Geweben wurde neben dem reifen NGF auch nicht prozessiertes Pro-Protein, ProNGF nachgewiesen. Für ProNGF wird eine proapoptische Aktivität postuliert, während für den reifen Wachstumsfaktor eine proliferative Wirkung bekannt ist. Die Struktur des Pro-Peptids und die Art der Wechselwirkung des Pro-Peptids mit dem reifen Teil waren zu Beginn der Arbeit unbekannt.

Ziel der vorliegenden Arbeit war die biophysikalische Charakterisierung des isolierten und des NGF-gekoppelten Pro-Peptids sowie die Untersuchung des Einflusses des Pro-Peptids auf den reifen Teil. Weiterhin sollten strukturelle Eigenschaften bzw. die Strukturbildung des Pro-Peptids in Abhängigkeit von der Anwesenheit des reifen Teils analysiert werden.

In diesem Zusammenhang sollte (I) mit ProNGF die so genannte "*loop-threading*"-Hypothese überprüft werden, die die langsame Entfaltung von NGF mit einem Zurückfädeln des N-Terminus durch den Cystin-Knoten erklärt. (II) Ein Vergleich der Struktur und Stabilität von NGF-gekoppelten und isolierten Pro-Peptid sollte zeigen, welchen Einfluss der native Teil auf das Pro-Peptid besitzt. Die Analyse der Wechselwirkung zwischen NGF und Pro-Peptid sollte zur Identifizierung des Interaktionsbereiches führen. (III) Im Rahmen einer Kooperation sollte der Einfluss des Pro-Peptids auf die Rezeptorbindung untersucht werden.

(zu I) Die Untersuchung der Denaturierung von NGF und ProNGF zeigte in beiden Fällen die Population eines Entfaltungsintermediats, welches nur sehr langsam zum völlig entfalteten Zustand denaturierte. Im Falle von NGF wurde in der "*loop-threading*"-Hypothes postuliert, dass der N-Terminus durch die Ringstruktur des Cystin-Knotens hindurchfädelt (De Young et al., 1996). NGF und ProNGF zeigen eine vergleichbare Geschwindigkeit der Entfaltung, allerdings eine Unabhängigkeit der Länge des N-Terminus und wiesen damit auf eine andere molekulare Ursache hin. Ein Vergleich des Intermediatzustands und völlig denaturierten Zustands zeigte deutlich die Gegenwart von Reststrukturen im Intermediatzustand, deren Auflösung für die beobachtete langsame Entfaltung verantwortlich gemacht wurde. Es wurden Hinweise erhalten, dass diese Reststrukturen in räumlicher Nähe des Cystin-Knotens liegen.

(zu II) Spektroskopische Vergleiche von NGF-gekoppelten und isolierten Pro-Peptid wiesen auf einen geringen, gleichgroßen Anteil an definierter Sekundärstruktur in beiden Pro-

Peptiden hin. Im Gegensatz dazu konnte nur im kovalent verknüpftem Pro-Peptid eine definierte Tertiärstruktur nachgewiesen werden, welche durch Wechselwirkung mit dem reifen Teil entsteht, wohingegen das isolierte Pro-Peptid keine kooperativ stabilisierte Tertiärstruktur ausbildet. Während der Denaturierung und Renaturierung des NGF-gekoppelten Pro-Peptids konnte ein Faltungsintermediat sowohl thermodynamisch als auch kinetisch identifiziert und charakterisiert werden. Dieses Faltungsintermediat repräsentiert einen Zustand ohne native Sekundärstrukturen, aber mit definierten Tertiärstrukturen, welche eine Assoziation des Pro-Peptids mit dem nativen NGF über einen hydrophoben Bereich darstellt.

Untersuchungen der Wechselwirkungsregion zwischen NGF und Pro-Peptid erlaubten die Identifizierung der Aminosäuresequenz Gln<sup>-84</sup>-Ala<sup>-63</sup> innerhalb des Pro-Peptids als die Region, welche mit dem reifen Teil des ProNGF interagiert. Umgekehrt konnte der Tryptophanrest-21 (Trp<sup>21</sup>) im reifen Teil ermittelt werden, welcher sehr wahrscheinlich an der Wechselwirkung mit dem Pro-Peptid beteiligt ist. Eine Beteiligung der Region um Trp<sup>21</sup> im NGF bei der Assoziation an die Rezeptoren TrkA und p75NTR könnte die reduzierte Affinität von ProNGF zu diesen Rezeptoren erklären.

(zu III) Weiterhin konnte auch zur Identifizierung eines weiteren Rezeptors, Sortilin beigetragen werden, welcher spezifisch sowohl ProNGF als auch das isolierte Pro-Peptid bindet. Somit interagiert das NGF-Pro-Peptid nicht nur als intramolekulares Chaperon während der Faltung mit der NGF-Domäne, sondern es kann dem Wachstumsfaktor in der Pro-Form auch eine veränderte biologische Funktion verleihen.



## 2 Einleitung & Hintergrund

### 2.1 Geschichte und Einordnung des Nervenwachstumsfaktors NGF

Eine auf Nervenzellen wachstumsstimulierende Wirkung einer biologischen Substanz, welche aus Mäusesarkomzellen isoliert worden war, wurde erstmals im Jahr 1952 beschrieben (Levi-Montalcini, 1987). Nach Zugabe dieser Substanz zu sympathischen und sensorischen Ganglienzellen aus Hühnerembryonen konnte *in vitro* und *in vivo* ein Neuritenwachstum beobachtet werden (Abb. 1.1) (Levi-Montalcini, 1987). Die biologische Substanz wurde später als *beta-nerve growth factor* (Nervenwachstumsfaktor, NGF) identifiziert. Immunohistochemische Untersuchungen zeigten, dass NGF in einer Vielzahl von Geweben vorkommt. In niedrigen Konzentrationen konnte NGF sowohl in der Plazenta, der Retina und in Haarfollikeln nachgewiesen werden (Chakrabarti et al., 1990; Delsite & Djakiew, 1999; Yardley et al., 2000). Hohe Konzentrationen an NGF wurden beispielsweise in einigen Schlangengiften und den submaxillaren Drüsen männlicher Mäuse gefunden, welche als Ausgangsmaterial zur Isolierung benutzt wurden (Cohen, 1960).

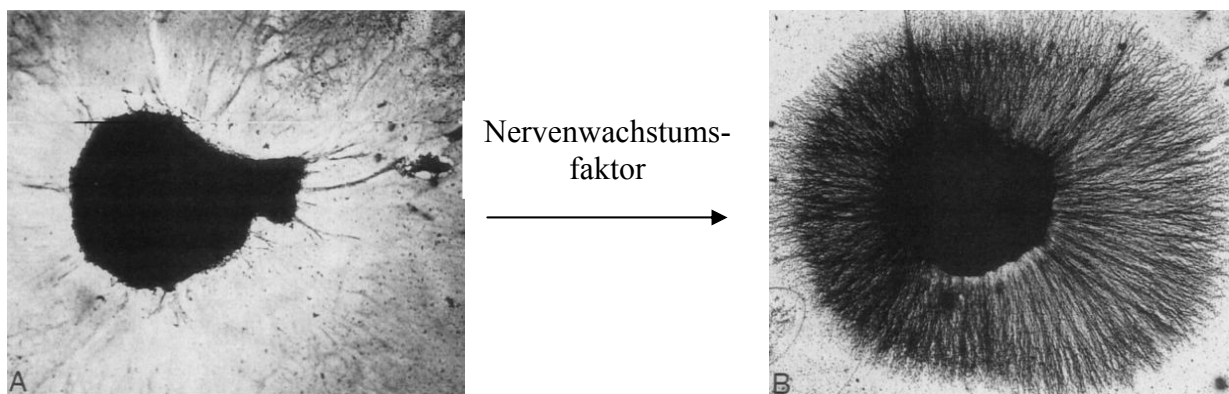


**Abb. 1.1:** Neuritenwachstum einer Ganglienzelle nach NGF-Stimulation (veröffentlicht unter <http://starklab.slu.edu/neuro/Cumulative.htm>).

Anhand der Sequenzhomologie bzw. der biologischen Aktivität konnten neben NGF fünf weitere Proteine identifiziert werden, welche eine wichtige Rolle während der neuronalen Entwicklung spielen: Der *brain derived neurotrophic factor* (BDNF), Neurotrophin-3 (NT-3), NT-4/5, NT-6 sowie NT-7 gehören deshalb neben NGF zur Familie der Neurotrophine (Leibrock et al., 1989; Ernfors et al., 1990; Hohn et al., 1990; Maisonpierre et al., 1990; Rosenthal et al., 1990; Ip et al., 1992). Als Neurotrophine werden die Proteine bezeichnet, die Wachstum, Differenzierung und Überleben bestimmter Nervenzellen vermitteln. Alle Mitglieder der Neurotrophine weisen untereinander eine über 50 %ige Sequenzidentität auf (Barde, 1990; Bradshaw et al., 1993).

Die Expression von NGF ist gewebespezifisch und abhängig vom postnatalen Entwicklungsstand (Large et al., 1986; Whittimore et al., 1986). Neben der wachstumsstimulierenden Wirkung von NGF konnte auch ein entgegengesetzter Effekt, die Induktion des programmierten Zelltods (Apoptose) nachgewiesen werden (Casaccia-Bonofil et al., 1996; Frade et al., 1996).

## 2.2 Struktur des Nervenwachstumsfaktors

Reifer NGF, welcher aus den Submaxillardrüsen von Mäusen (m-NGF) isoliert wurde, besteht aus 118 Aminosäuren. Die Primärsequenz von m-NGF ist nahezu identisch zu der von humanem NGF: Beide unterscheiden sich in lediglich 12 der 118 Aminosäurereste (Ullrich et al., 1983).

In der Aminosäuresequenz befinden sich sechs Cysteinreste, die durch drei Disulfidbrücken miteinander verbunden sind (Angeletti & Bradshaw, 1971). Diese sechs hoch konservierten Cysteinreste konnten bei allen Neurotrophinen nachgewiesen werden. Die drei Disulfidbrücken sind an der Bildung eines komplexen topologischen Strukturelements beteiligt; dem Cystin-Knoten. Im humanen NGF bilden die Disulfidbindungen Cys<sup>58</sup>-Cys<sup>108</sup> sowie Cys<sup>60</sup>-Cys<sup>110</sup> mit der Proteinhauptkette einen Ring aus insgesamt 14 Aminosäureresten. Die dritte Disulfidbrücke Cys<sup>15</sup>-Cys<sup>80</sup> ist so angeordnet, dass sie durch diesen Ring reicht (Abb. 1.2). Neben den Neurotrophinen befindet sich dieses charakteristische Strukturelement auch bei den Wachstumsfaktoren der TGF- $\beta$ -Superfamilie, wie PDGF (*platelet derived growth factor*) sowie bei einigen sehr kleinen Proteinen, wie den  $\omega$ -Conotoxinen und bestimmten Protease-Inhibitoren (Daopin et al., 1992; Oefner et al., 1992; Schlunegger & Grutter, 1992; McDonald & Hendrickson, 1993; Pallaghy et al., 1994; Price-Carter et al., 1996a; Wentzel et al., 1999).

Weiterhin ist auch die strukturelle Anordnung des nicht-kovalent assoziierten Homodimers allen Neurotrophinen gemeinsam (Abb. 1.2) (Bothwell & Shooter, 1977; Radziejewski et al., 1992; Narhi et al., 1993). Die beiden NGF-Monomere sind über starke hydrophobe Wechselwirkungen verbunden. Bei neutralem pH-Wert liegt die Dissoziationskonstante bei  $\leq 10^{-13}$  M (Bothwell & Shooter, 1977).

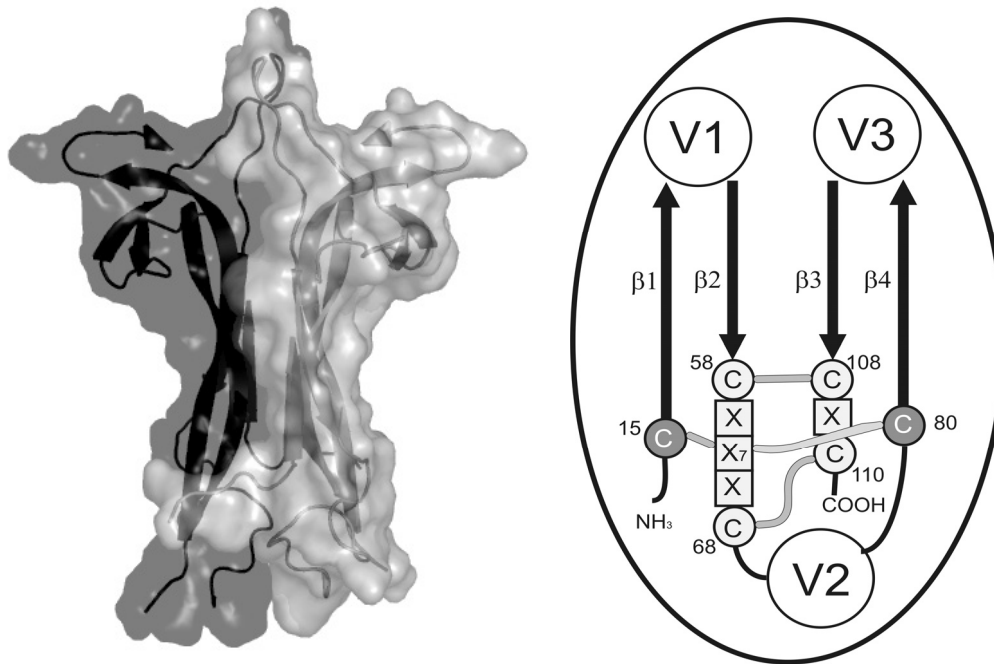


**Abb. 1.2: Strukturmodell des murinen NGF-Dimers und schematische Darstellung eines NGF-Monomers.** Das Strukturmodell wurde anhand der Kristallstrukturdaten berechnet (McDonald et al., 1991; pdb-Eintrag "1BET") und mit Hilfe "Pymol" dargestellt. Die schematische Darstellung (McDonald & Hendrickson, 1993) wurde modifiziert und zeigt die vier  $\beta$ -Faltblätter, drei *variable loop*-Regionen und den Cystin-Knoten, der aus den sechs Cystinen gebildet wird.

### 2.3 Biologie des NGF

NGF aus den submaxillaren Drüsen der Maus liegt mit weiteren Proteinen in einem hochmolekularen 7 S-Komplex von  $\sim 140$  kDa vor (Varon et al., 1967). NGF ist mit  $\alpha$ -NGF und  $\gamma$ -NGF im stöchiometrischen Verhältnis von  $\alpha_2\beta_2\gamma_2$  assoziiert (Silverman & Bradshaw, 1982). Nähere Untersuchungen haben gezeigt, dass es sich bei den  $\alpha$ - und  $\gamma$ -Untereinheiten um Serin-Proteasen der Kallikrein-Familie handelt (Varon et al., 1968; Mason et al., 1983). Die  $\alpha$ -Untereinheit liegt als degenerierte Serinprotease vor und besitzt im Gegensatz zur  $\gamma$ -Untereinheit keine proteolytische Aktivität. Daher ist die  $\alpha$ -Untereinheit nicht für die Prozessierung von NGF nötig (Greene et al., 1969; Isackson & Bradshaw, 1984). Die  $\gamma$ -Untereinheit ist *in vivo* an der N- und C-terminalen Prozessierung des NGF-Vorläuferproteins beteiligt, worauf später noch im Detail eingegangen wird (Edwards et al., 1988). Es wird diskutiert, ob der Komplex, der bisher nur bei Mäusen nachgewiesen werden konnte, eine physiologische Bedeutung als Schutz vor Degradation besitzt (Moore, Jr. et al., 1974; Mobley et al., 1976). Der 7 S-Komplex besitzt keine neurotrophe Aktivität (Bax et al., 1997). Eine ähnliche Komplexbildung zwischen Wachstumshormon und beteiligter Protease konnte auch beim *epidermal growth factor* (EGF) nachgewiesen werden (Taylor et al., 1970). Die Expression der NGF- $\alpha$ - und  $\gamma$ -Untereinheiten ist in der Maus gewebespezifisch. So konnten diese Unter-

einheiten in Fibroblasten- und Iriszellen, welche ebenso NGF exprimieren, nicht nachgewiesen werden (Pantazis, 1983).

NGF wird *in vivo* als Prä-Pro-Protein exprimiert (Berger & Shooter, 1977; Ullrich et al., 1983). Es konnten zwei unterschiedlich lange Pro-Sequenzen identifiziert werden, die *splice*-Varianten darstellen (Edwards et al., 1986; Selby et al., 1987). Die kürzere der beiden Isoformen mit einem Molekulargewicht von 27,5 kDa besitzt am N-Terminus ein 18 Aminosäurereste umfassendes Signalpeptid. Im Anschluss an die Signalsequenz folgen das Pro-Peptid mit einer Länge von 102 Aminosäuren sowie der reife Teil des Proteins. Zwei Aminosäuren am C-Terminus des reifen Teils stellen ebenfalls einen Teil der Pro-Sequenz dar. Die längere der beiden Isoformen mit einem Molekulargewicht von 34 kDa besitzt weitere 67 Aminosäurereste, die N-terminal vor der Signalsequenz der bereits erwähnten kurzen Isoform angeordnet sind. Die Expression der beiden Isoformen ist gewebespezifisch. Beobachtungen von Selby et al. deuten darauf hin, dass die kürzere Form das dominierende Translationsprodukt in den meisten Geweben darstellt (Selby et al., 1987). Dabei ist die biologische Bedeutung der Isoformen unbekannt, da aus beiden Formen biologisch aktiver NGF prozessiert werden kann. In der hier vorliegenden Arbeit wurde ausschließlich mit der kürzeren Isoform gearbeitet.

Die Abspaltung der Signalsequenz erfolgt nach Translokation des Proteins in das Endoplasmatische Retikulum (ER). Hier erfolgen unter oxidativen Bedingungen die Ausbildung der Disulfidbrücken und die Faltung des Proteins. ProNGF besitzt drei potenzielle Glykosylierungsstellen, davon zwei innerhalb des Pro-Peptids und eine im reifen NGF (Ullrich et al., 1983). Die Glykosylierung des reifen Teils wird bis auf wenige Ausnahmen nicht beobachtet. Dahingegen scheint die Glykosylierung an Asn<sup>8</sup> (im Pro-Peptid) sowohl für eine höhere Faltungseffizienz als auch für einen verbesserten Austritt aus dem ER von Bedeutung zu sein (Seidah et al., 1996). Eine Monoglykosylierung an der zweiten potenziellen Glykosylierungsstelle im Pro-Peptid wird seltener beobachtet (Murphy et al., 1989). ProNGF mit doppelt glykosyliertem Pro-Peptid konnte ebenso nachgewiesen werden wie eine unglykosylierte Form, die in vielen Geweben am häufigsten verbreitet ist (Edwards et al., 1988; Reinshagen et al., 2000; Chen et al., 1997; Fahnstock et al., 2001).

Die N- und C-terminalen Prozessierungen von ProNGF erfolgen im *trans-Golgi network* durch Furin beziehungsweise durch die weniger weit verbreiteten Prohormon-Convertasen (PC) PACE4 und PC5/6-B (Bresnahan et al., 1990; Seidah et al., 1996; Farhadi et al., 1997). Während der Prozessierung erfolgt die Abspaltung des N-terminalen Pro-Peptids sowie der beiden C-terminalen Aminosäuren. Neben verschiedenen Spaltprodukten des Pro-Peptids

konnte aber auch unprozessierter ProNGF als Sekretionsprodukt von Spermien- und Haarfollikelzellen nachgewiesen werden (Darling et al., 1983; Chen et al., 1997; Yardley et al., 2000). Spaltprodukte des Pro-Peptids mit Affinität zum NGF-Rezeptor TrkA konnten im Darmgewebe identifiziert werden (Dicou et al., 1997). Die korrekte Abspaltung der Pro-Sequenz scheint dabei essentiell für die konstitutive Sekretion zu sein, unprozessierter ProNGF wird hingegen regulatorisch sezerniert (Mowla et al., 1999). Bei einer Vielzahl von Geweben, wie Prostata, Spermien oder Haarfollikeln konnte inzwischen gezeigt werden, dass ProNGF und nicht NGF das Hauptsekretionsprodukt ist (Chen et al., 1997; Yardley et al., 2000). In vielen neuronalen, aber auch in anderen Geweben erfolgt die Sekretion in Abhängigkeit des Entwicklungsstadiums als Gemisch aus NGF und ProNGF (Hasan et al., 2003; Lobos et al., 2005). So wurde beispielsweise bei Alzheimer-Patienten eine Akkumulation von ProNGF im Gehirn nachgewiesen (Fahnestock et al., 2001). Aus diesen Beobachtungen lässt sich schließen, dass ProNGF nicht nur die Vorläuferform von NGF darstellt, sondern auch eigene biologische Funktionen erfüllt (Fahnestock et al., 2001).

## 2.4 Rezeptoren und Signalwege von Neurotrophinen

NGF und die anderen Mitglieder der Neurotrophinfamilie vermitteln ihre biologische Aktivität durch Bindung an zwei Klassen von Transmembranrezeptoren, den Tyrosin-Kinase-Rezeptoren (Trk), von denen bisher drei bekannt sind, und p75NTR, ein Mitglied der Tumornekrose-Faktor-Rezeptor-Familie. NGF aktiviert den Rezeptor TrkA (Klein et al., 1991a), BDNF und NT-4/5 binden an TrkB (Klein et al., 1991b; Ip et al., 1992), und NT-3 bindet TrkC mit hoher Affinität, interagiert aber auch mit TrkA und TrkB (Lamballe et al., 1991; Barbacid, 1995; Belliveau et al., 1997). Eine Bindung von NT-7 an TrkA konnte zwar nachgewiesen werden, die Affinität war aber deutlich geringer als die von NGF (Nilsson et al., 1998). Im Gegensatz zur spezifischen Aktivierung der Trk-Rezeptoren binden alle Neurotrophine mit ähnlicher Affinität an p75NTR (Philo et al., 1994; Friedman, 2000).

Beide Rezeptorklassen induzieren unabhängig von einander unterschiedliche Signalkaskaden (Miller & Kaplan, 2001). Die Aktivierung des TrkA-Rezeptors durch NGF bewirkt Wachstum, Differenzierung und Proliferation der Neuronen. Die Liganden-Rezeptorbindung induziert die Dimerisierung des Rezeptors und führt zur *trans*-Autophosphorylierung der Tyrosinreste der intrazellulären Rezeptordomänen. Nach Bindung intrazellulärer Signalmoleküle an die phosphorylierten Tyrosinresten der intrazellulären Domäne erfolgt die Aktivierung von zwei Signalwegen (Kaplan & Miller, 1997): Zum einen die Aktivierung von

PI3K (Phosphatidylinositol 3-Kinase) und Akt (Protein Kinase B) und zum anderen die Aktivierung des kleinen G-Proteins Ras, welches das Signal auf MAPK (*mitogen-activated protein kinase*) überträgt. Die Aktivierung beider Signalkaskaden führt zur Induktion verschiedener Transkriptionsfaktoren, die Einflüsse auf den Zellzyklus, das Neuritenwachstum und die synaptische Plastizität von Neuronen ausüben (Grewal et al., 1999; Kaplan & Miller, 2000; Lonze & Ginty, 2002; Chao, 2003).

Der durch p75NTR induzierte Signalweg kann zum programmierten Zelltod, der Apoptose der Nervenzellen führen (Casaccia-Bonnel et al., 1996; Frade et al., 1996; Hempstead, 2002). Im Gegensatz zu den Trk-Rezeptoren ist p75NTR keine Tyrosinkinase. Binden Neurotrophine an der extrazellulären Domäne von p75NTR, erfolgt über die intrazelluläre Domäne die Aktivierung von NRIF (*neurotrophin receptor interacting factor*), von JNK (Jun N-terminaler Kinase), NK- $\kappa$ B, p53 und Ceramid (Aloyz et al., 1998; Bamji et al., 1998; Le-Niculescu et al., 1999; Casademunt et al., 1999; Kaplan & Miller, 2000; ; Brann et al., 2002; Roux & Barker, 2002; Chao, 2003; Linggi et al., 2005). Die gleichzeitige Aktivierung der TrkA- und p75NTR-vermittelten Signalkaskaden durch NGF unterdrückt die Induktion der Apoptose (Majdan et al., 2001). Neben der Apoptoseinduktion vermittelt p75NTR weitere biologische Funktionen, die über andere Signalkaskaden reguliert werden. So steuert p75NTR beispielsweise das Wachstum von Axonen, die Migration von Schwann'schen Zellen sowie die Myelinbildung (Yamashita et al., 2005).

TrkA wird vom reifen NGF mit einer Dissoziationskonstante ( $K_D$ ) von  $\sim 10^{-11}$  M gebunden und daher auch oft als hoch affiner Rezeptor bezeichnet. Demgegenüber ist die Bindung an p75NTR, der als niedrig affiner Rezeptor bezeichnet wird, deutlich schwächer ( $K_D = \sim 10^{-9}$  M) (Kaplan & Miller, 2000; Fahnstock et al., 2004a). Dabei ist die Affinität zu den Rezeptoren abhängig, ob NGF mit jeweils einem oder beiden Rezeptoren interagiert. Sind beide Rezeptoren an der Bindung beteiligt, beeinflusst dies die Zellantwort auf das assoziierte Neurotrophin (Dechant, 2001). Die Bindung von NGF an TrkA und p75NTR führt zu einer Konformationsänderung von TrkA und der Ausbildung einer hoch affinen Bindestelle. Dies führt zu einer Verstärkung der TrkA-Signalkaskade (Hempstead et al., 1991; Chao & Hempstead, 1995; Ryden et al., 1997; Esposito et al., 2001) und einer Inhibierung der Apoptose induzierenden Signalkaskade über p75NTR (Yoon et al., 1998). Dadurch konnte bei der gleichzeitigen Bindung von NGF an TrkA und p75NTR ein höheres Neuritenwachstum beobachtet werden als bei der alleinigen Bindung an TrkA (Davey & Davies, 1998; Bibel et al., 1999). Wahrscheinlich besitzt TrkA nur in Verbindung mit p75NTR die oben genannten hoch affinen Bindungseigenschaften (Mahadeo et al., 1994). Daher ist die ursprüngliche

Einteilung der Rezeptoren in hoch und nieder affine Rezeptoren nicht korrekt und wird in neuerer Literatur wenig verwendet.

Die Wechselwirkung zwischen NGF und TrkA erfolgt über den N-Terminus von NGF (Aminosäure 2 bis 13) sowie Abschnitte des  $\beta$ -Faltblatts des NGF, wie anhand von Deletionsmutanten und der Kristallstruktur gezeigt werden konnte (Kahle et al., 1992; Ibanez et al., 1993; Woo et al., 1995; Woo & Neet, 1996; Kullander et al., 1997; Wiesmann et al., 1999; O'Connell et al., 2000). Diese Erkenntnis unterstützt die Hypothese, dass ProNGF mit dem Pro-Peptid als N-terminaler Domäne die Bindung an TrkA einschränkt. So wurde mit Hilfe einer spaltresistenten Mutante von ProNGF eine erhöhte Affinität zu p75NTR ( $K_d = \sim 10^{-10}$  M) nachgewiesen. Hingegen besitzt diese Mutante eine gegenüber NGF verminderte Affinität zu TrkA (Lee et al., 2001). Dies korreliert mit früheren Ergebnissen, die eine weniger starke Bindung von ProNGF als von NGF an TrkA zeigten (Edwards et al., 1988). Im Gegensatz dazu beobachtete die Arbeitsgruppe von Fahnstock mit Hilfe einer Spaltmutante von ProNGF, in der die dibasische Spaltstelle gegen zwei Alaninreste ausgetauscht war, eine ähnlich hohe Affinität von ProNGF wie von NGF zu TrkA (Fahnstock et al., 2004b).

Die Bereiche im NGF, welche eine Assoziation mit p75NTR vermitteln, konnten ebenfalls durch Mutationssysteme und Strukturmodellen identifiziert werden (Ibanez et al., 1992; Urfer et al., 1994). Anhand der Kristallstruktur wurde die Wechselwirkung zwischen NGF und p75NTR detailliert aufgeklärt. Ein NGF-Homodimer interagiert mit einem p75NTR-Rezeptormolekül. Es wird postuliert, dass die Bindung eine Konformationsänderung im NGF bewirkt und dadurch die Bindung eines weiteren p75NTR-Moleküls inhibiert wird (He & Garcia, 2004). Diese Daten wurden allerdings mit Hilfe von unglykosyliertem p75NTR-Rezeptor gewonnen. Mittels analytischer Ultrazentrifugation, Massenspektrometrie und Röntgenkleinwinkelstreuung konnte dagegen gezeigt werden, dass die Glykosylierung des Rezeptors eine wichtige Rolle bei der Assoziation spielt: Zwei glykosylierte p75NTR-Rezeptormoleküle assoziieren mit einem NGF-Homodimer (Aurikko et al., 2005).

Mit Sortilin (Petersen et al., 1997) konnte ein weiterer Rezeptor identifiziert werden, der an der Signaltransduktion von NGF bzw. ProNGF beteiligt ist. Dabei wurde für ProNGF ( $K_D = 5$  nM) eine höhere Affinität zu Sortilin nachgewiesen als für NGF ( $K_D = 87$  nM). Bei weiteren Versuchen konnte eine vergleichbar hohe Affinität wie für ProNGF auch für das isoliertes NGF-Pro-Peptid ( $K_D = 8$  nM) beobachtet werden. Daraus wurde geschlossen, dass das Pro-Peptid die Assoziation mit Sortilin vermittelt. *cross-linking*-Experimente deuteten auf einen

Komplex aus p75<sup>NTR</sup> und Sortilin, welcher für die Induktion von Apoptose durch ProNGF verantwortlich ist (Abb. 1.3) (Nykjaer et al., 2004).

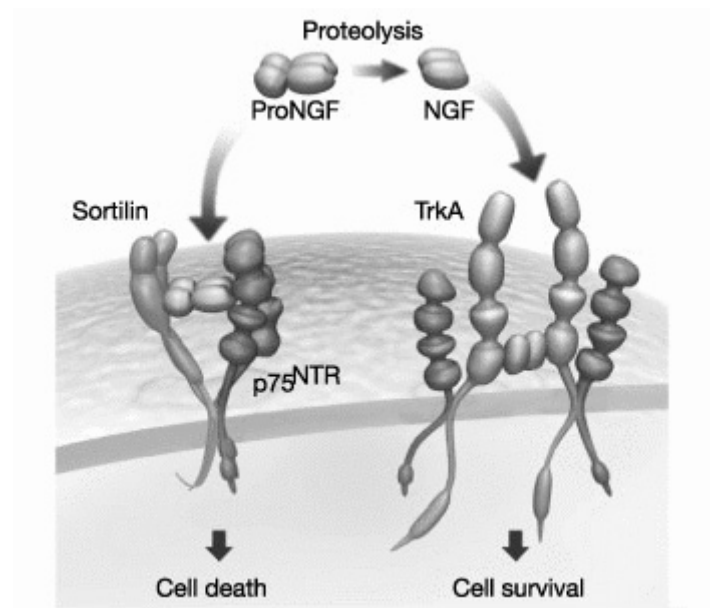


Abb. 1.3: Modell der NGF- und ProNGF-Bindung an die jeweiligen Rezeptoren (Nykjaer et al., 2004).

Ähnliche Beobachtungen wurden jüngst mit BDNF gemacht. So wurde die Induktion von Apoptose durch Interaktion von proBDNF mit den Rezeptoren p75<sup>NTR</sup> und Sortilin, nicht aber mit TrkB, welcher für das Nervenzellwachstum verantwortlich ist, beobachtet (Teng et al., 2005). Im Gegensatz zu diesen Ergebnissen wurde von einer anderen Forschungsgruppe die Bindung von proBDNF an TrkB mit hoher Affinität sowie die Stimulation des Neuritenwachstum beobachtet (Fayard et al., 2005). Ob ProNGF bzw. die Pro-Formen der Neurotrophine eher neurotroph oder apoptotisch wirken, bleibt kontrovers (Fahnestock et al., 2004a).

## 2.5 Pro-Proteine und Pro-Peptide

Proteine sind sich selbst organisierende Moleküle, deren dreidimensionale Struktur durch ihre Primärsequenz bestimmt wird (Anfinsen, 1973). Eine Vielzahl von Proteinen faltet jedoch nicht spontan zur nativen Struktur. Bei verschiedenen Faltungsprozessen konnte *in vivo* die Beteiligung zusätzlicher Proteine nachgewiesen werden, die für eine korrekte und effiziente Faltung notwendig sind. So erhöhen beispielsweise Disulfidisomerasen, Peptidyl-Prolyl-*cis/trans*-Isomerasen (PPIasen) oder molekulare Chaperons die Faltungsausbeute *in vivo* und *in vitro* (Creighton, 1991; Fischer et al., 1998; Freedman et al., 1994).



Viele Proteine werden wie NGF als Prä-Pro-Proteine translatiert. Pro-Peptide können sich sowohl am N- bzw. C-Terminus wie auch innerhalb des Proteins zwischen zwei Domänen befinden. In der Regel erlangt nach Abspaltung des Pro-Peptids das prozessierte, reife Protein seine biologische Aktivität. Werden diese Proteine ohne ihre Pro-Sequenz translatiert, nehmen sie oft inaktive, falsch gefaltete Konformationen an (Bryan, 2002). Bekannte Beispiele sind verschiedene Proteasen, wie Subtilisin E,  $\alpha$ -lytische Protease oder Carboxypeptidase Y aber auch *bovine pancreatic trypsin inhibitor* (BPTI) und *guanylyl cyclase activating peptide* (GCAP). Bei diesen Proteinen konnten entsprechende Faltungsdefizite in Abwesenheit des Pro-Peptids nachgewiesen werden (Ikemura et al., 1987; Silen & Agard, 1989; Winther & Sorensen, 1991; Weissman & Kim, 1992; Shinde et al., 1993; Sorenson et al., 1993; Hidaka et al., 1998). Die Pro-Sequenzen fungieren während der Strukturbildung durch das Absenken der Aktivierungsenergie des Übergangszustands bei der Faltungsreaktion als Katalysatoren (Eder et al., 1993). Aufgrund dieser Eigenschaft werden die Pro-Peptide auch als "Intramolekulare Chaperone" (IMC) bezeichnet (Inouye, 1991). Die strukturbildende Funktion vermitteln diese Pro-Sequenzen manchmal auch in *trans*, so dass eine kovalente Verbindung zwischen dem Protein und Pro-Peptid nicht Voraussetzung für die Aktivität ist. Als Faltungshelfer besitzen die Pro-Sequenzen meist eine sehr hohe Substratspezifität (Silen & Agard, 1989; Winther et al., 1994). Neben der faltungsstimulierenden Wirkung besitzen die Pro-Sequenzen der Proteasen auch eine regulatorische Funktion und stellen hoch-affine Inhibitoren der jeweiligen Proteasen dar (Ohta et al., 1991; Baker et al., 1992; Fox et al., 1992).

In Proinsulin liegt das Pro-Peptid, das C-Peptid, zwischen der A- und B-Kette des reifen Insulins. Während der Faltung bewirkt das C-Peptid, dass sich die beiden Polypeptidketten in räumlicher Nähe befinden damit die interchenaren Disulfidbindungen ausgebildet werden können. Anschließend wird die Pro-Sequenz durch Proteolyse prozessiert und das reife Protein sezerniert (Steiner & Clark, 1968).

Hingegen ist im *bovine pancreatic trypsin inhibitor* (BPTI) ein freier Cysteinrest im Pro-Peptid an der Ausbildung einer temporären Disulfidbrücke beteiligt und begünstigt dadurch die Ausbildung der nativen Disulfidbrücken im reifen Teil (Weissman & Kim, 1992).

Neben NGF werden auch andere Cystin-Knoten-Proteine als Prä-Pro-Proteine synthetisiert. Pro-Sequenzen müssen dabei nicht immer direkt die Faltung katalysieren. Beim Von-Willebrand-Faktor vermitteln die Pro-Sequenzen die Assemblierung der einzelnen Monomere und begünstigen die Ausbildung von intermolekularen Disulfidbrücken (Wise et al., 1988; Voorberg et al., 1990).

Andere Pro-Peptide vermitteln nicht direkt die Proteinfaltung, stimulieren und aktivieren aber durch Interaktion mit faltungshelfenden Proteinen die Biogenese des Proteins. So bindet das Pro-Peptid des  $\alpha$ -Conotoxins an eine Protein Disulfidisomerase (PDI) und stimuliert dadurch die Faltung (Buczek et al., 2004).

Für TGF- $\beta$ 1 konnte gezeigt werden, dass aktives Protein nur dann sezerniert wird, wenn die Pro-Sequenz kovalent gebunden beziehungsweise *in trans* coexprimiert wird (Gray & Mason, 1990). Da das TGF- $\beta$ 1-Pro-Peptid selbst ein über eine Disulfidbrücke verknüpftes Dimer ist, lässt es sich nicht mit dem isolierten NGF-Pro-Peptid vergleichen, welches als Monomer vorliegt (Gentry & Nash, 1990; Rattenholl, 2001; Kliemannel et al., 2004). Ein weiterer Vertreter aus der TGF- $\beta$ -Superfamilie ist *macrophage inhibitory cytokine* (MIC-1). Das Pro-Peptid fungiert hier als Marker für die Faltung. Bei korrekt gefaltetem Protein wird das Cytokin von seinem Pro-Peptid abgespalten und sekretiert. Falsch gefaltetes Protein wird hingegen vom Pro-Peptid erkannt und das gesamte Molekül für den späteren Abbau durch den Ubiquitin-Proteasom-Komplexes markiert (Bauskin et al., 2000; Fairlie et al., 2001).

Für das N-terminale Pro-Peptid des NGF konnte die faltungsstimulierende Wirkung *in vitro* nachgewiesen werden. Für ProNGF konnte eine Renaturierungsausbeute von ca. 35 % erreicht werden, mit reifem NGF dagegen nur eine Ausbeute von ca. 1 % (Rattenholl et al., 2001a). Eine Analyse der oxidativen Strukturbildung von ProNGF ermöglichte dabei die Identifizierung unterschiedlich disulfidverbrückter Faltungsintermediate (Rattenholl et al., 2001b). Im Gegensatz zu den oben beschriebenen Proteasen und TGF- $\beta$ 1 konnte eine faltungsstimulierende Wirkung des Pro-Peptids *in trans* nicht nachgewiesen werden, so dass die kovalente Verknüpfung zwischen Pro-Peptid und NGF zumindest *in vitro* für die Renaturierung essentiell ist. Durch welche molekularen Mechanismen das Pro-Peptid die Faltung des reifen Teils vermittelt ist derzeit unbekannt. Es wird angenommen, dass das Pro-Peptid als eine Art Gerüst fungiert, welches die Faltung des reifen Teils unterstützt (Rattenholl et al., 2001a; Rattenholl et al., 2001b; Rattenholl, 2001).

Die beiden Aminosäuren Arg<sup>119</sup> und Ala<sup>120</sup> bilden die C-terminale Pro-Sequenz des humanen NGF. Dabei ist die Funktion und Bedeutung dieser beiden Aminosäuren völlig unbekannt. Ein Einfluss des C-terminalen Pro-Peptids auf Stabilität, Struktur oder die Faltungseffizienz konnte nicht beobachtet werden (Kliemannel, 2001). Dass auch einzelne Aminosäuren Auswirkungen auf die Effizienz der Proteinfaltung haben können, konnte anhand des  $\omega$ -Conotoxin aus Meeresschnecken gezeigt werden. Hier wird das C-terminale Glycin posttranslational in eine Amid-Gruppe umgewandelt. Eine Deletionsmutante, welche

kein C-terminales Glycin besaß, zeigte *in vitro* eine deutlich reduzierte Faltungsausbeute (Price-Carter et al., 1996b).

Allerdings ist nur wenig über die Strukturen und proteinchemischen Eigenschaften der verschiedenen Pro-Peptide bekannt. Bei der Protease Subtilisin wurde nachgewiesen, dass das Pro-Peptid in der isolierten Form im Gegensatz zum kovalent verknüpften pro-Subtilisin wenig bzw. keine Struktur besitzt (Ruvinov et al., 1997). Ähnliche Beobachtungen wurden auch für das Pro-Peptid der Carboxypeptidase Y gemacht. So wurde unter nativen Bedingungen nur partiell strukturiertes Pro-Peptid beobachtet. Strukturelle Analysen ergaben eine definierte Sekundärstruktur, aber nur sehr geringe Anteile an Tertiärkontakten. Aufgrund dieser Ergebnisse wurde für das Pro-Peptid ein "*molten globule state*" postuliert (Sorenson et al., 1993). Neben diesen Erkenntnissen liegen über die Strukturen von Pro-Peptiden und Pro-Proteinen nur wenige Daten auf atomarer Ebene vor. Eine Aufklärung der Struktur mittels Röntgenstrukturanalyse gelang bisher nur bei Vertretern der Serin- und Cystein-Proteasen, wie Procathepsin und Prosubtilisin (Gallagher et al., 1995; Podobnik et al., 1997; Jain et al., 1998; LaLonde et al., 1999).

## 2.6 Biotechnologie & Herstellung von NGF und ProNGF

Durch die mitotische und apoptische Aktivität von NGF und ProNGF sind beide Proteine für einen therapeutischen Einsatz von hohem Interesse. Potenzielle Einsatzgebiete sind primäre Neuropathien wie die Alzheimer'sche Krankheit (AD) oder Parkinson'sche Krankheit (PD) und sekundäre Neuropathien, die bei Diabetes oder nach Chemotherapien auftreten (Tuszynski et al., 2005). Es wurde beispielsweise im Tiermodell eine Reduktion sensorischer Neuropathien nach Verabreichung von NGF nachgewiesen (Apfel et al., 1992). Ebenfalls konnte durch NGF das Axonenwachstum bei Ratten angeregt werden, denen die Hinterwurzelganglien durchtrennt worden waren (Ramer et al., 2000). Weiter wurde nach Applikation von NGF ein Einfluss auf periphere Nervenzellen sowie die Induktion anderer Neurotrophine beobachtet (Apfel & Kessler, 1996). Dabei ist die Applikationsform von zentraler Bedeutung, denn NGF kann aufgrund seiner Ladung und Polarität nicht die Blut-Hirn-Schranke passieren (Tuszynski, 2002).

NGF und ProNGF kommen in Geweben von Säugetieren in nur geringen Konzentrationen vor. Hohe Extraktionskosten und mögliche Verunreinigungen mit Pathogenen sprechen gegen eine Gewinnung von NGF und ProNGF aus diesen Quellen für die Therapie. Daher kommt für die Herstellung derzeit nur die rekombinante Produktion in Betracht. Hierzu stehen zwei

etablierte Methoden zur Wahl. Die Expression in eukaryotischen Zellen bietet den Vorteil einer korrekten *post*-translationalen Prozessierung, wie Glykosylierung und Spaltung des Zielproteins. Gut etabliert und industriell häufig angewendet ist beispielsweise die Expression in Insektenzellen (Sf9), welche über ein Baculovirussystem mit dem ProNGF-Gen transfiziert werden (Fahnestock et al., 2004a).

Eine andere Methode um kostengünstig und in hohen Ausbeuten NGF und ProNGF herzustellen, ist die Expression in prokaryotischen Zellen. Bei der Expression von NGF und ProNGF in *E. coli* erfolgt die Produktion des Proteins im reduzierenden Milieu des Cytoplasmas, und es wird dort unlöslich in Aggregaten, sogenannten *inclusion bodies* akkumuliert (Rattenholl et al., 2001a; Rattenholl, 2001). Dieses Phänomen wird häufig bei der Expression disulfidverbrückter Proteine in Bakterienzellen beobachtet. Durch das reduzierende cytosolische Milieu ist die Ausbildung von Disulfidbrücken, welche in der Regel für die Faltung essentiell sind, nicht möglich. Die *inclusion bodies* können aber mit Hilfe geeigneter chaotroper Substanzen solubilisiert werden (Rudolph & Lilie, 1996; De Bernardez et al., 1999). Anschließend erfolgt die Renaturierung unter Zuhilfenahme niedermolekularer Substanzen wie Arginin, welche eingesetzt werden um aggregationsanfällige Faltungsintermediate in Lösung zu halten. Gleichzeitig wird durch ein geeignetes *oxido-shuffling*-System wie zum Beispiel die Kombination von reduziertem und oxidiertem Glutathion die Ausbildung der Disulfidbrücken ermöglicht. So wurde im Fall der Rückfaltung von ProNGF eine gegenüber der Renaturierung des reifen NGF drastisch erhöhte Ausbeute und Kinetik dokumentiert (Rattenholl et al., 2001b). Nach der Faltung ProNGF wurde reifer NGF durch *in vitro*-Proteolyse mit Trypsin hergestellt. Mit Hilfe des DRG (*dorsal root ganglion*)–Assay konnte gezeigt werden, dass in *E. coli* exprimierter und *in vitro* renaturierter ProNGF, welcher anschließend zu reifem NGF prozessiert wurde, dieselbe biologische Aktivität wie herkömmlicher, aus Mäusesakromzellen gewonnener NGF besitzt (Rattenholl, 2001).

## 2.7 Biophysikalische Charakterisierung von NGF und ProNGF

Wie im Kapitel 1.2 beschrieben, liegen NGF und ProNGF als Homodimere vor (Bothwell & Shooter, 1977; Rattenholl, 2001). Für dimere Proteine beschreibt ein Drei-Zustandsmodell (Gl. 1.1) das Gleichgewicht aus nativem Dimer ( $N_2$ ), nativem Monomer (N) und entfaltetem Monomer (D).



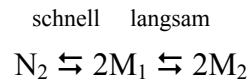
wobei  $K_1 = [N]^2 / [N_2]$  und  $K_2 = [D] / [N]$  Gl. 1.2

Wenn  $K_1$  größer als  $K_2$  ist, folgt, dass natives Monomer populiert wird. Daraus ergibt sich, dass die stabilisierenden Wechselwirkungen im Monomer stärker sind als die Assoziation der beiden monomeren Untereinheiten. Ist  $K_1$  deutlich kleiner als  $K_2$ , stellt die Assoziation der Monomere den Hauptbeitrag zur Stabilisierungsenergie dar und natives Monomer ist nur gering gegenüber dem entfalteten Zustand stabilisiert. Beim NGF kann unter nativen Bedingungen ausschließlich das Dimer und kein Monomer beobachtet werden. Auch bei Entfaltungs- und Faltungsstudien von NGF unter oxidativen Bedingungen in GdmCl und Harnstoff ließ sich kein natives Monomer nachweisen. Das NGF-Dimer dissoziiert unter gleichzeitiger Entfaltung der beiden monomeren Untereinheiten (Timm & Neet, 1992). Ähnliche Beobachtungen wurden auch bei anderen dimeren Proteinen, wie dem Arc-Repressor gemacht (Bowie & Sauer, 1989). Daher kann das Gleichgewicht auch vereinfacht als Zwei-Zustandsmodell beschrieben werden (Gl. 1.3).



Das gefaltete NGF-Dimer ist unter nativen Bedingungen (pH 7.0) mit  $\Delta G_{N \rightarrow D} = 80,9$  kJ/mol stabilisiert (Timm & Neet, 1992; Timm et al., 1994).

Allerdings ist die De- und Renaturierung von NGF weitaus komplexer als ursprünglich angenommen wurde. Wird NGF aus der Maus für kurze Zeit unter denaturierenden Bedingungen inkubiert, so ist die Denaturierung vollständig reversibel (Radziejewski et al., 1992; Timm & Neet, 1992; Timm et al., 1994). De- und Renaturierungen bei Denaturationskonzentrationen im Übergangsbereich benötigen 24 bis 72 h bis zur Gleichgewichtseinstellung (Timm & Neet, 1992). Bei Denaturierungsübergängen mit GdmCl wurde mit steigender Inkubationszeit eine Verschiebung des Übergangsmittelpunkts zu niedrigeren GdmCl-Konzentrationen beobachtet (De Young et al., 1996). Das aus der kurzzeitigen Denaturierung erhaltene, entfaltete Protein stellte ein Intermediat dar und wandelte sich sehr langsam in den vollkommen entfalteten Zustand um (Gl. 1.4). Dadurch wird der erste Entfaltungszustand aus dem Gleichgewicht mit dem nativen Zustand entfernt und eine Verschiebung des Übergangsmittelpunktes beobachtet. Aus diesem Ergebnis schlossen die Autoren auf die Existenz von zwei monomeren Entfaltungszuständen.



Gl. 1.4

In Anwesenheit von GdmCl denaturiert das Dimer ( $\text{N}_2$ ) bei gleichzeitiger Dissoziation zu zwei monomeren Untereinheiten ( $2\text{M}_1$ ) (siehe Gl. 1.3). Bei längeren Inkubationszeiten unterliegt das Monomer  $\text{M}_1$  weiteren strukturellen Veränderungen, und es entsteht das völlig entfaltete Monomer  $\text{M}_2$  (De Young et al., 1996; De Young et al., 1999). Da der Übergang von  $\text{M}_1$  zu  $\text{M}_2$  bei 25 °C über einen Zeitraum von mehreren Tagen verläuft, ist anzunehmen, dass sich die meisten publizierten Daten zur De- und Renaturierung von NGF auf den Übergang vom nativen Dimer zum ersten Entfaltungszustand beschränken. Auch bei anderen Neurotrophinen wurde die Gegenwart verschiedener Entfaltungszuständen in Abhängigkeit der Inkubationszeit nachgewiesen (Philo et al., 1993; De Young et al., 1999). Worin sich die beiden Zustände  $\text{M}_1$  und  $\text{M}_2$  unterscheiden, konnte nicht genau identifiziert werden. Beim *brain derived neurotrophic factor* (BDNF) wird ein "molten globule" postuliert, welches selbst nicht dimerisieren kann (Philo et al., 1993).

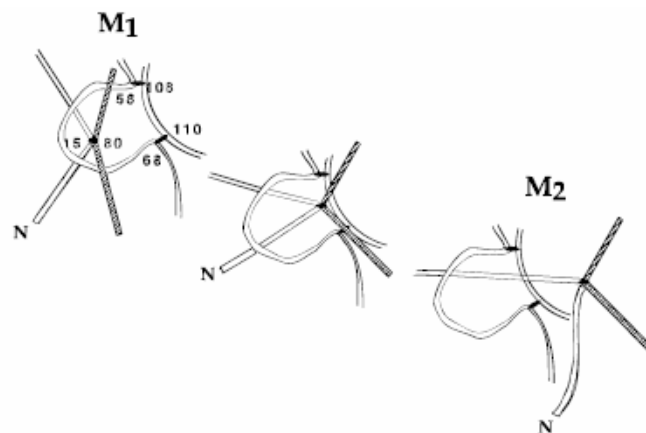


**Abb. 1.4:** Schematische Darstellung des "loop-threading"-Mechanismus nach De Young et al., 1996 und De Young et al., 1999. Die Spezies  $\text{M}_2$  repräsentiert gegenüber der Spezies  $\text{M}_1$  den Zustand, in dem der N-Terminus des NGF durch die Ringstruktur des Cystin-Knotens gefädelt wurde. Die Zahlen kennzeichnen die Cysteine.

Bei NGF wurde die Theorie aufgestellt, dass der Unterschied zwischen  $\text{M}_1$  und  $\text{M}_2$  auf einem Durchfädeln der Disulfidbrücke ( $\text{Cys}^{15}\text{-Cys}^{80}$ ) mit dem N-Terminus durch den Peptid-Ring des Cystin-Knotens beruht (Abb. 1.4). Unterstützt wurde diese "loop-threading"-Hypothese mit Mutanten, welche verkürzte N-Termini aufwiesen. Bei diesen Mutanten konnte ein schnellerer Übergang von  $\text{M}_1$  zu  $\text{M}_2$  beobachtet werden. Andere Ursachen für die langsame Umwandlung, wie eine Peptidyl-Prolyl-*cis/trans*-Isomerisierung, die häufig

Ursache für eine langsame Faltungsreaktion ist (Schmid & Baldwin, 1979), wurden aufgrund der gegenüber einer Prolinisomerisierung erhöhten Aktivierungsenergie ausgeschlossen (De Young et al., 1996).

## 2.8 Problemstellung und Ziele der Arbeit

Aus vorangegangenen Arbeiten war bekannt, dass das Pro-Peptid des ProNGF als intramolekulares Chaperon bei der oxidativen Faltung von NGF fungiert (Rattenholl et al., 2001a,b). In der vorliegenden Arbeit sollte der wechselseitige Einfluss von Pro-Peptid und NGF auf die Struktur und Strukturbildung der jeweiligen Domäne im ProNGF mit bereits korrekt ausgebildeten Disulfidbrücken untersucht werden. Dies beinhaltet (I) den Einfluss des Pro-Peptids auf die Renaturierung des denaturierten NGF mit intakten Disulfidbrücken. In diesem Zusammenhang sollte ebenfalls geprüft werden, ob die Anwesenheit des Pro-Peptids einen Einfluss auf die langsame Entfaltung des NGF-Teils hat und die "loop-threading"-Hypothese als Erklärung für das beobachtete Phänomen Gültigkeit besitzt (De Young et al., 1996; De Young et al., 1999). Neben "loop-threading" sollten auch alternative Mechanismen als Ursache für die langsame Entfaltungsreaktion überprüft werden.

(II) Parallel zur Untersuchung des Einflusses des Pro-Peptids auf die De- und Renaturierung des reifen Teils sollte umgekehrt der Einfluss des nativ strukturierten reifen Teils auf die De- und Renaturierung des Pro-Peptids analysiert werden. Ein Vergleich der Struktur und Stabilität von NGF-gebundenem und isoliertem Pro-Peptid sollte dabei Einblicke in die intramolekularen Wechselwirkungen zwischen reifem NGF und seinem Pro-Peptid geben und zum besseren Verständnis der Funktionen von ProNGF und Pro-Peptid beitragen.

Neben der Funktion als Faltungshelfer spielt das Pro-Peptid wahrscheinlich auch eine Rolle bei der biologischen Aktivität, welche durch Bindung an p75NTR hervorgerufen wird (Lee et al., 2001; Beattie et al., 2002). (III) Daher sollten in einer Zusammenarbeit mit der Arbeitsgruppe von Dr. Anders Nykjaer ProNGF und das isolierte Pro-Peptid hinsichtlich ihrer biologischen Aktivität näher charakterisiert werden.

### 3 Ergebnisse

#### 3.1 Untersuchungen der langsamen Entfaltung der Pro-Form des Nervenwachstumsfaktors sprechen gegen die "loop-threading"-Hypothese bei NGF

Kliemann, M., Weininger, U., Balbach, J., Schwarz, E., and Rudolph, R. (2006). Examination of the slow unfolding of pro-nerve growth factor argues against a loop threading mechanism for nerve growth factor. *Biochemistry*, **45**:3517-3524.

Wie in der Einleitung ausgeführt, konnten während der Denaturierung von NGF zwei Phasen der Entfaltung beobachtet werden. Laut Literatur spiegelt die erste schnelle Phase die Dissoziation des NGF-Dimers bei gleichzeitiger Entfaltung der Monomere wider (Timm & Neet, 1992). Mit längerer Inkubationszeit unter denaturierenden Bedingungen wurde eine zweite langsame Entfaltungsphase zum vollständig entfalteten Monomer beobachtet (De Young et al., 1996). Aus diesen Beobachtungen wurde der folgende sequentielle Entfaltungsweg postuliert:



In diesem Modell stellt  $N_2$  das native NGF-Dimer,  $M_1$  das partiell entfaltete NGF-Monomer und  $M_2$  das vollständig entfaltete Monomer dar. Untersuchungen mittels NMR-, fern-UV-CD- und Fluoreszenzspektroskopie zeigten, dass weder der  $M_1$ - noch der  $M_2$ -Zustand definierte Sekundär- oder Tertiärstrukturelemente besitzen. Mit der "loop-threading"-Hypothese wurde postuliert, dass der Übergang von  $M_1$  zu  $M_2$  ein Rückfädeln der durch den Ring des Cystin-Knoten gezogenen Disulfidbrücke mit dem N-Terminus darstellt (De Young et al., 1996; De Young et al., 1999). Die langsame Entfaltung sollte durch einen Gewinn an Entropie durch den flexibleren (entfädelten) N-Terminus getrieben werden. Die "loop-threading"-Hypothese wurde experimentell durch Ergebnisse mit N-terminal verkürzten NGF-Varianten gestützt, bei denen eine Beschleunigung des  $M_1 \rightarrow M_2$  Übergangs beobachtet wurde (De Young et al., 1996).

Da ProNGF das N-terminale, 102 Aminosäuren umfassende Pro-Peptid enthält, müsste nach Aussage der "loop-threading"-Hypothese diese sehr lange N-terminale Sequenz zu einer deutlichen Verlangsamung des Übergangs von  $M_1$  zu  $M_2$  führen. Aufgrund der unterschiedlichen Hydrophobizitäten der beiden Faltungszustände konnten  $M_1$  and  $M_2$  mittels *reversed-phase*-Chromatographie aufgetrennt und die Änderung ihrer Populationen über die Zeit der Denaturierung verfolgt werden. Durch Rechromatographie der getrennten Spezies wurde nachgewiesen, dass durch die Chromatographie das Verhältnis der beiden Zustände nicht



beeinflusst wird. Bei Untersuchungen des reifen NGF konnte für die Reaktion  $M_1 \rightarrow M_2$  die in der Literatur publizierte Geschwindigkeitskonstante von  $0,03 \text{ h}^{-1}$  bestätigt werden (Abb. 1, Seite 37) (De Young et al., 1996). Die Untersuchung der langsamen Entfaltung von ProNGF zeigte überraschenderweise eine nur unwesentlich kleinere Geschwindigkeitskonstante von  $0,024 \text{ h}^{-1}$  (Abb. 2B, Seite 37). Dieses Resultat konnte nicht mit Hilfe der "loop-threading"-Hypothese erklärt werden. Ein direkter Einfluss des Pro-Peptids auf den Übergang vom nativen zum ersten Denaturierungszustand ( $N \rightarrow M_1$ ) konnte ausgeschlossen werden, da bekannt war, dass das Pro-Peptid schon bei geringen GdmCl sehr schnell und vollständig entfaltet; spezifische Wechselwirkungen des Pro-Peptids mit dem Zustand  $M_1$ , welche diesen stabilisieren und somit seine Umwandlung in den vollständig denaturierten Zustand  $M_2$  inhibieren könnten, wurden daher ausgeschlossen. Die Denaturierung von ProNGF und NGF vom nativen in den ersten Denaturierungszustand erfolgte sehr schnell und beeinflusste nicht die langsame Denaturierung (Abb. 2A, Seite 37). Da davon auszugehen war, dass der langsamen Entfaltung von NGF und ProNGF dieselben molekularen Mechanismen zu Grunde liegen, stellte dieses Ergebnis die "loop-threading"-Hypothese in Frage und erforderte eine alternative Erklärung für den Mechanismus der langsamen Faltung und Entfaltung.

#### *Mögliche Ursachen der langsamen Entfaltungsreaktion*

Häufig sind Peptidyl-Prolyl-*cis/trans*-Isomerisierungen die molekularen Ursachen für langsame Faltungs- und Entfaltungsreaktionen. Da die erhaltenen Ergebnisse der "loop-threading"-Hypothese widersprachen, sollte eine mögliche Peptidyl-Prolyl-*cis/trans*-Isomerisierung als geschwindigkeitsbestimmende Reaktion untersucht werden. Für den Übergang  $M_1 \rightarrow M_2$  von NGF wurde eine Aktivierungsenergie von 108-112 kJ/mol bestimmt (De Young et al., 1996), ein Wert, der deutlich über dem typischen Wert der Aktivierungsenergie einer Prolinisomerisierung (75-91 kJ/mol) (Schmid & Baldwin, 1979) lag. Aufgrund dieser Tatsache wurde eine Prolinisomerisierung als Ursache für die langsame Entfaltung ausgeschlossen.

Zur Berechnung der Aktivierungsenergie der langsamen ProNGF-Entfaltung wurde die Geschwindigkeit der Reaktion  $M_1 \rightarrow M_2$  in Abhängigkeit von der Temperatur bestimmt (Abb. 3A und Tabelle 1, Seite 38). Aus diesen Daten konnte für den Übergang des ProNGF vom  $M_1$ - zum  $M_2$ -Zustand eine Aktivierungsenthalpie ( $\Delta H^\ddagger$ ) von  $88,8 \pm 5,3 \text{ kJ/mol}$ , eine Aktivierungsentropie ( $\Delta S^\ddagger$ ) von  $20,5 \pm 2,0 \text{ J mol}^{-1} \text{ K}^{-1}$  und eine Aktivierungsenergie ( $\Delta G^\ddagger$ ) bei  $20^\circ\text{C}$  von  $82,8 \pm 6,6 \text{ kJ/mol}$  berechnet werden (Abb. 3B, Seite 38). Aufgrund der berechneten Aktivierungsenergie konnte daher eine Prolinisomerisierung als molekulare

Ursache für die langsame Entfaltung des NGF-Teils nicht ausgeschlossen werden. Die Diskrepanz der hier bestimmten Aktivierungsenergie zu dem von De Young und Mitarbeitern bestimmten Wert konnte nicht aufgeklärt werden (De Young et al., 1996).

Da Reduktions- und Oxidationsreaktionen der Cysteine und eine damit verbundene Umverknüpfung der Disulfidbrücken als Ursache für die beobachtete langsame Reaktion in Betracht kamen, sollte die langsame Entfaltung von ProNGF hinsichtlich möglicher Reduktions- und Oxidationsreaktionen näher untersucht werden. Da Reduktions- und Oxidationsreaktionen pH-Wert-abhängig sind dies aber nicht beobachtet wurde, konnte eine Neuverknüpfung der Disulfidbindungen während der langsamen Entfaltung ausgeschlossen werden (Daten nicht gezeigt).

#### *Strukturelle Untersuchung des M<sub>1</sub>- und M<sub>2</sub>-Zustands von NGF und ProNGF*

Da sowohl mittels Fluoreszenz- als auch fern-UV-CD-Spektroskopie keine strukturellen Unterschiede zwischen M<sub>1</sub> und M<sub>2</sub> bei ProNGF detektiert werden konnten (Daten nicht gezeigt), wurde eine Strukturanalyse des M<sub>1</sub>- und M<sub>2</sub>-Zustandes mittels 1D-NMR-Spektroskopie von ProNGF durchgeführt. Hierzu wurde die langsame Denaturierung mittels 1D-NMR-Spektroskopie beobachtet. Das 1D-NMR-Spektrum der M<sub>2</sub>-Spezies zeigte eine charakteristische Signalverteilung eines vollständig entfalteten Proteins ohne Sekundär- oder Tertiärstrukturelemente (Abb. 4A, unteres Spektrum, Seite 38). Im Gegensatz dazu zeigte das 1D-NMR-Spektrum der M<sub>1</sub>-Spezies für Reststrukturen typische Hochfeldverschiebungen von Seitenkettenresonanzen unter 0,7 ppm und eine Niederfeldverschiebung der H<sup>α</sup> Resonanzen zwischen 4,8 und 5,2 ppm (Abb. 4A, oberes Spektrum, Seite 38). Unterschiede in den Resonanzen der aromatischen Aminosäurereste deuteten auf eine lokale Reststruktur, die wahrscheinlich um den Cystin-Knoten im M<sub>1</sub>-Zustand erhalten ist.

Eine Auswertung der Geschwindigkeitskonstante des mittels 1D-NMR-Spektroskopie detektierten M<sub>1</sub> zu M<sub>2</sub> Übergangs anhand der Hochfeldverschiebung ergab eine Geschwindigkeitskonstante von  $0,28 \pm 0,01 \text{ h}^{-1}$  bei 45°C (Abb. 4B, Seite 38) und war identisch mit der mittels HPLC bestimmten Geschwindigkeitskonstante (Abb. 2B, Seite 37). Zur detaillierteren Auflösung von Reststrukturen wurde NGF einheitlich mit <sup>15</sup>N markiert und der M<sub>1</sub> zu M<sub>2</sub> Übergang mittels <sup>1</sup>H-<sup>15</sup>N-HSQC-NMR-Spektroskopie untersucht. Einige beobachtete chemische Verschiebungen deuteten auf einen nicht vollständig entfaltenen Bereich im M<sub>1</sub>-Zustand. Hingegen zeigten die meisten Signale eine konstante Intensität und wiesen auf den völlig denaturierten Zustand während der gesamten Entfaltungsreaktion von M<sub>1</sub> zu M<sub>2</sub> (Abb. 5, Seite 39). Auffällig war die Beobachtung, dass mindestens 50 % der

Amidssignale der Peptidbindungen aufgrund der chemischen Verbreiterung fehlten. Während des Übergangs  $M_1$  zu  $M_2$  konnten sowohl Intensitätszunahmen als auch Intensitätsabnahmen beobachtet werden (Abb. 6A, C, D, Seite 40), welche Geschwindigkeitskonstanten zeigten, die identisch mit der mittels HPLC bestimmten Geschwindigkeitskonstante waren (Abb. 2B, Seite 37).

#### *Lokalisierung der beobachteten Reststruktur*

Insgesamt konnten damit drei experimentelle Beobachtungen gemacht werden, welche auf einen strukturellen Unterschied zwischen  $M_1$  und  $M_2$  deuteten. (I) Beide Zustände ließen sich aufgrund unterschiedlicher Hydrophobizitäten mittels *reverse-phase*-HPLC trennen. (II) Es wurden Unterschiede in der Verteilung der  $^1\text{H}$  Resonanzen im 1D-NMR-Spektren beobachtet. (III) Fehlende *cross-peaks* im 2D-HSQC-Spektrum des  $M_1$ -Zustandes gegenüber dem  $M_2$ -Zustand deuteten ebenfalls auf strukturelle Unterschiede.

Aufgrund der erhaltenen Ergebnisse wurde auf eine Reststruktur in räumlicher Nähe des Cystin-Knotens geschlossen. Die Auswirkung dieser Struktur auf den Cystin-Knoten sollte anhand der Reduktionsgeschwindigkeit des Cystin-Knotens untersucht werden. In Gegenwart von 100 mM DTT konnte dabei eine 30fach schnellere Reduktion des Cystin-Knotens von ProNGF im  $M_2$ -Zustand als im  $M_1$ -Zustand beobachtet werden (Abb. 7, Seite 40). Dies deutete auf eine wesentlich bessere Zugänglichkeit der Disulfidbrücken für DTT im  $M_2$ -als im  $M_1$ -Zustand. Das Ergebnis impliziert gleichzeitig eine Reststruktur im  $M_1$ -Zustand, welche in räumlicher Nähe des Cystin-Knotens lokalisiert sein sollte.

#### *Analyse der Renaturierung des $M_2$ -Zustands*

Sollte die  $M_2$ -Spezies einen Zustand repräsentieren, bei der der N-Terminus durch den aus den zwei Disulfidbrücken gebildeten Ring hindurchgefädelt wurde, so war zu erwarten, dass eine Renaturierung zum nativen Zustand nicht möglich ist. Eine Untersuchung der Zeitabhängigkeit der Renaturierung des  $M_2$ -Zustands sollte weiteren Aufschluss über Unterschiede zwischen  $M_1$  und  $M_2$  geben. Die Analyse der Renaturierung erfolgte wie bei der Denaturierung mittels RP-HPLC. Diese Methode erlaubte allerdings nur eine Unterscheidung zwischen  $M_1$  und  $M_2$ , da natives Protein unter HPLC-Bedingungen zu  $M_1$  denaturiert wird. Jedoch steht der denaturierte Zustand  $M_1$  im schnellen Gleichgewicht mit dem nativen Zustand, so dass die Methode zur Detektion der Renaturierung geeignet war (De Young et al., 1996).

Mit zunehmender Renaturierungszeit konnte eine Abnahme der M<sub>2</sub>-Spezies und eine Zunahme der M<sub>1</sub>-Spezies beobachtet werden (Abb. 8A, Seite 41). Aus der Zu- und Abnahme der beiden Spezies wurde eine Geschwindigkeitskonstante von 0,083 h<sup>-1</sup> bei 20°C und eine Gesamtausbeute von ca. 75 % berechnet (Abb. 8B, Seite 41). Eine nähere Analyse der im Faltungsansatz enthaltenen inhomogenen Proteinspezies erfolgte mittels Größenausschlusschromatographie, da bekannt war, dass ausschließlich nativer ProNGF zur Dimerisierung fähig ist (Bothwell & Shooter, 1977; Timm & Neet, 1992; Rattenholl et al., 2001a). Die Fern-UV-CD- und Fluoreszenzspektren des renaturierten ProNGF waren identisch mit dem Spektrum der nativen Referenz (Abb. 9A und 9B, Seite 41). Folglich war es möglich, vollständig denaturierten ProNGF aus dem M<sub>2</sub>-Zustand zur nativen Struktur zu renaturieren.

Eine Bestimmung der Faltungsausbeute mittels Gelfiltration ergab allerdings, dass nur ca. 30 % der Moleküle in der nativen Konformation vorlagen (Daten nicht gezeigt), also weitaus weniger als die zuvor durch RP-HPLC ermittelten 75 %. Eine Tatsache, die darauf hindeutete, dass die durch RP-HPLC detektierte Fraktion neben faltungskompetentem ProNGF auch irreversibel denaturierten ProNGF einschloss. Die Faltungsausbeute von 30 % konnte zudem durch Denaturierungskinetiken des Faltungsansatzes bestätigt werden (Daten nicht gezeigt).

### *Zusammenfassung*

Zwei der drei Prolinreste (Pro<sup>61</sup> und Pro<sup>63</sup>) in NGF sind in der Ringstruktur des Cystin-Knoten lokalisiert und konnten weder durch Cokristallisation mit dem TrkA- noch mit p75NTR-Rezeptor aufgelöst werden (Wiesmann et al., 1999; He & Garcia, 2004). Der dritte Prolinrest befindet sich am N-Terminus und liegt in der *trans*-Konformation vor (Wiesmann et al., 1999). Zur Analyse, ob die langsame Faltungs- und Entfaltungsreaktion durch eine Prolinisomerisierung hervorgerufen wird, wurden drei Peptidyl-Prolyl-*cis/trans*-Isomerasen (Cyclophilin 12, FKBP 18 und SlyD) hinsichtlich ihrer Auswirkung auf die Beschleunigung der Faltungsreaktion getestet. Bei keiner der getesteten Prolinisomerasen konnte eine Beschleunigung nachgewiesen werden. Dennoch konnte eine Prolinisomerisierung als Ursache für die sehr langsamen Umwandlungsprozesse nicht vollständig ausgeschlossen werden, da keine Aussagen über die Zugänglichkeit der Prolinreste für die Prolinisomerasen getroffen werden konnte.

Die aufgeführten Ergebnisse zeigten, dass die "*loop-threading*"-Hypothese als molekulare Ursache für die langsame Entfaltung nicht weiter in Betracht kommt: (I) Die Gegenwart des Pro-Peptids verlangsamt die Entfaltung von M<sub>1</sub> zu M<sub>2</sub> nicht signifikant. Nach der "*loop-*

*threading*"-Hypothese wurde erwartet, dass der um das Pro-Peptid verlängerte N-Terminus deutlich langsamer durch den Ring fädelt. (II) Vollständig in  $M_2$  vorliegender ProNGF konnte wieder renaturiert werden. Der "*loop-threading*"-Hypothese folgend, wäre ein Zurückfädeln des N-Terminus durch den Ring nicht zu erwarten. (III) Im Gegensatz zur "*loop-threading*"-Hypothese, welche beinhaltet, dass beide Zustände quasi vollständig entfaltet vorliegen und sich nur im Bezug auf den ein- bzw. ausgefädelten N-Terminus unterscheiden, konnten strukturelle Unterschiede mittels NMR-Spektroskopie nachgewiesen werden. So konnte eine Reststruktur in räumlicher Nähe des Cystin-Knotens im  $M_1$ -Zustand beobachtet werden, welche im  $M_2$ -Zustand nicht detektiert wurde. (IV) Die eingeschränkte Zugänglichkeit der Disulfidbrücken gegenüber DTT im  $M_1$ -Zustand im Vergleich zum  $M_2$ -Zustand bestätigte die Zuordnung der Reststrukturen im  $M_1$ -Zustand in der Nähe des Cystin-Knoten.

Diese Reststrukturen stellen den Unterscheid zwischen den beiden Zuständen  $M_1$  und  $M_2$  dar. Die Auflösung der Reststruktur unter denaturierenden Bedingungen wurde als sehr langsame Entfaltung beschrieben und irrtümlich mit der "*loop-threading*"-Hypothese erklärt. Die Lokalisierung um den Cystin-Knoten und die damit verbundene sterische Einschränkung könnten Ursache für die ungewöhnlich langsame Entfaltung sein. Darüber hinaus stellen diese Reststrukturen wahrscheinlich einen Kern dar, aus denen eine effiziente und schnelle Faltung von NGF (Timm & Neet, 1992) und ProNGF möglich ist.

### 3.2 Die native NGF-Domäne induziert die Struktur des Pro-Peptids im ProNGF

Kliemann, M., Rattenholl, A., Golbik, R., Balbach, J., Lilie, H., Rudolph, R., and Schwarz, E. (2004). The mature part of ProNGF induces the structure of its pro-peptide. *FEBS Lett.*, **566**:207-212.

Neben der biologischen Funktion als *in vitro*-Faltungshelfer stimuliert das NGF-Pro-Peptid durch Bindung sowohl an p75NTR als auch an TrkA auch eine pro-apoptotische Aktivität (Lee et al., 2001; Nykjaer et al., 2004). Eine biophysikalische Charakterisierung sollte über die Struktur und Stabilität des isolierten NGF-Pro-Peptids und des an NGF kovalent gekoppelten Pro-Peptids Aufschluss geben. Verschiedene Methoden zur Untersuchung des Oligomerzustands wie analytische Ultrazentrifugation oder Gelfiltration zeigten, dass das isolierte Pro-Peptid im Gegensatz zum NGF bzw. ProNGF als Monomer vorliegt (Abb. 2, Seite 44) (Timm & Neet, 1992; Rattenholl et al., 2001a).

#### *Das NGF-Pro-Peptid ist nur gering strukturiert*

Um weitere Kenntnisse über die Struktur des isolierten Pro-Peptids zu erhalten, wurde die intrinsische Fluoreszenz des Proteins untersucht. Der einzelne Tryptophanrest des Pro-Peptids lag sowohl unter nativen als auch unter denaturierenden Bedingungen lösungsmittel exponiert vor. Dies bedeutete, dass der Tryptophanrest nicht an der Ausbildung einer Tertiärstruktur beteiligt ist (Abb. 3A, Seite 45). Eine Analyse der Fluoreszenzeigenschaften der vier sich im Pro-Peptid befindenden Phenylalaninreste zeigte dagegen eine Abnahme der Fluoreszenzintensität unter denaturierenden Bedingungen, welche auf einen verminderten Energietransfer von dem angeregten Phenylalaninrest zum Tryptophanrest im denaturierten Zustand wies (Abb. 3B, Seite 45). Das fern-UV-CD-Spektrum zeigte ein Plateau zwischen 218 und 223 nm sowie ein Minimum bei 205 nm (Abb. 3C, Seite 45). Dieses Spektrum wurde als ein Indiz für einen geringen Anteil an  $\beta$ -Faltblattstruktur und einen hohen Anteil an "random coil"-Struktur interpretiert. Eine Auswertung des fern-UV-CD-Spektrums mit Hilfe des Programms CDNN (Bohm et al., 1992) ergab einen  $\beta$ -Faltblattanteil von 24% und einen "random coil"-Anteil von 34%.

Zur Untersuchung der Stabilität wurde das isolierte Pro-Peptid mit GdmCl titriert und die Denaturierung mit der damit verbundenen Änderung der Sekundärstruktur mit Hilfe von fern-UV-CD-Spektroskopie verfolgt. Die Detektion erfolgte bei 220 nm, einer Wellenlänge, bei der der spektroskopische Unterschied zwischen nativem und denaturiertem Zustand am

größten ist. Die reversibel verlaufende Denaturierung zeigte einen nicht-kooperativen Übergang; die Struktur des isolierten Pro-Peptids ist demnach nicht durch kooperativ wirkende Wechselwirkungen stabilisiert (Abb. 4A, Seite 45). Dieses Ergebnis konnte auch mit Hilfe der Analyse der Phenylalaninfluoreszenz bestätigt werden. Bei Versuchen mit steigenden Konzentrationen von Ammoniumsulfat konnte keine Stabilisierung der Pro-Peptid-Struktur nachgewiesen werden (Abb. 4B-D, Seite 45). Vermutlich enthält das Pro-Peptid keinen ausgeprägten hydrophoben Kern.

Der Vergleich der 1D-Protonen-NMR-Spektren (Abb. 5, Seite 46) von nativem und denaturiertem isolierten Pro-Peptid bestätigte die zuvor mit Hilfe der Fluoreszenzspektroskopie gewonnenen Daten. Das isolierte Pro-Peptid liegt unter beiden Bedingungen nahezu vollständig entfaltet vor. Geringe Unterschiede zwischen beiden Zuständen konnten auf lokale Kontakte zurückgeführt werden. Eine definierte Tertiärstruktur des isolierten Pro-Peptids konnte nicht nachgewiesen werden.

Zusammenfassend wurde sowohl aus der chemisch induzierten Entfaltung als auch aus den NMR-Experimenten ersichtlich, dass das isolierte Pro-Peptid keine kooperativ stabilisierte Tertiärstrukturelemente besitzt. Darüber hinaus konnte mittels fern-UV-CD-Spektroskopie definierte Sekundärstrukturanteile nachgewiesen werden. Der Energietransfer der angeregten Phenylalaninreste zum Tryptophanrest zeigte die kompaktere Anordnung des isolierten Pro-Peptids unter nativen gegenüber denaturierenden Bedingungen. Zum Vergleich der Stabilität und Struktur wurde das an NGF gekoppelte Pro-Peptid mittels fern-UV-CD- und Fluoreszenzspektroskopie untersucht.

#### *Stabilisierung des NGF-gekoppelten Pro-Peptids durch den reifen Teil*

Die komplette Denaturierung von ProNGF zeigte zwei kooperative Übergänge (Abb. 6B, Seite 46), wobei der zweite Denaturierungsübergang mit einem Mittelpunkt bei 3,5 M GdmCl die Denaturierung der reifen NGF-Domäne widerspiegelte (Timm & Neet, 1992; Rattenholl et al., 2001a). Der erste Übergang mit einem Mittelpunkt bei 0,85 M GdmCl resultierte aus der Denaturierung des Pro-Peptids. Das schmale Plateau zwischen beiden Übergängen repräsentierte eine Spezies, in der das Pro-Peptid denaturiert und der NGF-Teil nativ strukturiert war. Dass dieser partiell denaturierte ProNGF wie nativer ProNGF als Homodimer vorlag, konnte mittels analytischer Ultrazentrifugation nachgewiesen werden (Daten nicht gezeigt). Die Denaturierung des Pro-Peptids im ProNGF bewirkte im Gegensatz zum isolierten Pro-Peptid eine Änderung der Lösungsmittelzugänglichkeit von mindestens einem Tryptophanrest. Ob die während der Pro-Peptid-Denaturierung beobachtete

Fluoreszenzänderung durch einen Tryptophanrest im reifen oder im Pro-Peptid-Teil verursacht wurde, konnte dabei nicht unterschieden und aufgeklärt werden. Die geringe GdmCl-Konzentration, welche ausreichte um das Pro-Peptid zu denaturieren und vom reifen Teil zu dissoziieren, deutete auf eine nur geringe Stabilisierung. Für die reversible Entfaltung des Pro-Peptids wurde ein  $\Delta G^{\circ}$  von  $-7,8$  kJ/mol berechnet (Abb. 6C, Seite 46).

Reifer NGF enthält drei Tryptophan-, zwei Tyrosin- und sieben Phenylalaninreste (McDonald et al., 1991; Wiesmann et al., 1999). Aus den Strukturmodellen des humanen und murinen NGF war bekannt, dass zwei Tryptophanreste in der Dimerisierungsfläche lokalisiert sind. Der dritte Tryptophanrest ist an der Rezeptorbindung mit TrkA und p75TNR beteiligt und auf der Oberfläche des Moleküls teils lösungsmittel exponiert lokalisiert (Wiesmann et al., 1999; He & Garcia, 2004).

Wechselwirkungen, welche die Struktur des ProNGF-Pro-Peptids im Gegensatz zum isolierten Pro-Peptid stabilisieren, konnten mittels Ammoniumsulfat verstärkt werden. Mit steigenden Ammoniumsulfatkonzentrationen konnte eine Verschiebung des Übergangsmittelpunkts zu höheren GdmCl-Konzentrationen beobachtet werden (Abb. 7B-D, Seite 47).

Wie aus den vorgestellten Ergebnissen hervorgeht, besteht eine Wechselwirkung zwischen dem Pro-Peptid und dem reifen Teil im Kontext des nativen ProNGF. Da das Pro-Peptid aber auch einen Einfluss auf die Strukturbildung des reifen Teils während des Prozesses der oxidativen Faltung nimmt, ist während der Faltung auch eine Wechselwirkung des Pro-Peptids mit Faltungsintermediaten anzunehmen. Daher beschränken sich Wechselwirkungen des Pro-Peptids mit dem reifen Teil nicht auf einige wenige strukturell definierte Wechselwirkungen, sondern deutet auf eine Assoziation des relativ flexiblen Pro-Peptids mit mehreren und unterschiedlich strukturierten Abschnitten des reifen Teils.



### 3.3 Das Pro-Peptid des ProNGF: Strukturbildung und intramolekulare Assoziation mit NGF

Kliemann, M., Golbik, R., Rudolph, R., Schwarz, E. and Lilie, H. (2006) The pro-peptide of NGF: structure formation and intramolecular association with NGF. eingereicht bei *Prot. Sci.*

Wie in vorherigen Arbeiten gezeigt werden konnte, führt die GdmCl induzierte Gleichgewichtsdenaturierung des NGF-gekoppelten Pro-Peptids im Gegensatz zum isolierten Pro-Peptid, welches einen reversiblen nicht-kooperativen Übergang zeigt, zu einem reversiblen kooperativen Übergang (Abb. 1, Seite 50) (Kliemann et al., 2004). Der mittels Fluoreszenzspektroskopie gemessene kooperative Denaturierungsübergang wies daraufhin, dass die Struktur des NGF-gekoppelten Pro-Peptids im Gegensatz zum isolierten Pro-Peptid durch tertiäre Wechselwirkungen stabilisiert ist. Ebenfalls konnte anhand der fern-UV-CD-Spektren ein identischer Anteil an Sekundärstruktur für das isolierte und das NGF-gekoppelte Pro-Peptid nachgewiesen werden (Kliemann et al., 2004).

Für eine detailliertere Untersuchung der De- und Renaturierung wurden die mittels fern-UV-CD- und Fluoreszenzspektroskopie ermittelten Übergänge miteinander verglichen. Überraschenderweise waren die mit Fluoreszenz und fern-UV-CD gemessenen Übergangskurven nicht identisch (Abb. 2, Seite 51). Der Übergang der fern-UV-CD-Messung erfolgte bei einer geringeren GdmCl-Konzentration als der der Fluoreszenzmessungen. Aufgrund der Änderung der Elliptizität während der Denaturierung konnten ein Rückschluss auf die Sekundärstruktur gezogen werden. Im Gegensatz dazu spiegelten die Änderungen der Fluoreszenzintensität während der Denaturierung die Umgebungsänderung der Fluorophore wider, welche mit einer Änderung der Tertiärstruktur korreliert. Die nichtkongruenten Kurven deuteten auf eine ungewöhnliche entkoppelte Entfaltung der Sekundär- und Tertiärstrukturen. Daher implizierte dieses Ergebnis die Existenz eines Intermediats, in dem die native Sekundärstruktur aufgelöst ist, aber Tertiärkontakte, nachgewiesen über die Tryptophanfluoreszenz, vorhanden sind. Dabei kann der Tryptophanrest, der in den Tertiärkontakt involviert ist, prinzipiell im reifen NGF-Teil als auch im Pro-Peptid-Teil lokalisiert sein. Mit Hilfe eines Fusionproteins bestehend aus dem reifen NGF und dem Pro-Peptid des Neurotrophins-3, welches keinen Tryptophanrest enthält, wurde während der Denaturierung eine ähnliche Änderung der Tryptophanfluoreszenz beobachtet (Manuskript in Vorbereitung). Folglich ist der Tryptophanrest, welcher zumindest für einen Teil der Fluoreszenzänderung verantwortlich ist, wahrscheinlich im reifen Teil lokalisiert.

### *Lokalisierung der mit NGF wechselwirkenden Region im Pro-Peptid*

Zur Identifizierung der Pro-Peptid-Region, welche mit der reifen NGF-Domäne interagiert, wurden H/D-Austauschexperimente mit gekoppelter massenspektrometrischer Untersuchung durchgeführt. Diese Methode erlaubte die Identifizierung von Peptidfragmenten anhand ihres Molekulargewichts, welche aufgrund ihrer Wechselwirkung nur eingeschränkt Wasserstoff gegen Deuterium austauschen. Dazu wurde ProNGF in D<sub>2</sub>O inkubiert und nach anschließender Ansäuerung durch Pepsin verdaut. Unter diesen experimentellen Bedingungen wurde ausschließlich die Pro-Peptid-Domäne des ProNGF in unterschiedliche lange Proteolyseprodukte fragmentiert. Die Masse der erhaltenen Fragmente wurde anschließend mittels MALDI-TOF analysiert und mit Hilfe des Programms FindPept™ (<http://www.expasy.ch/tools/findpept.html>) der Primärsequenz zugeordnet (Tab. "Table 1", Seite 52).

Neben der Mehrzahl von Fragmenten, welche einen vollständigen H/D-Austausch zeigten, konnten die Peptide Trp<sup>-83</sup>-Ala<sup>-63</sup> and Gln<sup>-80</sup>-Ala<sup>-64</sup> im ProNGF identifiziert werden, welche einen reduzierten H/D-Austausch zeigten (Tab. "Table 1", Seite 52). Im Gegensatz zur spezifischen Fragmentierung des NGF-gekoppelten Pro-Peptids konnten keine definierten Spaltprodukte nach der Proteolyse des isolierten Pro-Peptids identifiziert werden. Potenzielle Spaltstellen im NGF-gekoppelten Pro-Peptid waren daher wahrscheinlich durch Wechselwirkung mit dem reifen Teil vor Proteolyse geschützt. Mit den Peptiden Trp<sup>-83</sup>-Ala<sup>-63</sup> and Gln<sup>-80</sup>-Ala<sup>-64</sup> konnte eine Region identifiziert werden, welche wahrscheinlich an einer Wechselwirkung mit dem reifen NGF beteiligt ist. Eine Sequenzanalyse bezüglich des hydrophoben Moments nach der Eisenberg-Methode ergab, dass dieser Sequenzabschnitt die höchste Hydrophobizität innerhalb des Pro-Peptids besitzt (Eisenberg et al., 1984). Unter Annahme einer helikalen Struktur stellt dieser Bereich einen hoch amphiphilen Abschnitt dar.

### *Kinetische Untersuchung der Entfaltung und Faltung des NGF-gekoppelten Pro-Peptids*

Die Änderung der Tryptophanfluoreszenz während der Denaturierung des ProNGF stellte eine Änderung der Wechselwirkung zwischen NGF und Pro-Peptid dar, da die Intensität der Tryptophanfluoreszenz des isolierten Pro-Peptids unter nativen und denaturierenden Bedingungen unverändert war (Abb. 3A, Seite 52). Zur Untersuchung der Wechselwirkung zwischen NGF und Pro-Peptid im ProNGF wurde die Faltung und Entfaltung des Pro-Peptids kinetisch untersucht. Eine Änderung des Fluoreszenzsignals im Bereich von 0 - 2 M GdmCl resultierte dabei ausschließlich von Strukturänderungen des NGF-gekoppelten Pro-Peptids,

da die NGF-Domäne erst ab GdmCl-Konzentrationen von über 3 M denaturiert (Timm & Neet, 1992; De Young et al., 1996; Kliemann et al., 2004).

Die Fluoreszenzamplituden während der Faltung und Entfaltung in Abhängigkeit von der GdmCl-Konzentration entsprachen dabei den Fluoreszenzamplituden, welche während der Gleichgewichtsmessungen analysiert wurden (Daten nicht gezeigt) und deuteten darauf, dass beide Messungen denselben Prozess beschrieben. Während der Faltung des NGF-gekoppelten Pro-Peptids konnte eine monophasische Zunahme des Fluoreszenzsignals beobachtet werden (Abb. 3A, Seite 52). Eine monophasische Zunahme war aufgrund des aus den Gleichgewichtsübergängen erwarteten Intermediats überraschend. Eine Analyse der Faltung des NGF-gekoppelten Pro-Peptids mittels fern-UV-CD-Spektroskopie bei 220 nm zeigte ebenfalls eine monophasisch verlaufende Kurve (Abb. 3A, Seite 52), welche die gesamte zu erwartende Amplitude aufzeigte, so dass keine schnelle vorangehende Reaktion anzunehmen war. Eine weitere langsame Reaktion im Anschluss konnte ebenfalls nicht nachgewiesen werden.

Da innerhalb des Pro-Peptids neun Prolinreste lokalisiert sind, konnte eine Prolin-*cis/trans*-Isomerisierung als geschwindigkeitsbestimmender Schritt der Reaktion nicht ausgeschlossen werden. Allerdings wurde weder mit Hilfe verschiedener Prolinisomerasen noch mittels Doppelsprungexperimenten eine Prolinisierung als geschwindigkeitsbestimmender Schritt für die Faltung nachgewiesen.

Eine kinetische Untersuchung der Denaturierung des NGF-gekoppelten Pro-Peptids in 1,75 M GdmCl mittels Fluoreszenzspektroskopie zeigte im Gegensatz zur Renaturierung einen biphasischen Verlauf der Reaktion (Abb. 3B, Seite 52). Aufgrund des schnellen Ablaufs der Reaktion war im Gegensatz zur Fluoreszenzmessung eine Bestimmung der Denaturierungsgeschwindigkeit mittels *stopped-flow*-fern-UV-CD-Spektroskopie nicht möglich (Abb. 3B, Seite 52). Diese ungewöhnliche Reihenfolge der Denaturierung entsprach den Ergebnissen aus den Gleichgewichtsmessungen, die zeigten, dass sich die Sekundärstruktur vor den Tertiärkontakten auflöste. Um Aufschluss zu erhalten, ob eine parallele oder serielle Reaktion die Ursache für den biphasischen Denaturierungsverlauf ist, wurde Doppelsprungexperimente durchgeführt. NGF-gekoppeltes Pro-Peptid wurde unterschiedlich lange unter denaturierenden Bedingungen inkubiert, anschließend renaturiert und die Strukturänderung mittels Fluoreszenzspektroskopie analysiert. Dabei wurde beobachtet, dass eine Denaturierungszeit von 25 s in 1,75 M GdmCl des NGF-gekoppelte Pro-Peptids zu einem monophasischen Verlauf der Renaturierung führt, welcher der Renaturierung des vollständig denaturierten Pro-Peptids entsprach. Im Gegensatz dazu wurde

bei kürzeren Denaturierungszeiten eine biphasische Faltungsreaktion mit einer ca. 20-fach schnelleren ersten Reaktion beobachtet (Abb. 4A, Seite 53). Das Ergebnis dieses Experiments wies eindeutig auf die Existenz eines Intermediats (I) während der Denaturierung des Pro-Peptids. Dabei resultierte die schnelle Reaktion aus der Umwandlung des Intermediats zum nativen Zustand (N), die langsame Reaktion spiegelte die Faltung des entfalteten Zustands (U) zum nativen Zustand wider;  $U \rightarrow I \rightarrow N$ . Der geschwindigkeitsbestimmende Schritt der Reaktion war die Umwandlung von  $U \rightarrow I$ , so dass die Reaktion  $I \rightarrow N$  innerhalb der Gesamtreaktion nicht spektroskopisch erfasst werden konnte.

Die Akkumulation des Intermediats konnte während der Denaturierung in 1,75 M GdmCl nur innerhalb der ersten Sekunde beobachtet werden, da anschließend die vollständige Entfaltung des Intermediats erfolgte. Durch unterschiedlich lange Denaturierungszeiten in den Doppelsprungexperimenten konnte die zeitabhängige Akkumulation des Intermediats beobachtet werden (Abb. 4A, Seite 53). Die Amplituden der beiden Renaturierungsphasen reflektierten dabei die Populationen des Intermediats und der entfalteten Spezies. Anhand der Amplituden konnten daher sowohl die Zu- und Abnahme des Intermediats als auch die Akkumulation des entfalteten Zustands beobachtet werden (Abb. 4B, Seite 53). Die aus diesen Messungen berechnete Geschwindigkeit für die Abnahme des Intermediats korrelierte dabei mit den Kinetiken der biphasischen, mittels *stopped-flow*-Fluoreszenzmessung analysierten Denaturierung.

Da das Fluoreszenzspektrum des Intermediats aufgrund der schnellen Reaktion von  $I \rightarrow U$  nicht direkt gemessen werden konnte, wurde versucht, das Spektrum aus den Denaturierungskinetiken bei verschiedenen Wellenlängen zu berechnen. Dazu wurde das NGF-gekoppelte Pro-Peptid in 1,8 M GdmCl denaturiert und die Kinetik bei verschiedenen Emissionswellenlängen zwischen 330 und 360 nm analysiert. Anhand der kinetischen Daten konnte ein Fluoreszenzmaximum für den denaturierten und intermediären Zustand bei 345-350 nm und für den nativen Zustand bei 337 nm bestimmt werden (Abb. 5, Seite 54). Demnach ist der Tryptophanrest, der für den spektroskopischen Unterschied des ProNGF mit nativem bzw. denaturiertem Pro-Peptid verantwortlich war, bereits im Faltungsintermediat exponiert.

Anhand der Fluoreszenzänderung während der Denaturierung konnte sowohl die Bildung des Intermediats als auch die Entstehung des denaturierten Zustands beobachtet werden. Demgegenüber wurde während der Renaturierung nur die Umwandlung von  $U \rightarrow I$  beobachtet. Zur Bestimmung der Renaturierungsrate von  $I \rightarrow N$  wurden Doppelsprungexperimente durchgeführt, wobei das NGF-gekoppelte Pro-Peptid für eine Sekunde bei 1,8 M

GdmCl denaturiert und anschließend rückgefaltet wurde. Die gemessenen Geschwindigkeitskonstanten der Faltung und Entfaltung in Abhängigkeit der GdmCl-Konzentration sind in Abb. 6 (Seite 54) als Chevron-Plot dargestellt. Die Extrapolationen der Daten ergaben die mikroskopischen Geschwindigkeitskonstanten für die Faltung und Entfaltung sowohl des nativen und denaturierten Zustands als auch des Intermediats unter nativen Bedingungen. Darüber hinaus konnte die thermodynamische Stabilität des nativen Zustands und des Intermediats berechnet werden (Abb. 6, Seite 54). Für die Gesamtreaktion  $N \leftrightarrow U$  konnte eine Stabilisierungsenergie von 20,9 kJ/mol berechnet werden, welche sich aus den Teilreaktionen  $N \leftrightarrow I$  mit 14,8 kJ/mol und  $I \leftrightarrow U$  mit 6,1 kJ/mol zusammensetzt. Die mikroskopischen Geschwindigkeitskonstanten für die beiden Reaktionen  $N \rightarrow I$  und  $I \rightarrow U$  waren mit  $k_{\text{q}} = 0.0025 \text{ s}^{-1}$  und einer Aktivierungsenergie von 86,3 kJ/mol identisch. Aufgrund der schnellen, mittels fern-UV-CD-Spektroskopie nicht quantifizierbaren Entfaltungsreaktion des NGF-gekoppelten Pro-Peptids stellt der Chevron-Plot nicht die gesamten Faltungs- und Entfaltungsprozesse dar.

Wie gezeigt werden konnte, beschreiben die tertiären Wechselwirkungen intramolekulare Interaktionen zwischen NGF und seinem Pro-Peptid, welche hauptsächlich auf hydrophoben Interaktionen beruhen (Kliemann et al., 2004). Hydrophoben Wechselwirkungen bei fehlender Sekundärstruktur wurde auch für andere Proteine beobachtet (Neri et al., 1992; Saab-Rincon et al., 1996). Dabei stellt die Wechselwirkung unter denaturierenden Bedingungen zwischen NGF und Pro-Peptid weniger einen hydrophoben Kern dar, sondern eher die Assoziation über hydrophobe Aminosäuren. Die strukturelle Wechselwirkung zeichnet sich dabei wahrscheinlich nicht durch eine hohe Selektivität und Spezifität aus, da dass Pro-Peptid sowohl den reifen NGF bindet als auch während der Faltung des reifen Teils als intramolekulares Chaperon fungiert (Rattenholl et al., 2001a).

An der Wechselwirkung zwischen NGF und Pro-Peptid sind, wie gezeigt werden konnte, ein oder mehrere Tryptophanrest(e) beteiligt. Dabei konnte anhand einer Chimäre aus NGF und dem verwandten Neurotrophin-Pro-Peptid des NT-3 nachgewiesen werden, dass einer dieser Tryptophanreste im NGF lokalisiert ist (Veröffentlichung in Vorbereitung). Aufgrund der zur Verfügung stehenden Daten der Röntgenstrukturanalyse konnte der Tryptophanrest Trp<sup>21</sup> identifiziert werden, welcher lösungsmittel exponiert vorliegt (Abb. 7, Seite 56) (McDonald et al., 1991). Im Gegensatz dazu befinden sich die beiden anderen Tryptophanreste innerhalb der Dimerisierungsschnittstelle und sind unter nativen Bedingungen nicht zugänglich. Im ProNGF schränkt das gefaltete Pro-Peptid die Lösungsmittelzugänglichkeit dieses Tryptophanrests ein. Nach Denaturierung des Pro-Peptids liegt der Tryptophanrest

wieder lösungsmittlexponiert vor. Aufgrund der Annahme, dass das Pro-Peptid weder die Struktur noch die Dimerisierung des NGF beeinflusst, konnten Hinweise erhalten werden, dass das Pro-Peptid im Bereich von Trp<sup>21</sup> mit dem reifen Teil interagiert.

#### *Biologische Bedeutung des NGF-gekoppelten Pro-Peptids*

Der Tryptophanrest Trp<sup>21</sup>, welcher wahrscheinlich an der Wechselwirkung mit dem Pro-Peptid beteiligt ist, trägt zur Interaktion von NGF mit den beiden Rezeptoren TrkA und p75NTR bei (Wiesmann et al., 1999; He & Garcia, 2004). So befinden sich beispielsweise im NGF-TrkA-Komplex sieben Aminosäuren des Rezeptors in der Nähe von 8 Å zum Trp<sup>21</sup> (Abb. 7, Seite 56). Daher ist es sehr wahrscheinlich, dass das Pro-Peptid mit den beiden Rezeptoren TrkA und p75NTR um die NGF-Bindungsstelle konkurriert. Diese Vermutung wird durch die Beobachtung unterstützt, dass die Gegenwart des Pro-Peptids die Affinität von NGF zu diesen Rezeptoren senkt (Nykjaer et al., 2004). Um eine Dissoziation des Pro-Peptids vom reifen Teil zu bewirken und eine Rezeptorbindung zu ermöglichen, muss ein Energiebetrag von 14,8 kJ/mol aufgebracht werden. Andererseits wäre es möglich, dass eine Dissoziation des Pro-Peptids für eine Rezeptorbindung nicht notwendig und eine Delokalisierung ausreichend ist, welche sich in einer Senkung der Affinität von ProNGF zum Rezeptor äußern würde. Der Energiebetrag für eine Delokalisierung ist abhängig von der Größe und der Überlappung der Kontaktfläche des Pro-Peptids und den Rezeptoren und wahrscheinlich energetisch begünstigt. Solange allerdings keine Strukturdaten auf atomarer Ebene von ProNGF mit den Rezeptoren zur Verfügung stehen, bleiben diese Interpretationen der Ergebnisse spekulativ.

### 3.4 Sortilin ist essentiell für den ProNGF induzierten neuronalen Zelltod

Nykjaer, A., Lee, R., Teng, K. K., Jansen, P., Madsen, P., Nielsen, M. S., Jacobsen, C., Kliemann, M., Schwarz, E., Willnow, T. E., Hempstead, B. L., and Petersen, C. M. (2004). Sortilin is essential for ProNGF-induced neuronal cell death. *Nature*, **427**:843-848.

In Kooperation mit der Arbeitsgruppe von Prof. Petersen konnte dazu beigetragen werden, neue Erkenntnisse über die Affinitäten von ProNGF und isoliertem NGF-Pro-Peptid im Vergleich zu NGF zu den beiden Rezeptoren TrkA und p75NTR zu gewinnen. Dabei konnte keine Affinität des isolierten Pro-Peptids zu den Rezeptoren TrkA und p75NTR und eine etwa 10-fach geringere Affinität des ProNGF zu den Rezeptoren als die von reifem NGF beobachtet werden. Darüber hinaus wurde ein weiterer Rezeptor, Sortilin, identifiziert, welcher spezifisch ProNGF über die Pro-Peptid-Domäne bindet. Der identifizierte Sortilin-Rezeptor aus der Familie der Vps10P-Domänen-Rezeptoren (Hermey et al., 2003) besitzt *in vitro* eine 10- bis 15-fach höhere Affinität zu ProNGF bzw. zum isolierten Pro-Peptid als zum reifen NGF (Abb. 1, Seite 59). Mittels *in vivo*-Experimenten wurde die spezifische Aufnahme von NGF in die Zellenlinie 293 über TrkA und p75NTR, nicht aber über den Sortilin-Rezeptor nachgewiesen. Im Gegensatz dazu erfolgt die Aufnahme von ProNGF über einen Komplex aus Sortilin und p75NTR (Abb. 2, Seite 60). Dieser Komplex scheint eine hoch affine Bindestelle für das Pro-Peptid zu bilden und essentiell für die Apoptoseinduktion durch ProNGF zu sein. Als Modell dieses Komplexes wurde eine Stöchiometrie von einem p75NTR-Molekül, einem Sortilin-Molekül und einem ProNGF-Dimer vorgeschlagen (Abb. 4H, Seite 61).

## 4 Veröffentlichungen

Biochemistry 2006, 45, 3517–3524

3517

### Examination of the Slow Unfolding of Pro-Nerve Growth Factor Argues against a Loop Threading Mechanism for Nerve Growth Factor<sup>†</sup>

Marco Kliemannel,<sup>‡</sup> Ulrich Weininger,<sup>§</sup> Jochen Balbach,<sup>§</sup> Elisabeth Schwarz,<sup>\*,‡</sup> and Rainer Rudolph<sup>‡</sup>

*Institut für Biotechnologie der Martin-Luther-Universität Halle-Wittenberg, Kurt-Mothes-Strasse 3, 06120 Halle, Germany, and Fachbereich Physik, Arbeitsgruppe Biophysik der Martin-Luther-Universität Halle-Wittenberg, Hoher Weg 8, 06099 Halle, Germany*

*Received September 16, 2005; Revised Manuscript Received January 25, 2006*

**ABSTRACT:** Nerve growth factor (NGF), a member of the neurotrophin family, is an all- $\beta$ -sheet protein with a characteristic structure motif, the cystine knot. Unfolding of NGF in 6 M GdnHCl has been described previously to involve an initial partial loss of structure and a subsequent very slow conversion to a second, completely unfolded state. This latter conversion was postulated to represent a back-threading of the disulfide bond that passes through the cystine knot (loop threading hypothesis). Here, this hypothesis was questioned with the pro form of the protein (proNGF). In proNGF, the mature part is preceded by the 103-amino acid pro-peptide. Consequently, loop threading of the N-terminally extended protein should be significantly delayed. However, unfolding kinetics of proNGF monitored by RP-HPLC, intrinsic fluorescence, and NMR spectroscopy were comparable to those of mature NGF. Time-resolved <sup>1</sup>H–<sup>15</sup>N HSQC spectra revealed a slow time-dependent loss of residual structure of which the kinetics correlated well with the transition observed by RP-HPLC. Refolding from the completely unfolded state led to a partial recovery of natively folded proNGF. In summary, the sequential unfolding of proNGF only marginally differed from that of mature NGF. Therefore, it is very unlikely that a loop threading mechanism is the cause of the slow unfolding step.

NGF<sup>1</sup> belongs to the neurotrophin protein family and promotes growth, maintenance, and differentiation of neurons in the central and peripheral nervous system. NGF conveys its biological activity by binding to the TrkA receptor. The pro form of NGF, proNGF, on the other hand, has been postulated to induce apoptosis via interaction with both p75 and the sortilin receptor (1–5). NGF is a noncovalent homodimer in which both monomers are tightly associated via hydrophobic interactions. The  $K_D$  value for the monomer–dimer equilibrium has been reported to be  $\leq 10^{-13}$  M at neutral pH (6). NGF, like other neurotrophins, contains a characteristic structure motif, the cystine knot. In NGF, two disulfide bridges connect the polypeptide backbone to a 14-amino acid loop that is penetrated by the third disulfide bridge (7–9).

In vivo, NGF is translated as a pre-pro-protein. The pre-sequence confers secretion and is cleaved upon translocation into the endoplasmic reticulum where disulfide bond formation occurs. The pro-peptide of NGF with 103 amino acids is nearly as large as the mature part with 118 residues. The

pro-peptide is known to promote correct maturation and secretion of NGF in vivo (10, 11). Moreover, we could demonstrate that the pro-peptide of NGF guides effective oxidative folding of the mature protein also in vitro (12, 13). Furthermore, we could show that the mature part stabilizes the pro-peptide (14). At low guanidinium hydrochloride (GdnHCl) concentrations, the pro-peptide unfolds fast and does not influence the unfolding of the mature NGF moiety (14).

Analysis of structure formation of mouse NGF (the sequence of which is 90% identical with that of human NGF examined here) by unfolding experiments revealed a rapid initial unfolding (15, 16). With longer incubation times under denaturing conditions, murine NGF exhibited a second slow unfolding reaction that resulted in the completely unfolded species (17). On the basis of these results, De Young et al. postulated the following sequential unfolding:



The model includes an initial loss of structure, which likely reflects the dissociation of the dimer and partial unfolding to monomer  $M_1$  followed by a slow subsequent complete unfolding to  $M_2$ . By NMR measurements, De Young et al. (17) analyzed  $M_1$  and concluded that no defined secondary structural elements were retained. However, according to this model,  $M_1$  still contains an intact cystine knot. The transition from  $M_1$  to  $M_2$  was proposed to involve a back-threading of the N-terminal sequence, in which Cys15 is in a disulfide linkage with Cys80, through the ring formed by the other

<sup>†</sup> This work was supported by Deutsche Forschungsgemeinschaft Grant SCHW 375/4 1-3 (E.S.) and the INTAS-2001 program (J.B.).

<sup>\*</sup> To whom correspondence should be addressed. E-mail: elisabeth.schwarz@biochemtech.uni-halle.de. Phone: +49 345 55 24 856. Fax: +49 345 55 27 013.

<sup>‡</sup> Institut für Biotechnologie der Martin-Luther-Universität Halle-Wittenberg.

<sup>§</sup> Arbeitsgruppe Biophysik der Martin-Luther-Universität Halle-Wittenberg.

<sup>1</sup> Abbreviations: NGF, nerve growth factor; HSQC, heteronuclear single-quantum correlation; RP-HPLC, reversed phase HPLC; GdnHCl, guanidinium hydrochloride.



3518 *Biochemistry*, Vol. 45, No. 11, 2006

Kliemann et al.

two disulfides (17, 18). Accordingly,  $M_2$  was assumed to represent an unfolded species in which the N-terminal sequence has slipped out of the ring (17). A gain in entropy was suggested as the driving force for threading. A rearrangement of disulfide bonds, as an alternative explanation for the slow conversion, was excluded since unfolding was independent of pH. The loop threading hypothesis was supported by the observation that NGF variants with truncated N-termini underwent the transition from  $M_1$  to  $M_2$  considerably faster (17). In proNGF, the mature part is preceded by the pro-peptide comprising 103 amino acids. Accordingly, threading through the ring should be significantly retarded in proNGF. Here, we compare the folding and unfolding of proNGF with that of mature NGF. Our results show that the N-terminal pro-peptide has no influence on the slow  $M_1$  to  $M_2$  conversion. Furthermore, NMR experiments revealed new insight into the structural differences between the  $M_1$  and  $M_2$  states. Taken together, our results suggest that the  $M_1$  and  $M_2$  states differ in the residual structure in the  $M_1$  state probably close to the cystine knot.

## MATERIALS AND METHODS

**Preparation of Recombinant Human proNGF and NGF.** Inclusion bodies of human proNGF were produced with pET11a in *Escherichia coli* BL21(DE3), and the fully folded protein was obtained as described previously (12). Mature NGF was obtained from proNGF by digestion with bovine pancreatic trypsin (Roche) (1:415 molar ratio). After a 30 min digestion in 50 mM Tris-HCl (pH 8.0) at 0 °C, trypsin and cleavage products were removed by ion exchange chromatography on a SP-Sepharose column (GE Healthcare) (12).

**NMR Spectroscopy.** For  $^{15}\text{N}$  labeling of *E. coli* BL21(DE3) cells containing recombinant cDNA for proNGF, cells were cultured in M9 medium with  $^{15}\text{NH}_4\text{Cl}$  as the sole nitrogen source. Proton spectra of 0.435 mM proNGF samples and 1 mM uniformly  $^{15}\text{N}$ -labeled NGF samples were acquired at 45 °C with a Bruker DRX 500 spectrometer. The residual water resonance in the  $\text{D}_2\text{O}$  samples of the unfolding buffer, containing 6 M GdnHCl and 50 mM sodium phosphate (pH 7.0), was presaturated during the relaxation delay. Due to the fast exchange of water and GdnHCl protons and thus the complete saturation transfer to the GdnHCl resonance at 45 °C, an additional suppression of the denaturant was not necessary. The concentration of GdnHCl was determined by refraction without correction for the isotopic effect of  $\text{D}_2\text{O}$ . Exchangeable protons of the buffer were removed by dissolving the sample in  $\text{D}_2\text{O}$  three times and subsequent lyophilization. Unfolding reactions were started by manually dissolving the lyophilized protein in the unfolding buffer. The unfolding kinetics of proNGF were measured in  $\text{D}_2\text{O}$  (6 M GdnDCl and 50 mM sodium phosphate, pD 7.0 pH-meter reading), recording 800 one-dimensional (1D)  $^1\text{H}$  spectra (64 scans each) over 19 h. Spectra were recorded over a spectral width of 13 ppm. A squared cosine window function was applied prior to Fourier transformation. The unfolding of  $^{15}\text{N}$ -NGF was followed via 28  $^1\text{H}$ - $^{15}\text{N}$  HSQC spectra over 24 h in 6 M GdnHCl (90%  $\text{H}_2\text{O}$ /10%  $\text{D}_2\text{O}$ ). The spectral widths for the HSQC spectra were 13 and 32 ppm for the  $^1\text{H}$  and  $^{15}\text{N}$  dimensions, respectively. Quadrature detection in the indirect dimension was achieved using the States-TPII method. The GdnHCl signal was suppressed

by a 1 s presaturation and the water signal by the WATERGATE pulse train of the FHSQC sequence (19).

Data were processed and analyzed using Felix. The 1D spectra depicted in Figure 4A are averages of 100 1D spectra. The spectrum of  $M_2$  was recorded after the unfolding reaction had reached completion. For the  $M_1$  state, the first 100 1D spectra during refolding were averaged. According to the unfolding kinetics, 75% of this average NMR intensity belongs to  $M_2$ . Therefore, after subtraction of these 75% using the plain  $M_2$  spectrum recorded after the unfolding reaction, the 1D spectrum of  $M_1$  could be derived. For more details about this deconvolution of 1D real-time NMR spectra, see refs 20 and 21. The two-dimensional (2D) HSQCs of  $M_1$  and  $M_2$  were derived by the similar approach using averages of five spectra.

For the kinetic studies, the high-field-shifted methyl groups of the proNGF 1D  $^1\text{H}$  spectra between 0.3 and 0.6 ppm were integrated and plotted against the unfolding time. For the analysis of the 2D HSQC, the intensities of the amide cross-peaks were followed. Kinetic analyses were performed using GraFit (Erithacus Software Ltd.).

**Reversed Phase High-Pressure Liquid Chromatography (RP-HPLC).** RP-HPLC was performed with a C4-RP-HPLC column (Vydac, C4, 5  $\mu\text{m}$ ; 4.6 mm  $\times$  250 mm; Hesperia) on a Gynkotek HPLC system (Dionex, Idstein, Germany). The samples were loaded after incubation at different temperatures and time points. The column was equilibrated in 6% buffer B [buffer A was 0.1% (v/v) TFA in water; buffer B was 80% (v/v) acetonitrile and 0.08% (v/v) TFA in water]. Samples were eluted with the following gradient: 6% B from 0 to 4 min, 6 to 30% B from 4 to 9 min, 30 to 69% B from 9 to 24 min, and 69 to 100% B from 24 to 25 min at a flow rate of 1 mL/min. Peak areas were calculated with Chromeleon version 4.32 (Dionex).

**Circular Dichroism (CD) Measurements.** Far-UV CD spectra were recorded on a Jasco J710 spectropolarimeter from 190 to 260 nm with a 1 nm light path. Measurements were performed in 50 mM sodium phosphate (pH 7.0) at 20 °C. Spectra were buffer corrected, and ellipticities related to the mean residue weight of amino acid residues were calculated according to the method described in ref 22.

**Fluorescence Measurements.** Measurements were carried out with a FluoroMax-2 fluorescence spectrometer (Jobin-Yvon-Spex). Slit widths for both excitation and emission wavelengths were 5 nm. Experiments were performed in 50 mM sodium phosphate (pH 7.0) and 1 mM EDTA at 20 °C in 1 cm cuvettes. For emission spectra, excitation was at 280 nm. Spectra were collected from 300 to 400 nm. Kinetics were recorded upon excitation at 280 nm and by monitoring emission at 325 nm in 1 cm cuvettes with stirring.

**Refolding of ProNGF from the  $M_2$  State.** Fully unfolded proNGF (6 M GdnHCl at 45 °C over 4 days) was refolded by pulse renaturation in 50 mM sodium phosphate (pH 7.0) and 1 mM EDTA. The protein concentration of each pulse was 200  $\mu\text{g}/\text{mL}$ . ProNGF was refolded in five pulses over 120 h, and the final residual concentration of GdnHCl was 0.2 M.

**Gel Filtration.** For separation of dimeric species from monomeric species, size exclusion chromatography was performed on a Superdex75 10/300 column with the ÄKTA explorer system (Amersham Bioscience) at a flow rate of 0.5

## Slow Unfolding of ProNGF

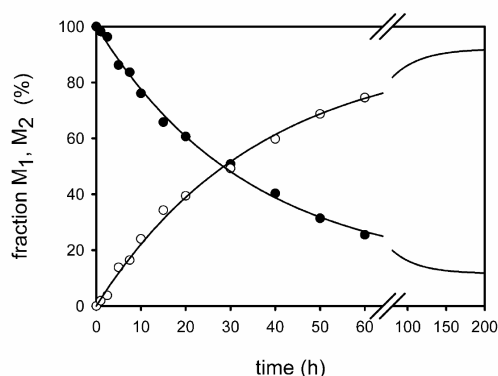


FIGURE 1: Unfolding kinetics of NGF. NGF (300  $\mu\text{g}/\text{mL}$ ) was incubated in 6 M GdnHCl, 50 mM sodium phosphate (pH 7.0), and 1 mM EDTA at 25  $^{\circ}\text{C}$ . At different time points, 30  $\mu\text{g}$  of protein was loaded on a C4-RP-HPLC column: (●) proNGF in the  $M_1$  state and (○) NGF in the  $M_2$  state. Rate constants were calculated by integration of peak areas and by assuming a first-order reaction ( $k = 0.029 \text{ h}^{-1}$ ).

mL/min. The mobile phase consisted of 0.33 M L-arginine, 50 mM sodium phosphate (pH 7.0), and 1 mM EDTA.

## RESULTS AND DISCUSSION

*Influence of the Pro-Peptide on the Unfolding Kinetics of the Mature Domain.* The kinetics of NGF unfolding upon denaturation with GdnHCl were studied in detail by De Young et al. (17, 18). The authors separated the partially unfolded monomeric species,  $M_1$ , from the fully denatured species,  $M_2$ , that eluted at higher acetonitrile concentrations than  $M_1$  on a C4-RP-HPLC column. As performed by De Young et al., conversion of  $M_1$  to  $M_2$  during RP-HPLC analysis can be excluded, since rechromatography of the  $M_1$  and  $M_2$  species via RP-HPLC did not result in changes in the elution properties of either species (data not shown). The results of De Young et al. could be confirmed in our lab by identical analyses. The rate constant ( $k$ ) for the  $M_1$  to  $M_2$  transition equaled  $0.029 \text{ h}^{-1}$  and was thus very similar to that determined by De Young et al. ( $0.03 \text{ h}^{-1}$ ) (Figure 1).

The loop threading hypothesis is supported by the observation that rate constants of dimer loss increased with longer deletions of N-terminal segments in mutant variants of NGF (17). Accordingly, N-terminal extensions of NGF should lead to severely retarded conversions of  $M_1$  to  $M_2$ . To this end, unfolding kinetics of proNGF, in which the mature part is preceded by the 103-residue pro-peptide, were measured. Experimental conditions were identical to those in the studies with mature NGF. GdnHCl-induced unfolding of native proNGF to  $M_1$ , which is supposed to be coupled with the dissociation of the dimer, was monitored by fluorescence. At 20  $^{\circ}\text{C}$ , the fast unfolding reaction (N to  $M_1$ ) was complete after 2 min (Figure 2A). Conversion of  $M_1$  to  $M_2$  was monitored by RP-HPLC. Due to the fast unfolding of the pro-peptide, which is already at low GdnHCl concentrations in the millisecond range (data not shown), an influence of any residual structure(s) in the pro-peptide on the transition of  $M_1$  to  $M_2$  could be excluded.

In proNGF, conversion of  $M_1$  to  $M_2$  occurred with a rate constant  $k$  of  $0.024 \text{ h}^{-1}$  (Figure 2B). The rate of conversion

## Biochemistry, Vol. 45, No. 11, 2006 3519

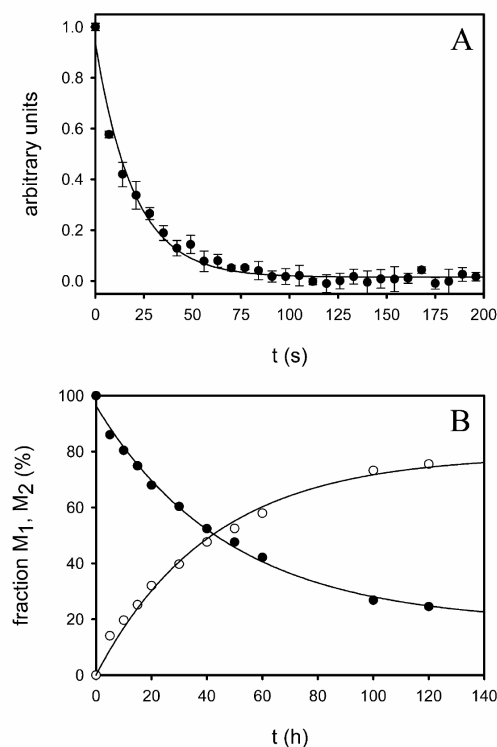


FIGURE 2: (A) Unfolding kinetics of proNGF from the native to the  $M_1$  state. ProNGF (20  $\mu\text{g}/\text{mL}$ ) was incubated in 6 M GdnHCl, 50 mM sodium phosphate (pH 7.0), and 1 mM EDTA. The fluorescence was measured at 20  $^{\circ}\text{C}$  at 325 nm upon excitation at 280 nm. The decay of the signal was fitted to a first-order reaction ( $k = 0.04 \text{ s}^{-1}$ ). (B) Unfolding kinetics of proNGF from the  $M_1$  state to the  $M_2$  state. ProNGF (10  $\mu\text{g}$ ) was incubated in 6 M GdnHCl, 50 mM sodium phosphate (pH 7.0), and 1 mM EDTA. After different incubation intervals, samples were loaded onto a C4-RP-HPLC column: (●) proNGF in the  $M_1$  state and (○) proNGF in the  $M_2$  state. Rate constants were calculated by integration of peak areas and by subsequently assuming a first-order reaction ( $k = 0.024 \text{ h}^{-1}$ ).

was independent of the pH (data not shown), excluding the possibility of disulfide rearrangements. The determined rate constant is very close to that of the corresponding reaction of mature NGF ( $k = 0.029 \text{ h}^{-1}$ ). Thus, it is unlikely that the slow unfolding reaction that is observed in both NGF and proNGF is caused by a loop threading mechanism since in the case of proNGF considerably longer unfolding rates for the threading of the 103-amino acid pro-peptide would be expected.

*Temperature-Dependent Unfolding of ProNGF.* Proline isomerizations with activation energies of 75–91 kJ/mol (23) are known to cause slow unfolding reactions. However, a higher energy barrier of 108–112 kJ/mol was calculated from temperature-dependent conversion of  $M_1$  to  $M_2$  in NGF by De Young et al. (17). On the basis of these results, the authors excluded proline isomerization(s) as a reason for the slow unfolding. To characterize the activation energies of proNGF unfolding, rate constants were determined at various temperatures (Figure 3A and Table 1). For the slow  $M_1$  to  $M_2$  transition, an activation enthalpy ( $\Delta H^{\ddagger}$ ) of  $88.8 \pm 5.3 \text{ kJ/mol}$  and an entropy ( $\Delta S^{\ddagger}$ ) of  $20.5 \pm 2.0 \text{ J mol}^{-1} \text{ K}^{-1}$ , resulting in a  $\Delta G^{\ddagger}$  of  $82.8 \pm 6.6 \text{ kJ/mol}$  at 20  $^{\circ}\text{C}$ , were calculated (Figure 3B). This considerably smaller  $\Delta G^{\ddagger}$  value,

3520 *Biochemistry*, Vol. 45, No. 11, 2006

Kliemann et al.

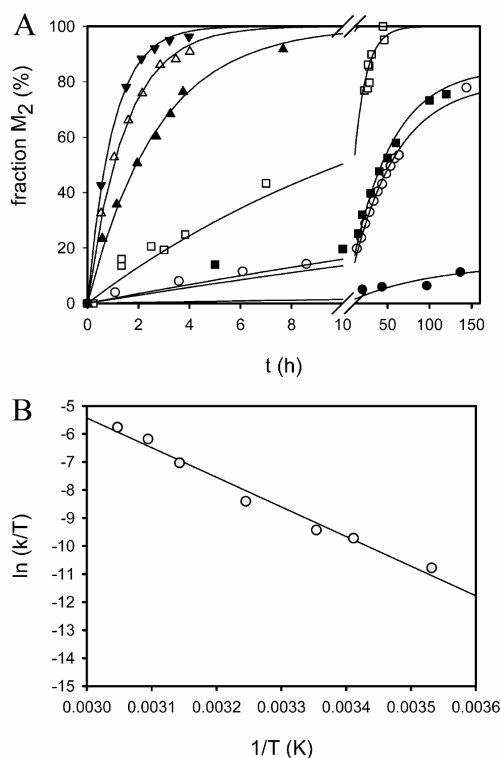


FIGURE 3: (A) Temperature dependence of the  $M_1$  to  $M_2$  transition of proNGF. Protein ( $10 \mu\text{g/mL}$ ) was incubated in 6 M GdnHCl, 50 mM sodium phosphate (pH 7.0), and 1 mM EDTA: (●) 10, (○) 20, (■) 25, (□) 35, (▲) 45, (△) 50, and (▼) 55 °C. Resulting rate constants (Table 1) were derived by a first-order reaction. (B) Arrhenius plot of the rate constants.

Table 1: Temperature Dependence of the Apparent First-Order Rate Constants for the Conversion of  $M_1$  to  $M_2$

temp (°C)	$k_{\text{obs}}$ ( $\text{h}^{-1}$ )	temp (°C)	$k_{\text{obs}}$ ( $\text{h}^{-1}$ )
10	$0.0053 \pm 0.001$	45	$0.28 \pm 0.025$
20	$0.0176 \pm 0.004$	50	$0.67 \pm 0.037$
25	$0.024 \pm 0.0018$	55	$1.03 \pm 0.015$
35	$0.069 \pm 0.008$		

compared to that determined by De Young et al., corresponds to the observed activation energies of proline isomerizations. A possible influence of the pro-peptide on the  $\Delta G^\ddagger$  of the mature part is very unlikely, since a small stabilization energy ( $\Delta G^0$ ) of  $-7.8 \text{ kJ/mol}$  for the pro-peptide had been determined previously (14). Thus, proline isomerization(s) accounting for the slow unfolding can presently not be excluded on the basis of the thermodynamic results.

*1D NMR Studies of ProNGF in the  $M_1$  State and the Transition to  $M_2$ .* For a more detailed investigation of the  $M_1$  state of proNGF in terms of residual structure, a time-resolved 1D NMR experiment was performed (24). Unfolding at 45 °C was induced by dissolving a lyophilized sample of proNGF to a final protein concentration of 1 mM in  $\text{D}_2\text{O}$  containing 6 M GdnDCI. During the dead time of  $\sim 15$  min for this experiment, native species were no longer populated. Each of the 800 1D NMR spectra, recorded after the unfolding reactions had been started, contained a superposition of the  $M_1$  and  $M_2$  state. Deconvolution of this real-time NMR data set as described previously (20, 21) revealed the

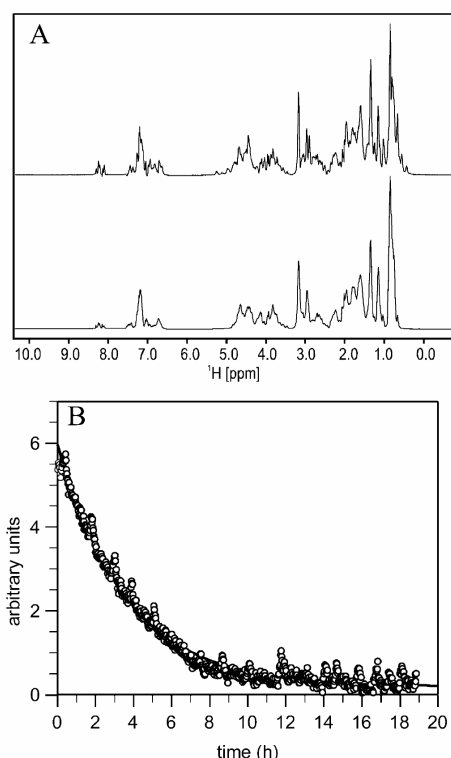


FIGURE 4: (A) 1D NMR spectra of proNGF in the  $M_1$  state (top) and the  $M_2$  state (bottom) at 45 °C in 6 M GdnDCI and 50 mM sodium phosphate (pD 7) in 100%  $\text{D}_2\text{O}$ . The top spectrum of the kinetic intermediate was derived from deconvoluting the 1D real-time NMR data according to the unfolding kinetics. (B) Decrease in the NMR integral of the high-field-shifted methyl groups between 0.3 and 0.6 ppm upon unfolding in 6 M GdnDCI. The solid line represents a fit of a single-exponential function to the NMR intensity resulting in a rate constant of  $0.28 \pm 0.01 \text{ h}^{-1}$  at 45 °C.

1D spectrum of  $M_1$  (Figure 4A, top spectrum) and  $M_2$  (Figure 4A, bottom spectrum). The 1D NMR spectrum of  $M_2$  shows the characteristic dispersion of a completely unfolded polypeptide chain without secondary or tertiary interactions. In contrast, the 1D spectrum of the  $M_1$  state revealed some high-field-shifted side chain resonances below 0.7 ppm and several low-field-shifted  $\text{H}^\alpha$  resonances between 4.8 and 5.2 ppm, which are indicative of residual structure. The resonances of nonexchangeable protons from the 26 aromatic side chains are located between 6.5 and 7.5 ppm, and those of the  $\text{H}^{\epsilon 1}$  protons of the nine histidine residues were between 8.0 and 8.5 ppm. These resonances have a low dispersion in both the  $M_1$  and  $M_2$  states, indicating an unfolded conformation. All 26 aromatic residues are well distributed along the primary sequence, and only Tyr79 is close to the cystine knot in the three-dimensional structure (8). Therefore, it is likely that only a local residual structure is preserved around the cystine knot in  $M_1$ , which cannot be unambiguously resolved by 1D NMR spectroscopy.

The high-field-shifted NMR signals were used to determine the unfolding kinetics for the transition from the  $M_1$  state to the  $M_2$  state. A single-exponential function has been fitted to the decay of the integral between 0.3 and 0.6 ppm during the 19 h monitoring as depicted in Figure 4B. The unfolding rate constant ( $k$ ) of  $0.28 \pm 0.01 \text{ h}^{-1}$  at 45 °C in  $\text{D}_2\text{O}$  at NMR concentration is identical to the rate

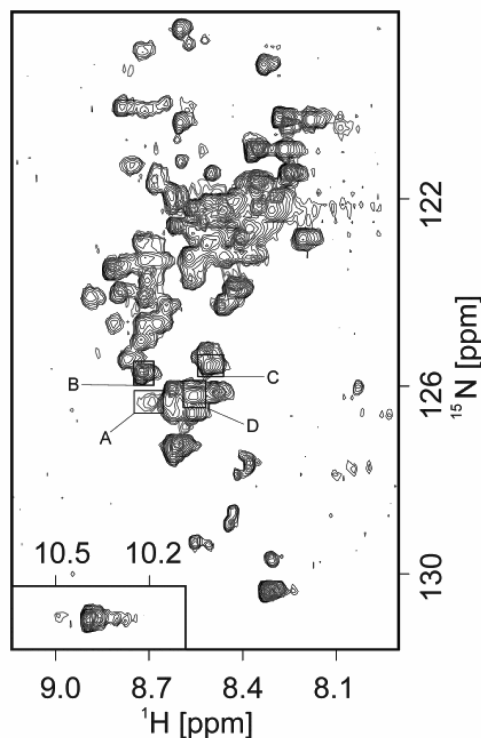


FIGURE 5:  $^1\text{H}$ - $^{15}\text{N}$  HSQC spectra of uniformly  $^{15}\text{N}$ -labeled NGF in 6 M GdnHCl at 45 °C. The spectrum of completely unfolded NGF ( $M_2$  state) is colored black, and the spectrum of the intermediate  $M_1$  state derived after deconvolution of the 2D real-time NMR experiment is colored red. Cross-peaks, for which a kinetic analysis is provided in Figure 6, are denoted with boxes (A–D). The inset shows the horizontally shifted side chain resonances of Trp.

constant observed by the HPLC approach at 45 °C ( $0.28 \text{ h}^{-1}$ ) (Figure 3A).

**2D NMR Studies for the  $M_1$  State and the Transition to  $M_2$  of NGF.** Unfolding of mature NGF has been studied by 1D real-time NMR (17). To increase the resolution of the NMR spectra, unfolding of uniformly labeled  $^{15}\text{N}$ -NGF at 45 °C in 6 M GdnHCl was monitored by a set of 28 2D  $^1\text{H}$ - $^{15}\text{N}$  HSQC spectra over 24 h. These 2D spectra again contained cross-peaks of the  $M_1$  and  $M_2$  states, which could be deconvoluted via unfolding kinetics (20, 21). The result is plotted in Figure 5. Black contours represent the cross-peaks of  $M_2$ , which is simply the last 2D spectrum recorded after completion of the unfolding reaction. Red resonances result from the amides of the  $M_1$  state. The cross-peaks around 10 ppm originate from the  $\text{H}^{\epsilon 1}$  protons of the three tryptophan side chains of NGF (inset of Figure 5). Their chemical shifts and intensities match exactly those of the reported 1D spectrum of the  $M_1$  and  $M_2$  states (17), confirming the reproducibility of these real-time NMR experiments.

The most prominent cross-peaks of the backbone and side chain amides of  $M_1$  (red in Figure 5) are located at chemical shifts, where  $M_2$  shows resonances as well. The few exceptions are the already mentioned  $\text{H}^{\epsilon 1}$  proton of three tryptophan side chains, the cross-peak marked by box A in Figure 5, and some side chain resonances between 120 and 122 ppm. They indicate not completely unfolded regions in

$M_1$ . All other observable signals of  $M_1$  originate from completely unfolded stretches of the polypeptide chain. These signals exhibited constant intensities during the entire unfolding experiment. One representative time course is shown in Figure 6B for the resonance indicated by box B in Figure 5. The striking observation was that at least 50% of the backbone amide cross-peaks in the 2D HSQC spectrum of  $M_1$  were missing probably due to chemical exchange broadening. The appearance of the 2D HSQC spectra of NGF resembles closely that of spectra of other folding intermediates such as the molten globule of  $\alpha$ -lactalbumin. In this case, both for the pH 2 state at equilibrium and for the kinetic molten globule under refolding conditions, the majority of cross-peaks were missing (25, 26). A molten globule-like structure of  $M_1$ , however, is unlikely since, for example, the far-UV CD spectra of  $M_1$  and  $M_2$  are superimposable (data not shown).

The time dependence of the intensities of those cross-peaks of  $M_2$ , which do not overlap with resonances of  $M_1$ , revealed uniform unfolding rates. Seventeen signals could be analyzed with an average unfolding rate  $k$  of  $0.28 \pm 0.03 \text{ h}^{-1}$ . Two of these kinetics are shown in panels C and D of Figure 6. They were derived from cross-peaks marked by boxes C and D in Figure 5. The decay of  $M_1$  (Figure 6A) could be monitored by the signal in box A, giving a rate constant  $k$  of  $0.29 \pm 0.05 \text{ h}^{-1}$ . These coinciding rate constants monitored by reporters of the  $M_1$  and  $M_2$  state indicate that no further, detectable kinetic intermediate is populated during the  $M_1$  to  $M_2$  transition.

**Characterization of the Structural Differences of the  $M_1$  and  $M_2$  States.** Three experimental observations verify structural differences between  $M_1$  and  $M_2$ . First, both states can be separated by RP-HPLC. Second, differences in the dispersion of the  $^1\text{H}$  resonances in the 1D spectra exist. Third, missing cross-peaks in the 2D HSQC spectrum of  $M_2$  were observed. However, far-UV CD spectroscopy of the two states revealed no differences in the secondary structure level (data not shown). To gain further insight into the structural differences between the two states, the kinetics of reduction of  $M_1$  and  $M_2$  species were monitored by RP-HPLC (Figure 7). Reduction with 100 mM DTT was 30 times faster with  $M_2$  than with  $M_1$ , pointing to a better accessibility of the disulfides in  $M_2$ . Accordingly, the residual structure in the  $M_1$  species is most likely close to the cystine knot, preventing fast reduction even in 6 M GdnHCl. We suggest that the integrity of this residual structure in  $M_1$  presents a nucleation structure enabling the much faster and more complete refolding from  $M_1$  than from  $M_2$  in both mature mouse NGF (16) and human proNGF (data not shown).

**Renaturation of ProNGF from the  $M_2$  State.** If  $M_2$  species would represent species in which the N-terminus had threaded out of the cystine knot, the reverse reaction, i.e., refolding of proNGF, would be inhibited. Therefore, we analyzed the time-dependent renaturation of proNGF starting from the  $M_2$  state. For quantification of refolding kinetics from  $M_2$ , the fully denatured protein was refolded by dialysis against refolding buffer. However, refolding of proNGF at high protein concentrations ( $> 60 \mu\text{M}$ ) was accompanied by aggregation. Thus, to suppress aggregation, refolding was initiated by rapid dilution of small amounts of denatured protein into refolding buffer to final concentrations of approximately  $8 \mu\text{M}$ . Refolding was monitored by RP-HPLC,

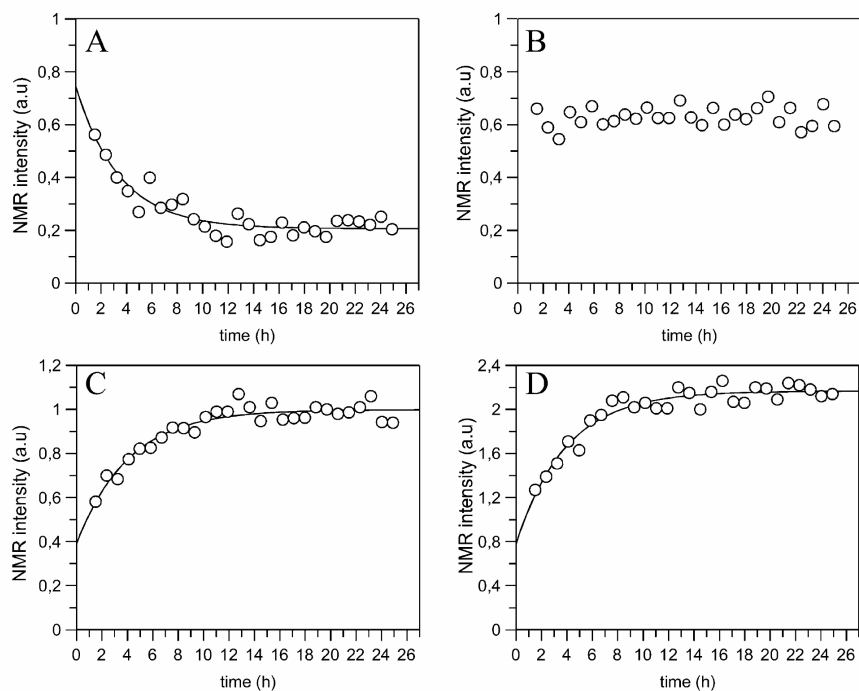


FIGURE 6: Time-dependent intensities of the four cross-peaks indicated in the 2D HSQC spectra of NGF recorded during the unfolding reaction. Single-exponential fits are given as solid lines. (A) Decay of the  $M_1$  state with a rate constant of  $0.29 \pm 0.05 \text{ h}^{-1}$ . (B) Invariant NMR intensity with unfolding time. (C and D) Increase in the level of of the  $M_2$  state with rate constants of  $0.27 \pm 0.03$  and  $0.26 \pm 0.04 \text{ h}^{-1}$ , respectively.

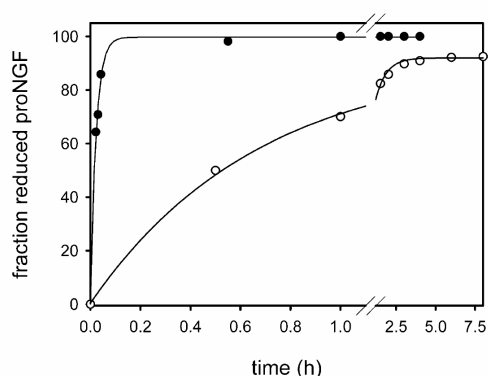


FIGURE 7: Kinetics of reduction of proNGF in the  $M_1$  (○) and  $M_2$  state (●) in 100 mM DTT, 6 M GdnHCl, 50 mM sodium phosphate, and 1 mM EDTA (pH 7.0) at 20 °C. Quantification of  $M_1$ ,  $M_2$ , and the reduced species was performed as described in Materials and Methods by RP-HPLC.

a method that allows differentiation between only  $M_2$  and  $M_1$ , since under the HPLC buffer conditions native protein is immediately converted to  $M_1$  (17). However, since  $M_1$  is in rapid equilibrium with native species, the technique is suitable for monitoring refolding from  $M_2$  (17) (Figure 8A).

With a prolonged incubation under refolding conditions, the peak area representing  $M_2$  gradually decreased (Figure 8A). Concomitantly, the earlier eluting peak representing  $M_1$  species increased. From the peak areas, the ratios of the two folding species were calculated. The decrease in the amount of  $M_2$  and the increase in the amount of refolded species were analyzed as a first-order reaction (Figure 8B). A rate constant  $k$  of  $0.083 \text{ h}^{-1}$  was determined. The yield of conversion was 75%. The sum of both peaks correlated with

the total protein concentration, indicating that no aggregation had taken place during the refolding reaction.

To confirm that natively folded protein had been obtained, the refolded species were analyzed by fluorescence, far-UV CD spectroscopy, and analytical ultracentrifugation. All analyses revealed inhomogeneous protein populations (data not shown). Hence, it was necessary to further purify the native species. Since only a dimeric species is supposed to represent the correctly folded conformation, purification was based on the separation of the dimeric species from monomeric species by size exclusion chromatography (6, 16). The far-UV CD spectrum of the purified dimeric protein was almost superimposable with that of native proNGF (Figure 9A). Furthermore, the fluorescence spectra of the refolded protein and the reference, native proNGF, were nearly identical (Figure 9B). These results demonstrate that proNGF refolded from  $M_2$  contains the same secondary and tertiary structure elements as the starting material. Further analysis by analytical ultracentrifugation demonstrated the dimeric state (data not shown) as already shown for native proNGF (12).

For quantification of the refolding yields, peak areas of the dimeric species obtained by SEC were calculated. A total yield of ca. 30% native proNGF was determined (data not shown). A refolding yield of 30% did not correlate with that determined by RP-HPLC (peak areas representing  $M_1$ ) (75%) (Figure 9B). This indicates that the  $M_1$  peak also contains besides native proNGF unproductive folding intermediates, which resemble under RP-HPLC conditions the  $M_1$  state. Native proNGF obtained upon refolding of  $M_2$  was additionally analyzed by unfolding kinetics. Here, the refolded protein without subsequent purification was tested. Unfolding was

## Slow Unfolding of ProNGF

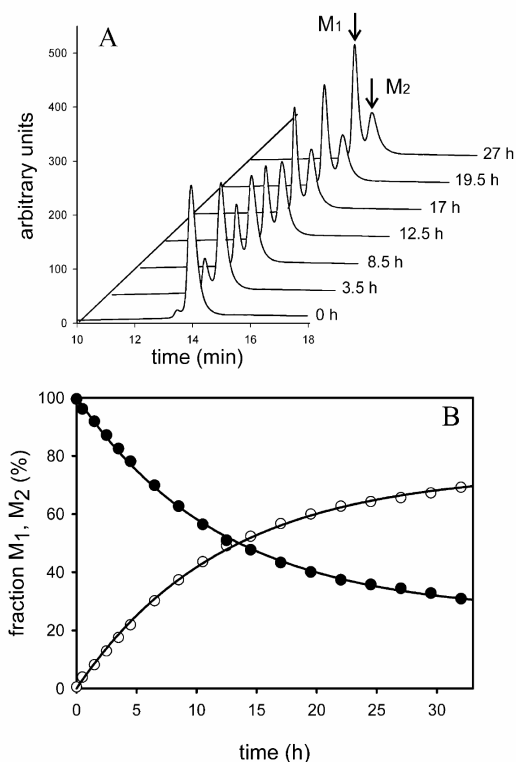


FIGURE 8: Refolding of proNGF from the  $M_2$  state. Refolding was performed at a concentration of  $200 \mu\text{g/mL}$  in  $50 \text{ mM}$  sodium phosphate ( $\text{pH } 7.0$ ) and  $1 \text{ mM}$  EDTA at  $20^\circ\text{C}$  (residual GdnHCl concentration of  $35 \text{ mM}$ ). At different time points, aliquots were withdrawn and analyzed by RP-HPLC. (A) RP-HPLC chromatograms during refolding of proNGF from the  $M_2$  state. (B) Refolding kinetics monitored by RP-HPLC. Peak areas of  $M_1$  ( $\circ$ ) and  $M_2$  ( $\bullet$ ) were fitted to a first-order reaction ( $k = 0.083 \text{ h}^{-1}$ ).

induced by chemical denaturation with GdnHCl and monitored by fluorescence spectroscopy. The same unfolding rate constant was observed as with the reference, but only ca. 30% of the expected amplitude, a finding that corresponded well with the renaturation yield of 30% determined before by gel filtration.

NGF contains three proline residues: Pro5, Pro61, and Pro63. The crystal structure of Pro5 shows a trans conformation (8). The states of Pro61 and Pro63 are located in the loop region of the cystine knot, which is not resolved in cocrystallizations of NGF with either TrkA or p75 (8, 9). The crystal structure of mouse NGF, which contains one conserved proline residue in the cystine knot, reveals that this prolyl bond is also in the trans conformation (7). To test whether slow unfolding may reflect cis–trans isomerization(s) of one or more proline residues, several well-known proline isomerases, cyclophilin 12, FKPB 18, and SlyD, were tested for their ability to accelerate the refolding rate. None of the isomerases resulted in an acceleration of the refolding reaction of proNGF (data not shown). Nevertheless, proline isomerization(s) as a reason for the very slow refolding kinetics cannot be fully ruled out since the accessibility of the isomerases to the proline residues may be sterically hindered.

Several lines of evidence have been collected in this work that argue against a loop threading mechanism that has been postulated to underlie the slow unfolding of NGF. First, the

## Biochemistry, Vol. 45, No. 11, 2006 3523

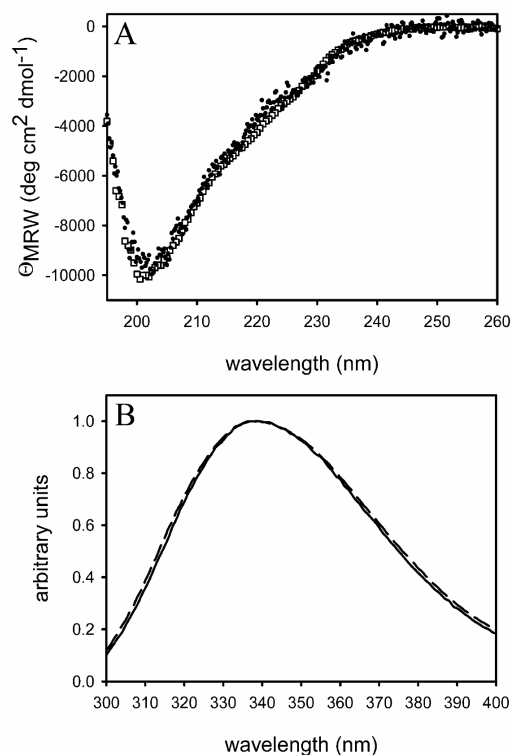


FIGURE 9: (A) Far-UV CD spectra of proNGF ( $0.55 \text{ mg/mL}$ ) in  $50 \text{ mM}$  sodium phosphate ( $\text{pH } 7.0$ ) in a  $0.5 \text{ mm}$  cuvette at  $20^\circ\text{C}$ : ( $\square$ )  $M_2$ -refolded proNGF and ( $\bullet$ ) native proNGF. (B) Fluorescence spectra ( $10 \mu\text{g/mL}$ ) in  $50 \text{ mM}$  sodium phosphate ( $\text{pH } 7.0$ ) and  $1 \text{ mM}$  EDTA upon excitation at  $280 \text{ nm}$ : (—)  $M_2$ -refolded proNGF and (---) native proNGF.

pro-peptide of NGF does not significantly retard the transition from  $M_1$  to  $M_2$ . A retarded unfolding would have been expected if loop threading were occurring since then the longer N-terminal sequence would require more time to slip through the ring. Second, the  $M_2$  state of proNGF can be refolded to the native form. Refolding to the native conformation with a yield of 30% cannot be reconciled with loop threading, since the N-terminal sequence would first have to find the ring and then have to pass through it. Third, NMR analyses showed in the  $M_1$  state residual structures. Loop threading would predict that  $M_1$  and  $M_2$  differ only by a not yet slipped N-terminal sequence through the cystine knot of the fully unfolded polypeptide chain. Therefore, the NMR spectra of both NGF and proNGF in the  $M_2$  and  $M_1$  states should be almost identical, which was not the case. Fourth, the residual structure in  $M_1$  which is most likely located close to the cystine knot is probably responsible for the slow unfolding.

Recently, an unfolding intermediate possibly similar to  $M_1$  was described for FGF-1 from newt (nFGF), an all- $\beta$ -sheet growth factor devoid of disulfide bonds (27). Renaturation from the intermediate state was almost fully reversible. Prolonged incubation under denaturing conditions led eventually to complete unfolding because renaturation from this second state was incomplete. The authors interpreted the slow unfolding as a final rearrangement of a hydrophobic core. This description of another slow unfolding protein lacking disulfide bridges and the results presented here render a loop threading mechanism very unlikely. Rather, evidence that

3524 *Biochemistry*, Vol. 45, No. 11, 2006

Kliemann et al.

NGF and proNGF may unfold via a partially structured intermediate was collected. Since neurotrophins share a high degree of sequence and structure homology, presumably, loop threading may not underlie the slow unfolding of the other members of this family.

#### ACKNOWLEDGMENT

We thank Gunter Fischer, Christian Lücke, and Monika Seidel at the Max-Planck research unit for enzymology of protein folding for the NMR time and assistance. We thank Hauke Lilie for helpful suggestions.

#### REFERENCES

- Levi-Montalcini, R. (1987) The nerve growth factor 35 years later, *Science* 237, 1154–1162.
- Hefti, F. (1994) Neurotrophic factor therapy for nervous system degenerative diseases, *J. Neurobiol.* 25, 1418–1435.
- Casaccia-Bonnel, P., Carter, B. D., Dobrowsky, R. T., and Chao, M. V. (1996) Death of oligodendrocytes mediated by the interaction of nerve growth factor with its receptor p75, *Nature* 383, 716–719.
- Frade, J. M., Rodriguez-Tebar, A., and Barde, Y. A. (1996) Induction of cell death by endogenous nerve growth factor through its p75 receptor, *Nature* 383, 166–168.
- Nykjaer, A., Lee, R., Teng, K. K., Jansen, P., Madsen, P., Nielsen, M. S., Jacobsen, C., Kliemann, M., Schwarz, E., Willnow, T. E., Hempstead, B. L., and Petersen, C. M. (2004) Sortilin is essential for proNGF-induced neuronal cell death, *Nature* 427, 843–848.
- Bothwell, M. A., and Shooter, E. M. (1977) Dissociation equilibrium constant of  $\beta$  nerve growth factor, *J. Biol. Chem.* 252, 8532–8536.
- McDonald, N. Q., Lapatto, R., Murray-Rust, J., Gunning, J., Wlodawer, A., and Blundell, T. L. (1991) New protein fold revealed by a 2.3-Å resolution crystal structure of nerve growth factor, *Nature* 354, 411–414.
- Wiesmann, C., Ultsch, M. H., Bass, S. H., and de Vos, A. M. (1999) Crystal structure of nerve growth factor in complex with the ligand-binding domain of the TrkA receptor, *Nature* 401, 184–188.
- He, X. L., and Garcia, K. C. (2004) Structure of nerve growth factor complexed with the shared neurotrophin receptor p75, *Science* 304, 870–875.
- Suter, U., Heymach, J. V., Jr., and Shooter, E. M. (1991) Two conserved domains in the NGF propeptide are necessary and sufficient for the biosynthesis of correctly processed and biologically active NGF, *EMBO J.* 10, 2395–2400.
- Seidah, N. G., Benjannet, S., Pareek, S., Savaria, D., Hamelin, J., Goulet, B., Laliberte, J., Lazure, C., Chretien, M., and Murphy, R. A. (1996) Cellular processing of the nerve growth factor precursor by the mammalian pro-protein convertases, *Biochem. J.* 314, 951–960.
- Rattenholl, A., Lilie, H., Grossmann, A., Stern, A., Schwarz, E., and Rudolph, R. (2001) The pro-sequence facilitates folding of human nerve growth factor from *Escherichia coli* inclusion bodies, *Eur. J. Biochem.* 268, 3296–3303.
- Rattenholl, A., Ruoppolo, M., Flagiello, A., Monti, M., Vinci, F., Marino, G., Lilie, H., Schwarz, E., and Rudolph, R. (2001) Pro-sequence assisted folding and disulfide bond formation of human nerve growth factor, *J. Mol. Biol.* 305, 523–533.
- Kliemann, M., Rattenholl, A., Golbik, R., Balbach, J., Lilie, H., Rudolph, R., and Schwarz, E. (2004) The mature part of proNGF induces the structure of its pro-peptide, *FEBS Lett.* 566, 207–212.
- Ullrich, A., Gray, A., Berman, C., and Dull, T. J. (1983) Human  $\beta$ -nerve growth factor gene sequence highly homologous to that of mouse, *Nature* 303, 821–825.
- Timm, D. E., and Neet, K. E. (1992) Equilibrium denaturation studies of mouse  $\beta$ -nerve growth factor, *Protein Sci.* 1, 236–244.
- De Young, L. R., Burton, L. E., Liu, J., Powell, M. F., Schmelzer, C. H., and Skelton, N. J. (1996) RhNGF slow unfolding is not due to proline isomerization: Possibility of a cystine knot loop-threading mechanism, *Protein Sci.* 5, 1554–1566.
- De Young, L. R., Schmelzer, C. H., and Burton, L. E. (1999) A common mechanism for recombinant human NGF, BDNF, NT-3, and murine NGF slow unfolding, *Protein Sci.* 8, 2513–2518.
- Mori, S., Abeygunawardana, C., Johnson, M. O., and van Zyl, P. C. (1995) Improved sensitivity of HSQC spectra of exchanging protons at short interscan delays using a new fast HSQC (FHSQC) detection scheme that avoids water saturation, *J. Magn. Reson., Ser. B* 108, 94–98.
- Balbach, J., Steegborn, C., Schindler, T., and Schmid, F. X. (1999) A protein folding intermediate of ribonuclease T1 characterized at high resolution by 1D and 2D real-time NMR spectroscopy, *J. Mol. Biol.* 285, 829–842.
- Zeeb, M., Rosner, H., Zeslawski, W., Canet, D., Holak, T. A., and Balbach, J. (2002) Protein folding and stability of human CDK inhibitor p19<sup>INK4d</sup>, *J. Mol. Biol.* 315, 447–457.
- Schmid, F. X. (1997) Spectral methods of characterizing protein conformation and conformational changes, in *Protein structure: A practical approach* (Creighton, T. E., Ed.) 1st ed., pp 251–286, IRL-Press, Oxford University Press, Oxford, U.K.
- Schmid, F. X., and Baldwin, R. L. (1979) The rate of interconversion between the two unfolded forms of ribonuclease A does not depend on guanidinium chloride concentration, *J. Mol. Biol.* 133, 285–287.
- Balbach, J., Forge, V., van Nuland, N. A., Winder, S. L., Hore, P. J., and Dobson, C. M. (1995) Following protein folding in real time using NMR spectroscopy, *Nat. Struct. Biol.* 2, 865–870.
- Balbach, J., Forge, V., Lau, W. S., van Nuland, N. A., Brew, K., and Dobson, C. M. (1996) Protein folding monitored at individual residues during a two-dimensional NMR experiment, *Science* 274, 1161–1163.
- Schulman, B. A., Kim, P. S., Dobson, C. M., and Redfield, C. (1997) A residue-specific NMR view of the non-cooperative unfolding of a molten globule, *Nat. Struct. Biol.* 4, 630–634.
- Kathir, K. M., Kumar, T. K., Rajalingam, D., and Yu, C. (2005) Time-dependent changes in the denatured state(s) influence the folding mechanism of an all  $\beta$ -sheet protein, *J. Biol. Chem.* 280, 29682–29688.

BI051896T

## The mature part of proNGF induces the structure of its pro-peptide

Marco Kliemannel<sup>a</sup>, Anke Rattenholl<sup>a,1</sup>, Ralph Golbik<sup>b</sup>, Jochen Balbach<sup>c</sup>, Hauke Lilie<sup>a</sup>,  
Rainer Rudolph<sup>a</sup>, Elisabeth Schwarz<sup>a,\*</sup>

<sup>a</sup>Institut für Biotechnologie, Martin-Luther-Universität Halle-Wittenberg, Kurt-Mothes-Strasse 3, 06120 Halle, Germany

<sup>b</sup>Institut für Biochemie, Martin-Luther-Universität Halle-Wittenberg, Kurt-Mothes-Strasse 3, 06120 Halle, Germany

<sup>c</sup>Laboratorium für Biochemie III, Universität Bayreuth, 95440 Bayreuth, Germany

Received 15 March 2004; revised 14 April 2004; accepted 14 April 2004

Available online 28 April 2004

Edited by Thomas L. James

**Abstract** Human nerve growth factor (NGF) belongs to the structural family of cystine knot proteins, characterized by a disulfide pattern in which one disulfide bond threads through a ring formed by a pair of two other disulfides connecting two adjacent  $\beta$ -strands. Oxidative folding of NGF revealed that the pro-peptide of NGF stimulates *in vitro* structure formation. In order to learn more about this folding assisting protein fragment, a biophysical analysis of the pro-peptide structure has been performed. While proNGF is a non-covalent homodimer, the isolated pro-peptide is monomeric. No tertiary contacts stabilize the pro-peptide in its isolated form. In contrast, the pro-peptide appears to be structured when bound to the mature part. The results presented here demonstrate that the mature part stabilizes the structure in the pro-peptide region. This is the first report that provides a biophysical analysis of a pro-peptide of the cystine knot protein family.

© 2004 Federation of European Biochemical Societies. Published by Elsevier B.V. All rights reserved.

**Keywords:** Cystine knot proteins; Oxidative folding; Pro-peptide stimulated folding; NGF

### 1. Introduction

Human nerve growth factor (NGF) belongs to the neurotrophin family, whose members control growth, survival, and differentiation of neuronal cells [1,2]. NGF is a non-covalent homodimer and contains a characteristic structural motif, the cystine knot, denoted by a ring structure formed by two disulfide bridges penetrated by a third disulfide bridge (Fig. 1A and B). The crystal structures of both mouse and human NGF have been reported [3,4].

NGF is expressed *in vivo* as a pre-pro-protein. The 18 amino acids long N-terminal signal sequence targets the pre-pro-protein to the endoplasmic reticulum. The 103 amino acids comprising pro-peptide that does not possess any cystine residues (Fig. 1C) is known to promote correct maturation *in vivo* and guides oxidative refolding of the mature moiety *in vitro* [5–8]. Thus, proNGF joins the group of those proteins, of

which structure formation is significantly aided by their pro-peptides that do not engage in redox reactions (for review, see [9,10]). Pro-sequence assisted folding appears to be a hallmark of the structure formation process of mainly proteases. Structure formation of the pro-peptides themselves is either dependent or independent of their mature moieties.

Besides its verified role *in vitro* as a folding facilitator, the pro-peptide modulates the function of NGF by eliciting pro-apoptotic responses that are likely to be transmitted by both, p75 receptor and sortilin [11,12]. In order to learn more about the biophysical properties of the pro-peptide, its stability and structure were studied in its isolated form and while covalently attached to NGF. Our results suggest that the pro-peptide is stabilized by association with the mature part and that in the absence of the mature moiety the pro-peptide lacks stabilizing tertiary contacts. Thus, the pro-peptide features of NGF described here closely resemble those of the pro-domain of subtilisin BPN<sup>1</sup> with respect to structure and stability [13,14].

### 2. Materials and methods

#### 2.1. Preparation of recombinant human proNGF

Inclusion bodies of proNGF were produced with pET11a in *Escherichia coli* BL21(DE3), and the fully folded protein was obtained as described previously [8].

#### 2.2. Chemical crosslinking

20  $\mu$ l pro-peptide (0.3 mg/ml) was incubated with an equal volume of 0.02% (w/v) glutaraldehyde for 30 min at room temperature. The reaction was stopped by addition of 5  $\mu$ l of 2 M sodium borohydride in 100 mM NaOH. The protein was precipitated with sodium desoxycholate [15] and analyzed by 15% SDS-PAGE-gel stained with Coomassie Brilliant Blue.

#### 2.3. Analytical ultracentrifugation

For analytical ultracentrifugation, the pro-peptide was analyzed in 20 mM Na-phosphate, pH 7.0, and 1 mM EDTA in a Beckman Optima XL-A centrifuge and a 50Ti rotor. Sedimentation equilibrium measurements (absorption at 230 and 280 nm) were carried out in double sector cells at 25 000 rpm and 20 °C. Data were analyzed with the software provided by Beckman Instruments (Palo Alto, CA).

#### 2.4. Fluorescence measurements

Measurements were carried out on a fluorescence-spectrometer FluoroMax-2 (Jobin-Yvon-Spex). Slit widths for both excitation and emission wavelengths were 5 nm. Experiments were performed in 50 mM Na-phosphate, pH 7.0, and 1 mM EDTA at 20 °C in 1 cm cuvettes. For determination of the denaturation/renaturation transitions,

\* Corresponding author. Fax: +49-345-55-27-013.

E-mail address: elisabeth.schwarz@biochemtech.uni-halle.de (E. Schwarz).

<sup>1</sup> Present address: Dermatologische Klinik der Universität Münster, Esmarch-Str. 58, 48149 Münster, Germany.



208

M. Kliemann et al. / FEBS Letters 566 (2004) 207–212

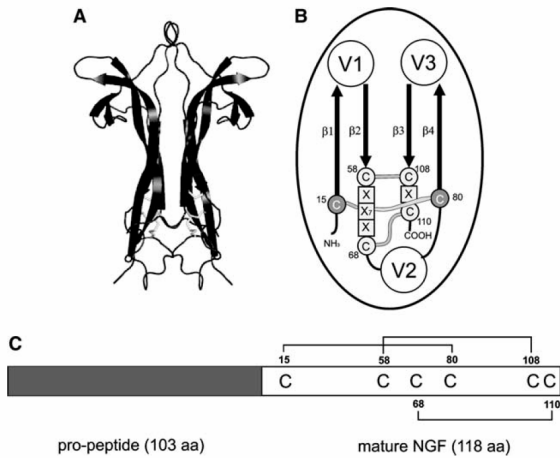


Fig. 1. Schematic presentation of NGF and proNGF. (A) Structure of the NGF dimer [3]. (B) Positions of  $\beta$ -strands and disulfide bridges in a NGF monomer (modified according to [21]). (C) Cysteine connectivities in proNGF.

proteins were incubated at the concentrations provided in the figure legends for at least 6 h. The recorded signals were normalized and linearly extrapolated [16].

### 2.5. Circular dichroism measurements

Far-UV CD spectra were recorded on an AVIV Model 62 ADS spectropolarimeter from 190 to 260 nm. Measurements were performed in 50 mM Na-phosphate, pH 7.0, at 20 °C. Spectra were buffer-corrected and ellipticities related to the mean residue weight of amino acid residues were calculated according to [17].

### 2.6. NMR spectroscopy

Proton spectra of 1.5 mM pro-peptide samples were acquired at a BRUKER DRX 500 spectrometer at 25 °C. 512 scans were averaged and a squared cosine window function was applied before Fourier transformation. The residual water resonance in the  $^2\text{H}_2\text{O}$  samples, containing 50 mM Na-phosphate, pH 7.0, and 1 mM EDTA, was weakly pre-saturated during the relaxation delay. The concentration of urea was determined by refraction without correction for the isotopic

effect of  $^2\text{H}_2\text{O}$ . Exchangeable protons of the buffer were removed by dissolving in  $^2\text{H}_2\text{O}$  three times and subsequent lyophilization.

## 3. Results and discussion

### 3.1. The isolated NGF pro-peptide is monomeric

The NGF pro-peptide was produced with pET11a in *E. coli* BL21(DE3) (Fig. 2A). In contrast to the recombinantly synthesized proNGF [8], the pro-peptide, which does not possess any cystine residues, remained soluble in the *E. coli* cytosol. Cell lysis and the first purification step on SP-Sepharose were performed in the presence of 8 M urea. After renaturation by dialysis against urea-free buffer, the protein was purified to near homogeneity by hydrophobic interaction chromatography and cation exchange chromatography (Fig. 2A). The protein migrated with an apparent molecular weight of ca. 16 kDa in SDS-PAGE.

We could show that oxidative folding in vitro giving rise to the native homodimer is significantly stimulated by the pro-peptide [7,8]. Thus, the question arises as to whether the pro-peptide exists in isolation in a dimeric form. Analytical ultracentrifugation was performed for the analysis of the oligomeric state of the recombinant pro-peptide. Sedimentation equilibrium analyses yielded an apparent molecular mass of 11.5 kDa, clearly indicating the monomeric state of the pro-peptide (Fig. 2B). Moreover, the correct mass of the pro-peptide (calculated molecular mass: 11.6 kDa) was verified by mass spectrometry (data not shown). The monomeric state of the pro-peptide was confirmed by chemical crosslinking with glutaraldehyde (Fig. 2C). The bands of apparent molecular weights lower than 16 kDa are probably due to intramolecular crosslinking caused by the prevalence of arginines and lysines in the basic protein domain (pI: 11.6).

### 3.2. The NGF pro-peptide contains only few structural elements

The pro-peptide contains a single tryptophan and four phenylalanine residues. The fluorescence properties of these aromatic amino acids were used to investigate the tertiary

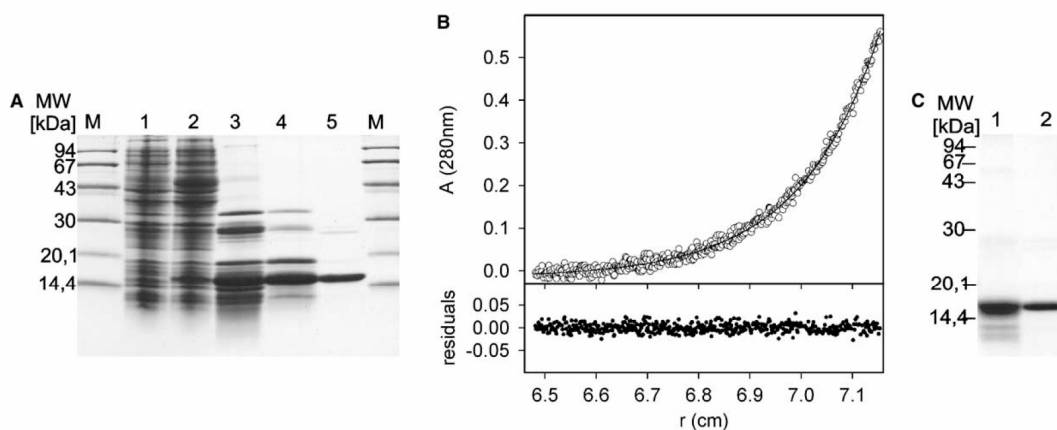


Fig. 2. (A) Isolation of recombinant human NGF pro-peptide from *E. coli* crude extract. 1: crude cell extract before induction, 2: crude cell extract after 3 h induction with 1 mM IPTG, 3: elution sample from the cation exchange chromatography in the presence of 8 M urea at pH 10, 4: sample after hydrophobic interaction chromatography, 5: sample after second cation exchange chromatography step at pH 7.0, M: marker. (B) Sedimentation equilibrium run of the pro-peptide (0.2 mg/ml). (C) Chemical crosslinking of the pro-peptide. 1: NGF pro-peptide after crosslinking with glutaraldehyde, 2: for negative control the protein was treated identically in the absence of crosslinker.

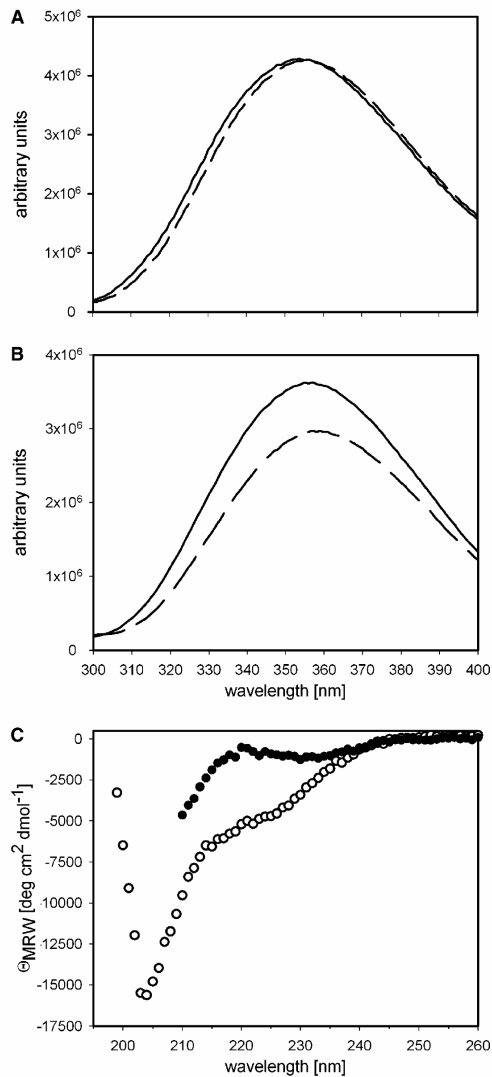


Fig. 3. (A) Fluorescence spectrum of the pro-peptide (50 µg/ml) upon excitation at 280 nm and (B) at 250 nm. Solid line, native pro-peptide; dashed line, pro-peptide denatured in 3.5 M GdmCl. (C) Far-UV CD spectra of the pro-peptide (1.5 mg/ml in 0.2 mm cuvettes). Open circles, native pro-peptide; closed circles, pro-peptide in the presence of 6 M GdmCl.

structure of the pro-peptide using fluorescence spectroscopy. The intrinsic tryptophan fluorescence signals of the native and denatured pro-peptide indicate that the single tryptophan residue is solvent-exposed under native conditions (Fig. 3A). When, however, fluorescence was measured at an excitation wavelength of 250 nm, a clear difference of the spectra of the native and the denatured protein was observed (Fig. 3B). This is due to the excitation of the four phenylalanines that contribute significantly to the overall fluorescence due to an energy transfer from excited phenylalanine to tryptophan. The

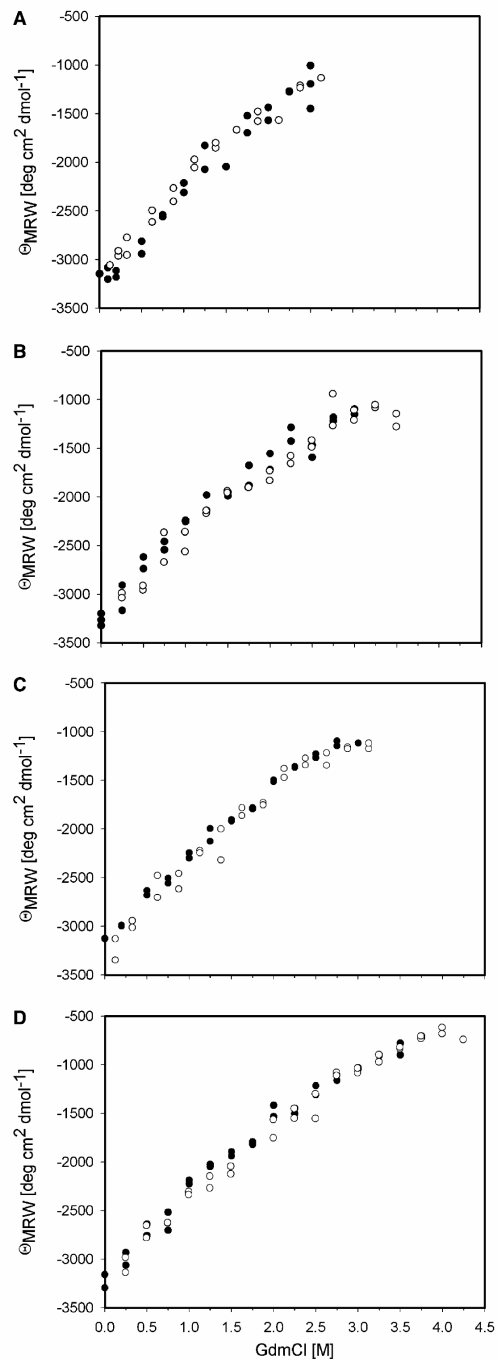


Fig. 4. Denaturation and renaturation transitions of the isolated pro-peptide. Measurements were monitored by far-UV CD spectroscopy. Ellipticities were measured at 220 nm in 1 mm cuvettes. Protein (0.4 mg/ml) was incubated at 20 °C for 6 h in the presence of the indicated GdmCl concentrations. Black circles, denaturation; open circles, renaturation of the pro-peptide. (A) Pro-peptide in 50 mM Na-phosphate, pH 7.0. (B) Pro-peptide as in (A), but +0.25 M (NH<sub>4</sub>)<sub>2</sub>SO<sub>4</sub>, +0.5 M (NH<sub>4</sub>)<sub>2</sub>SO<sub>4</sub> (C) and +0.75 M (NH<sub>4</sub>)<sub>2</sub>SO<sub>4</sub> (D).

210

M. Kliemannel et al. / FEBS Letters 566 (2004) 207–212

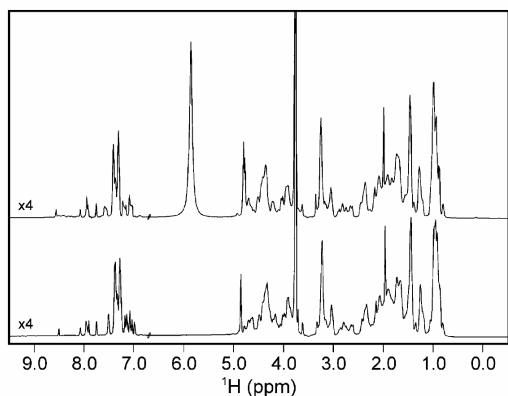


Fig. 5. 1D  $^1\text{H}$  NMR spectra of the pro-peptide. The measurements were performed in  $^2\text{H}_2\text{O}$  at 0 M urea (bottom) and 4.8 M urea (top). Residual resonances of protonated water and urea are located around 4.8 and 5.9 ppm, respectively. The intense resonance at 3.8 ppm belongs to EDTA. The aromatic region of the spectra between 6.8 and 9.5 ppm has been enlarged by a factor of 4.

higher fluorescence signal of the native protein is due to a more efficient energy transfer than in the denatured form.

In order to further analyze the contribution of secondary structure elements to the overall structure of the pro-peptide,

far-UV CD spectroscopy was performed. The small plateau in the wavelength range 218–223 nm and the minimum at 205 nm indicates a limited amount of  $\beta$ -sheet structure in addition to the prevailing random coil (Fig. 3C). Deconvolution of the spectrum using the program CDNN yielded 24%  $\beta$ -sheet and 34% random coil [18]. However, deviation of the pro-peptide CD spectrum from model spectra for helical,  $\beta$ -sheet or random coil structure suggests that these values should be treated with caution.

### 3.3. The pro-peptide exhibits only local intrachain contacts in the absence of the mature part

The stability of the pro-peptide was tested by stepwise denaturation with guanidinium-hydrochloride (GdmCl), and structural changes were monitored by far-UV CD spectroscopy. Changes in ellipticity were measured at 220 nm, a wavelength range where the largest difference between the species under native and denaturing conditions was observed (Fig. 3C). The unfolding and refolding changes in ellipticity showed a non-cooperative transition, indicating that the isolated pro-peptide does not possess a cooperatively stabilized structure (Fig. 4A). A similar result was obtained using the energy transfer from phenylalanines to tryptophan as a probe for denaturation (data not shown). Even stabilization by increasing concentrations of  $(\text{NH}_4)_2\text{SO}_4$  did not result in cooperative transitions (Fig. 4B–D).  $(\text{NH}_4)_2\text{SO}_4$  concentrations above 0.75 M resulted in aggregation of the pro-peptide (data

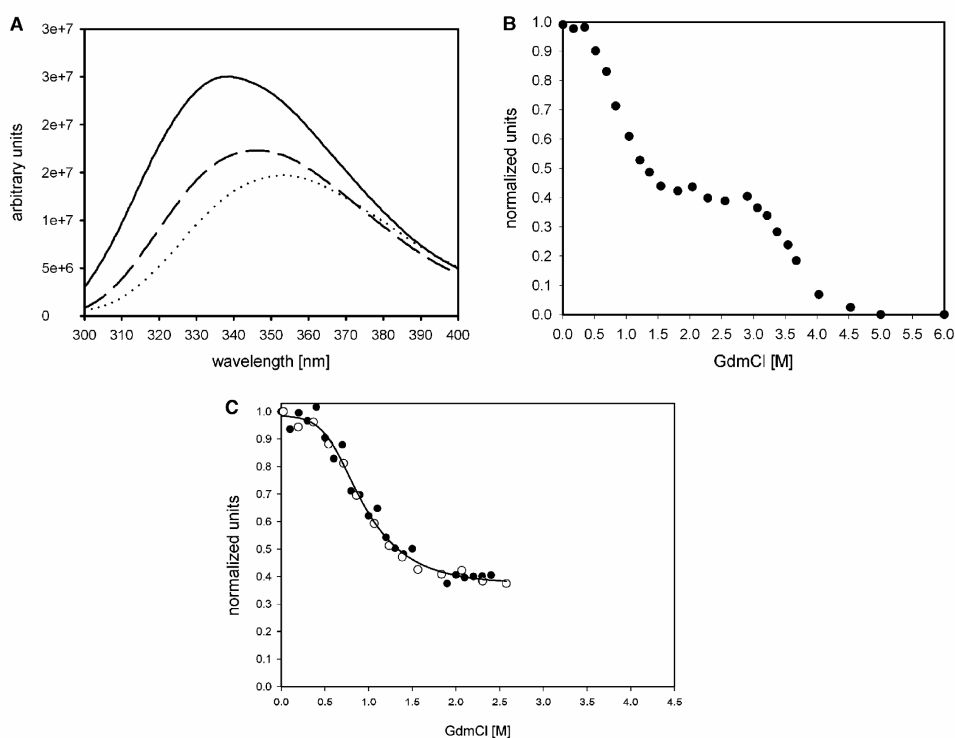


Fig. 6. (A) Fluorescence spectra of proNGF (20  $\mu\text{g}/\text{ml}$ ) upon excitation at 280 nm. Solid line, proNGF in the absence of GdmCl; dashed line, in the presence of 2.5 M GdmCl; dotted line, in the presence of 6 M GdmCl. (B) Denaturation of proNGF monitored by fluorescence. Protein was incubated at 20  $^\circ\text{C}$  for 24 h in the presence of the indicated GdmCl concentrations. Excitation and emission wavelengths were 280 and 325 nm, respectively. Data were normalized. (C) Transitions of the pro-peptide in proNGF. Black circles, denaturation; open circles, renaturation of the pro-peptide.

M. Kliemann et al. / FEBS Letters 566 (2004) 207–212

211

not shown) and therefore were not applied for stabilization experiments.

Missing tertiary interactions within the isolated pro-peptide could be confirmed by NMR spectroscopy. Fig. 5 depicts the 1D  $^1\text{H}$  spectra of the pro-peptide in 0 and 4.8 M urea, dissolved in  $^2\text{H}_2\text{O}$ . No high-field shifted aliphatic side chain resonances are observed below 0.7 ppm, which are sensitive measures for the tertiary structure of a protein. The only obvious deviation from random coil chemical shifts [19] shows a histidine  $\text{H}^{\epsilon 1}$  proton at 8.5 ppm and a  $\text{H}^{\gamma}$  proton at 4.9 ppm. Both resonances were only marginally affected by urea, indicating that these deviations are due to local contacts. 2D  $^1\text{H}$  NOESY experiments corroborated these findings (data not shown), especially for the  $\text{H}^{\gamma}$  proton at 4.9 ppm, which is very close to the residual water resonances at 4.8 ppm in the spectrum at 0 M urea. The very similar overall appearance of the two 1D spectra showed that the pro-peptide is unstructured and the small changes in chemical shifts are caused by a difference in the urea dependence of the individual resonances rather than structural changes upon addition of the denaturant (Fig. 5).

Taking these results together, both the chemical unfolding experiments and the NMR analysis indicate that the isolated pro-peptide lacks structure stabilizing tertiary contacts. Nevertheless, a limited amount of secondary structure appears to be present in the isolated pro-peptide as phenylalanine energy transfer to tryptophan by fluorescence and far-UV CD spectroscopy reveal clear differences between the native and denatured protein.

### 3.4. Tertiary contacts can only be detected when the pro-peptide is covalently attached to the mature part

For comparison of the structure of the pro-peptide when covalently attached to the mature NGF, fluorescence studies were performed with proNGF. Mature NGF contains three tryptophans, two tyrosines and seven phenylalanines. The crystal structures of mouse and human NGF show that the tryptophans are located close to the dimerization interface [3,4]. The fluorescence spectrum of native proNGF showed a maximum at 337 nm, indicating that the tryptophans are partially shielded from the solvent (Fig. 6A). Unfortunately, no conclusions about the surroundings of the tryptophan residing in the pro-peptide can be made from the spectrum of the native protein, since this signal is overlaid by the signal of the tryptophans in the mature part. However, changes in tryptophan fluorescence were observed upon denaturation of proNGF with low GdmCl concentrations that were not observed in the isolated pro-peptide. These changes are likely to reflect structural transitions of the pro-peptide, since the transition midpoint of the mature part is at a GdmCl concentration of about 3.5 M (see below).

The spectroscopic properties of proNGF allowed structural changes during denaturation to be monitored by fluorescence, so that the thermodynamic stability of the pro-peptide bound to the mature moiety could be explored. Upon chemical unfolding of proNGF with GdmCl, two distinct transitions were observed: one at 0.85 M GdmCl and a second transition at 3.5 M GdmCl (Fig. 6B). The second transition probably reflects the unfolding of the mature part, as the highly homologous murine NGF had been shown to unfold in this concentration range [20]. The small plateau at very low GdmCl concentrations probably represents native proNGF species. Thus, GdmCl concentrations as low as 0.85 M are sufficient to

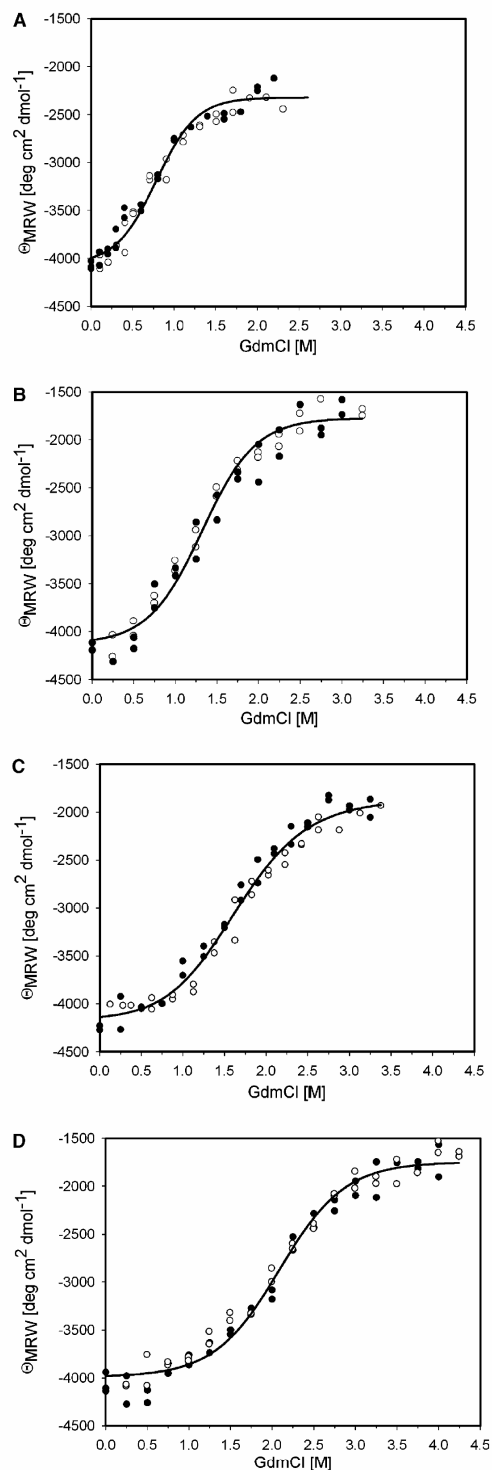


Fig. 7. Denaturation and renaturation of the pro-peptide (0.35 mg/ml) attached to the mature moiety followed by far-UV CD spectroscopy under the same conditions as described in the legend of Fig. 4. (A) in the absence of  $(\text{NH}_4)_2\text{SO}_4$ , (B) in the presence of 0.25 M, (C) in the presence of 0.5 M and (D) 0.75 M  $(\text{NH}_4)_2\text{SO}_4$ .

promote dissociation of the pro-peptide from the mature part. Dissociation may be concomitant with the unfolding of the pro-peptide. A  $\Delta G^0$  value of  $-7.8$  kJ/mol was calculated from the reversible unfolding/refolding of the pro-peptide (Fig. 6C).

Unfolding was also monitored by far-UV CD spectroscopy. As in the fluorescence measurements, a transition midpoint at 0.9 M GdmCl was observed (Fig. 7A). With increasing  $(\text{NH}_4)_2\text{SO}_4$  concentrations, the midpoint of the pro-peptide transition was shifted to higher GdmCl concentrations (Fig. 7B–D). Thus, while the pro-peptide in its isolated form cannot be stabilized by  $(\text{NH}_4)_2\text{SO}_4$ , stabilization was achieved when the pro-peptide was bound to the mature part, again indicating a significant difference in structure and molecular properties of the isolated and the NGF-bound pro-peptide. Structure stabilization is likely to be brought about via contact of the pro-peptide with the mature part; additional interactions may exist between the pro-peptide moieties themselves in the proNGF dimer.

Structure induction of the pro-peptide by the mature part also raises questions as to the role of the pro-peptide in the oxidative folding process. Clearly, the pro-peptide stimulates oxidative structure formation of the mature part, as proNGF could be renatured with yields of ca. 40%, while with mature NGF refolding yields of only ca. 4% were obtained [8]. These results indicate that, upon folding of mature NGF, the correct disulfide bonding is hardly energetically privileged compared to the multitude of non-native pairings. In contrast, the correctly disulfide-bonded form is the dominant species when proNGF is folded. It is likely that once the cystine knot has formed in a proNGF polypeptide to give rise to a native monomer, the pro-peptide part stabilizes the correct disulfide pattern by associating to this form and adopting a defined tertiary structure. Transient stabilization of correctly disulfide-bonded monomeric species by the pro-peptide is required until dimerization with a second natively folded monomer occurs, that finally results in the stably folded proNGF dimer. Certainly, this hypothesis has to be tested on the experimental level, as, e.g., by a comparison of the thermal unfolding of mature NGF and proNGF under equilibrium conditions in the presence of reducing agents.

*Acknowledgements:* We thank Milton Stubbs for improving the English. This work was supported by a grant from the Deutsche Fors-

chungsgemeinschaft (SCHW375/4-1/2) to E.S. and R.R. and by INTAS-2001-2347 to J.B.

## References

- [1] Barde, Y.A. (1990) *Prog. Growth Factor Res.* 2, 237–248.
- [2] Bradshaw, R.A., Blundell, T.L., Lapatto, R., McDonald, N.Q. and Murray-Rust, J. (1993) *Trends Biochem. Sci.* 18, 48–52.
- [3] McDonald, N.Q., Lapatto, R., Murray-Rust, J., Gunning, J., Wlodawer, A. and Blundell, T.L. (1991) *Nature* 354, 411–414.
- [4] Wiesmann, C., Ultsch, M.H., Bass, S.H. and de Vos, A.M. (1991) *Nature* 401, 184–188.
- [5] Seidah, N.G., Benjannet, S., Pareek, S., Savaria, D., Hamelin, J., Goulet, B., Laliberte, J., Lazure, C., Chretien, M. and Murphy, R.A. (1996) *Biochem. J.* 314, 951–960.
- [6] Suter, U., Heymach Jr., J.V. and Shooter, E.M. (1991) *EMBO J.* 10, 2395–2400.
- [7] Rattenholl, A., Ruoppolo, M., Flagiello, A., Monti, M., Vinci, F., Marino, G., Lilie, H., Schwarz, E. and Rudolph, R. (2001) *J. Mol. Biol.* 305, 523–533.
- [8] Rattenholl, A., Lilie, H., Grossmann, A., Stern, A., Schwarz, E. and Rudolph, R. (2001) *Eur. J. Biochem.* 268, 3296–3303.
- [9] Baker, D., Shiau, A.K. and Agard, D.A. (1993) *Curr. Opin. Cell Biol.* 5, 966–970.
- [10] Bryan, P.N. (2002) *Chem. Rev.* 102, 4805–4815.
- [11] Lee, R., Kermani, P., Teng, K.K. and Hempstead, B.L. (2001) *Science* 294, 1945–1948.
- [12] Nykjaer, A., Lee, R., Teng, K.K., Jansen, P., Madsen, P., Nielsen, M.S., Jacobsen, C., Kliemannel, M., Schwarz, E., Willnow, T.E., Hempstead, B.L. and Petersen, C.M. (2004) *Nature* 427, 843–848.
- [13] Eder, J., Rheinhecker, M. and Fersht, A.R. (1993) *J. Mol. Biol.* 233, 293–304.
- [14] Buevich, A.V., Shinde, U.P., Inouye, M. and Baum, J. (2001) *J. Biomol. NMR* 20, 233–249.
- [15] Arnold, U. and Ulbrich-Hofmann, R. (1999) *Anal. Biochem.* 271, 197–199.
- [16] Pace, C.N. (1986) *Meth. Enzymol.* 131, 266–280.
- [17] Schmid, F.X. (1997) in: *Protein Structure: A practical Approach* (Creighton, T.E., Ed.), second ed, pp. 261–297, IRL-Press, Oxford University Press, Oxford, New York, Tokio.
- [18] Böhm, G., Muhr, R. and Jaenicke, R. (1992) *Prot. Eng.* 5, 191–195.
- [19] Wüthrich, K. (1986) *NMR of proteins and nucleic acids*. Wiley, New York.
- [20] Timm, D.E. and Neet, K.E. (1992) *Protein Sci.* 1, 236–244.
- [21] McDonald, N.Q. and Hendrickson, W.A. (1993) *Cell* 73, 421–424.

Proof Only

## The pro-peptide of proNGF: Structure formation and intramolecular association with NGF

MARCO KLIEMANNEL,<sup>1</sup> RALPH GOLBIK,<sup>2</sup> RAINER RUDOLPH,<sup>1</sup>  
ELISABETH SCHWARZ,<sup>1</sup> AND HAUKE LILIE<sup>1</sup><sup>1</sup>Martin-Luther-Universität Halle-Wittenberg, Institut für Biotechnologie, 06120 Halle, Germany<sup>2</sup>Martin-Luther-Universität Halle-Wittenberg, Institut für Biochemie, 06120 Halle, Germany

(RECEIVED May 31, 2006; FINAL REVISION November 29, 2006; ACCEPTED November 30, 2006)

### Abstract

**ABSTRACT** The pro-peptide of human nerve growth factor (NGF) functions as an intramolecular chaperone during oxidative renaturation of proNGF in vitro and interacts intramolecularly with the mature part of native proNGF. Here, we analyzed the structure formation and stability of the pro-peptide in the context of proNGF and its intramolecular interaction with the native mature part. Folding and unfolding of the NGF-coupled pro-peptide, as analyzed by fluorescence, were biphasic reactions with both phases depending on the interaction with the mature part. This interaction was characterized by an overall stability of  $\Delta G = 20.9$  kJ/mol that was subdivided into two reactions, native  $\leftrightarrow$  intermediate state (14.8 kJ/mol) and intermediate  $\leftrightarrow$  unfolded state (6.1 kJ/mol). An additional very fast unfolding reaction was observed using circular dichroism (CD), indicating the presence of at least two kinetically populated intermediates in the unfolding of ProNGF. The part of the pro-peptide involved in the intramolecular association with mature NGF comprised the peptide Trp<sup>-83</sup>-Ala<sup>-63</sup> as determined by H/D exchange experiments. Spectroscopic analyses revealed that on the NGF side, a surface area around Trp<sup>21</sup> interacted with the pro-peptide. Trp<sup>21</sup> also participates in binding to TrkA and p75 receptors. These overlapping binding sites of the pro-peptide and the NGF receptors might explain the previously observed lower affinity of proNGF to its receptors as compared to NGF.

**Keywords:** pro-peptide; proNGF; NGF; folding; receptor binding; TrkA; p75; Trp21**Supplemental material:** see [www.proteinscience.org](http://www.proteinscience.org)

Nerve growth factor (NGF), a member of the neurotrophin family, as the neurotrophins 3–7 and brain-derived neurotrophic factor (BDNF) promotes growth, survival, and differentiation as well as apoptosis of neuronal cells (Barde 1990; Ernfors et al. 1990; Hohn et al. 1990; Bradshaw et al. 1993; Casaccia-Bonnel et al.

1996; Frade et al. 1996). NGF contains a typical structure motif, the cystine knot: Two disulfide bridges form a loop of 14 amino acids, which is penetrated by a third disulfide bridge. In vivo, NGF is expressed as a pre-pro-protein. The N-terminal signal sequence mediates translocation into the endoplasmic reticulum. Secretion of the growth factor occurs in a cell-type-specific manner as a mixture of proNGF and mature NGF, in which the pro-peptide with 103 amino acids is removed by furin or related pro-protein convertases (Seidah et al. 1996; Hasan et al. 2003; Fahnestock et al. 2004). Both mature NGF and proNGF exist in their active forms as homodimers (Bothwell and Shooter 1977; Rattenholl et al. 2001a).

The pro-peptide acts in vitro as an intramolecular chaperone by facilitating and stimulating oxidative folding of the mature part (Rattenholl et al. 2001a,b).

Reprint requests to: Elisabeth Schwarz, Martin-Luther-Universität Halle-Wittenberg, Institut für Biotechnologie, Kurt-Mothes-Str. 3, D-06120 Halle, Germany; Elisabeth.Schwarz@biochemtech.uni-halle.de; fax + 49 345 55 27 013.

**Abbreviations:** CD, circular dichroism; GdmCl, guanidinium hydrochloride; NGF, human nerve growth factor; proNGF, pro-form of NGF containing the 102-amino-acid-comprising pro-peptide and a start methionine at the N terminus.

Article and publication are at <http://www.proteinscience.org/cgi/doi/10.1110/ps.062376207>.

Kliemann et al.

Folding-promoting functions of pro-peptides have been reported for several proteins, which are expressed as (pre-)pro-proteins (Shinde and Inouye 2000). Prominent examples are bovine pancreatic trypsin inhibitor (BPTI), guanylyl cyclase activating peptide (GCAP), or the macrophage inhibitory cytokine-1 (MIC-1), and proteases such as  $\alpha$ -lytic protease, subtilisin, and carboxypeptidase Y (Ikemura et al. 1987; Winther and Sorensen 1991; Weissman and Kim 1992; Shinde et al. 1993; Hidaka et al. 1998; Fairlie et al. 2001). The pro-peptides of the  $\alpha$ -conotoxins, toxins of marine snails, are not directly involved in the folding of the mature part, but can facilitate the structure formation by interacting with protein disulfide isomerase in the endoplasmic reticulum (Buczek et al. 2004). It has also been reported that pro-peptides guide the assembly of subunits into active protein complexes as in case of the von Willebrand factor or caspase-3 (Wise et al. 1988; Feeney and Clark 2005). The pro-peptides of TGF- $\beta$  and very likely also bone morphogenetic proteins retard the biological activities of the mature growth factors (Böttinger et al. 1996; Degnin et al. 2004; Hillger et al. 2005). While for some pro-peptides their biological activities are displayed even when they are not covalently linked to their mature parts (Gray and Mason 1990), in the case of NGF, the pro-peptide has to be covalently linked to the mature part to promote oxidative structure formation (Rattenholl et al. 2001a). Besides aiding in structure formation, the pro-peptide of proNGF confers a pro-apoptotic activity to the growth factor and thus responses that are completely opposite to the mature growth factor (Lee et al. 2001). Pro-apoptotic responses of proNGF are elicited by binding to a pro-form specific receptor, sortilin (Nykjaer et al. 2004).

Besides their biological relevance, little is known about the structures and stabilities of the various pro-peptides. In the case of the protease subtilisin, the pro-peptide loses the structure in the absence of the mature part (Ruvinov et al. 1997; Buevich et al. 2001). A similar observation was made for the pro-peptide of carboxypeptidase Y: Under conditions where the protein is functional, the pro-peptide is only partially folded. The pro-peptide contains secondary structural elements but a very low content of defined tertiary structure and exists in a molten globule state (Sorenson et al. 1993).

Recently, we demonstrated that the isolated pro-peptide of NGF is a monomeric protein with a distinct secondary structural content. In the isolated form the structure was significantly less stable than in its NGF-coupled form, suggesting an interaction of the pro-peptide and the mature part in native proNGF (Kliemann et al. 2004). Here, we analyzed in detail the intramolecular interaction of the pro-peptide with the mature part of proNGF and the influence of the mature part on the structure formation process of the covalently linked pro-peptide.

## Results

### *Thermodynamic and structural properties of the NGF-coupled pro-peptide*

We have shown previously that the overall denaturation process of proNGF is biphasic with the first and second transition representing unfolding of the pro-peptide and NGF part, respectively (Kliemann et al. 2004). Furthermore, we observed that the subtraction far-UV circular dichroism (CD) spectrum of proNGF and mature NGF was identical to that recorded for the isolated pro-peptide, indicating that the pro-peptide contains the same amount of secondary structure elements in the isolated form and in the NGF-coupled pro-peptide ("NGF-coupled" refers to the pro-peptide in the context of proNGF) (Rattenholl et al. 2001a; Kliemann et al. 2004). This assumption could be confirmed by denaturation and renaturation transitions monitored by far-UV CD spectroscopy. It should be emphasized that the terms denaturation and renaturation as well as unfolding and folding refer in this work to the pro-peptide moiety, since at the denaturant concentrations used here the mature part retains its native structure (Kliemann et al. 2004). The observed differences in ellipticities between native and unfolded pro-peptide were independent of whether the isolated pro-peptide or that coupled to the mature part was analyzed (Kliemann et al. 2004). Equilibrium denaturation studies revealed a non-cooperative transition of the isolated pro-peptide, indicating that tertiary contacts are not involved in the stabilization of the pro-peptide. In contrast, the NGF-coupled pro-peptide showed a cooperative transition when unfolding was monitored by fluorescence measurements (Fig. 1). F1

Denaturation and renaturation under equilibrium conditions of the NGF-coupled pro-peptide were reversible (Kliemann et al. 2004). The transition midpoints

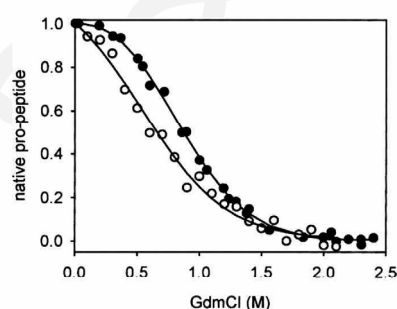


**Figure 1.** Equilibrium transitions of the NGF-coupled pro-peptide and the isolated pro-peptide. The proteins were incubated in 50 mM Na-phosphate, pH 7.0 at various GdmCl concentrations for 16 h at 20°C. Fluorescence signals of the NGF-coupled pro-peptide (●, 20  $\mu$ g/mL, excitation: 280 nm, emission: 325 nm) and the isolated pro-peptide (○, 50  $\mu$ g/mL, excitation: 250 nm, emission: 345 nm) were recorded.

## Interaction of NGF with its pro-peptide

occurred at a low guanidinium hydrochloride (GdmCl) concentration of 0.9 M, pointing to a low overall stabilization of the pro-peptide moiety. For a more comprehensive analysis of the unfolding reaction, a comparison of the transitions monitored by far-UV CD spectroscopy and fluorescence was carried out. Changes in ellipticities in the far-UV range reflect changes in secondary structure elements that are expected to occur during unfolding. Changes of the fluorescence represent alterations of solvent accessibilities of tryptophan residues and thus correspond to differences in tertiary contacts. Unexpectedly, the unfolding curves obtained by fluorescence and CD measurements did not coincide (Fig. 2). This result indicates that the loss of secondary structures and tertiary contacts are not coupled as would be expected. The transition midpoint measured by far-UV CD spectroscopy was at lower GdmCl concentrations than that measured by fluorescence. This unexpected fact predicts the existence of an intermediate where secondary structure is lost prior to the loss of specific tertiary contacts observed by tryptophan fluorescence.

On the basis of the obtained results, the intermediate could be characterized as a species with partly or fully unfolded secondary structure, though a tryptophan residue would still engage in tertiary interaction. In principle, the tryptophan residue(s) could either be localized in the mature part that contacts the pro-peptide or in the pro-peptide itself. Since a chimeric fusion protein consisting of NGF linked to the pro-peptide moiety of a related neurotrophin, NT-3, which lacks tryptophans, exhibited a change in tryptophan fluorescence upon unfolding, as well (in prep.), very likely part of the fluorescence signal is caused by a tryptophan residue in mature NGF.

#### Identification of pro-peptide regions involved in tertiary contacts

In order to identify those regions within the pro-peptide that could be involved in contacts with the mature part,

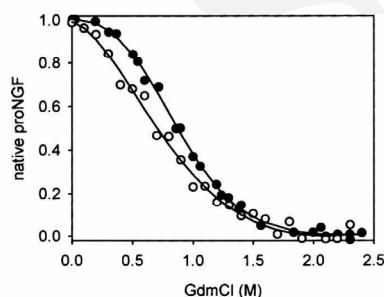


**Figure 2.** Comparison of the transitions of NGF-coupled pro-peptide measured by fluorescence (●) and far-UV CD spectroscopy (○). The fluorescence data were obtained as described in Figure 1. Signals were monitored at 220 nm.

mass spectrometry-coupled H/D exchange was employed. This method allows the identification of segments that are protected against H/D exchange due to their engagement in secondary and/or tertiary structure (Zhang and Smith 1993). For the analysis of the exchange of amide protons in the pro-peptide of proNGF, the protein was incubated in D<sub>2</sub>O. The exchange reaction was stopped by acidification to minimize a back exchange during the subsequent digestion with pepsin (Supplemental Fig. S1) and preparation for mass analysis (Bai et al. 1993). Analysis of the digestion products showed that the mature part of proNGF is completely intact under the applied experimental conditions. In contrast, defined proteolysis products were obtained from the pro-peptide moiety. The fragments were aligned with the program FindPept (<http://www.expasy.ch/tools/findpept.html>). The masses of the fragments were analyzed by MALDI-TOF, and exchange rates were corrected for the back exchange determined by control peptides (Table 1).

H/D exchange was impaired in peptides Trp<sup>-83</sup>-Ala<sup>-63</sup> and Gln<sup>-80</sup>-Ala<sup>-64</sup>. To determine if the observed amide proton protection would result from hydrogen bonds present in the isolated pro-peptide as well, the same experiment was repeated with the isolated pro-peptide. Here, no defined fragments were obtained upon proteolysis. Thus, in contrast to its isolated form, the pro-peptide in proNGF is partially protected when complexed with the mature part. Based on the H/D exchange data, it is very likely that a region of the pro-peptide containing the peptides Trp<sup>-83</sup>-Ala<sup>-63</sup> and Gln<sup>-80</sup>-Ala<sup>-64</sup> is involved in an interaction with the mature part itself or forms a structure that is stabilized by the interaction of the pro-peptide with the mature part.

#### Kinetic analyses of the pro-peptide unfolding and refolding in proNGF

Since the isolated pro-peptide did not alter its tryptophan fluorescence upon denaturation, the change of tryptophan fluorescence of the NGF-coupled pro-peptide should reflect specific tertiary contacts between the pro-peptide and the mature part in proNGF. Folding and unfolding kinetics of the NGF-coupled pro-peptide were analyzed by fluorescence spectroscopy. Changes in spectroscopic signals obtained in a range from 0–2 M GdmCl originate solely from structural alterations of the pro-peptide, which has been shown previously to possess only a marginal stability (Fig. 1), while the mature part is stable up to 3 M GdmCl (Fig. 1A; Timm and Neet 1992; De Young et al. 1996; Kliemann et al. 2004). Folding of the NGF-coupled pro-peptide exhibited a monophasic reaction (Fig. 3A). Since the pro-peptide contains nine prolyl residues, peptidyl prolyl *cis-trans* isomerization could be rate-limiting. However, the folding was neither accelerated by the addition of various



Kliemann et al.

**Table 1.** Protection of the NGF-coupled pro-peptide against H/D exchange

	M <sub>R</sub> in H <sub>2</sub> O (Da)	M <sub>R</sub> in D <sub>2</sub> O (Da)	Difference	Maximum incorporation <sup>a</sup>	Exchange (%)
Met <sup>-104</sup> -Ala <sup>-61</sup>	4653.22	4683.39 ± 8.6	30.18 ± 8.6	32.5	92.8 ± 26
Met <sup>-104</sup> -Ala <sup>-63</sup>	4470.25	4497.38 ± 8.3	27.13 ± 8.3	30.78	88.2 ± 26.9
Met <sup>-104</sup> -Leu <sup>-73</sup>	3461	3481.97 ± 8.7	20.97 ± 8.7	23.08	90.88 ± 38.1
Trp <sup>-83</sup> -Ala <sup>-63</sup>	<b>2236.5</b>	<b>2246.58 ± 0.8</b>	<b>10.08 ± 0.8</b>	<b>15.39</b>	<b>65.5 ± 5.1</b>
Phe <sup>-32</sup> -Phe <sup>-16</sup>	1937.8	1949.05 ± 0.8	11.25 ± 0.8	11.5	97.81 ± 7.2
Gln <sup>-80</sup> -Ala <sup>-64</sup>	<b>1819.25</b>	<b>1828.2 ± 7.7</b>	<b>8.96 ± 7.7</b>	<b>12.15</b>	<b>73.7 ± 64.1</b>
Ser <sup>-31</sup> -Phe <sup>-16</sup>	1791.58	1800.84 ± 0.5	9.26 ± 0.5	9.5	97.5 ± 4.4

ProNGF was submitted to H/D exchange by incubating the protonated protein in D<sub>2</sub>O. After blocking further exchange by acidification, proNGF was digested with pepsin. This led to a set of peptides derived from the pro-peptide, whereas the NGF part proved to be protease-resistant. The masses of the different peptides were determined by MALDI ToF analyses from which the amount of incorporated deuterium atoms could be calculated. The comparison with the maximum deuterium incorporation possible yields the exchange factor. The experimental data listed were collected after a 2-min incubation of proNGF in D<sub>2</sub>O and represent mean values of at least three independent measurements. By convention, the amino acids of the pro-peptide are assigned by negative numbers; the pro-peptide starts with Met<sup>-104</sup>.

<sup>a</sup>The theoretical maximum of deuterium incorporation was corrected by the experimentally determined back exchange of 12%.

peptidyl prolyl *cis-trans* isomerases nor in double-jump experiments (data not shown), indicating that peptidyl prolyl isomerization(s) may not to be a rate-limiting factor.

The same refolding kinetics as determined by fluorescence were observed by far-UV CD spectroscopy at 220 nm (Fig. 3A). The monophasic folding kinetics were surprising, because the equilibrium transitions clearly indicated the presence of an intermediate. Since the observed folding phase showed the full fluorescence amplitude, no fast reaction prior to the observed structure formation can be assumed; a fast phase following the observed folding reaction, however, would not be detectable. The GdmCl-dependent fluorescence amplitude of the folding phase fit well to the equilibrium transition measured by fluorescence (data not shown), indicating that the kinetic and equilibrium analyses describe the same process.

Denaturation kinetics of the NGF-coupled pro-peptide were more complex than refolding kinetics. When denaturation at 1.75 M GdmCl was monitored by fluorescence spectroscopy, a biphasic denaturation process was observed (Fig. 3B). Recording the unfolding by stopped flow CD measurements was not possible at this GdmCl concentration, since the process was too fast to be detectable (Fig. 3B). Thus, upon denaturation, secondary structure is lost first, followed by the disruption of tertiary contacts. This deduced order of reactions is unusual, but matches the data obtained from unfolding equilibria, which also pointed to a first loss of secondary structure(s) before disruption of tertiary contacts (Fig. 2).

In order to analyze whether the biphasic denaturation observed by fluorescence would reflect parallel or serial unfolding reactions with an intermediate accumulating, we performed double-jump experiments. In these experiments, the NGF-coupled pro-peptide was denatured for various times. Subsequently, the protein was transferred to native conditions, and refolding was monitored by fluorescence spectroscopy. When proNGF was denatured

for 25 sec in 1.75 M GdmCl, monophasic refolding kinetics were observed. In contrast, upon shorter denaturation times, a biphasic refolding reaction was recorded,

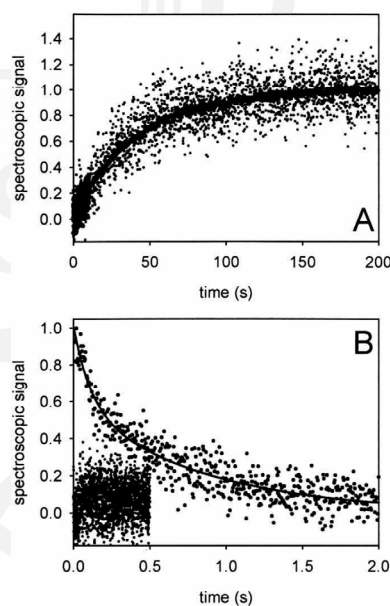


**Figure 3.** Kinetics of folding and unfolding of the NGF-coupled pro-peptide. (A) Folding of the NGF-coupled pro-peptide. ProNGF was denatured in 2 M GdmCl for at least 1 h at 20°C. Subsequently, refolding was initiated by a 1:11 dilution in 50 mM Na-phosphate, pH 7. Kinetics were monitored by stopped flow fluorescence (●) with an emission cut-off filter of 325 nm and stopped flow CD at 220 nm (circles). The data could be fitted to a single phase with  $k = 0.02 \text{ sec}^{-1}$ . (B) Unfolding of the NGF-coupled pro-peptide. Unfolding was started by a 1:11 dilution of proNGF in 50 mM Na-phosphate, pH 7, 2 M GdmCl at 20°C. Fluorescence and CD signals were measured as in A. The fluorescence data exhibited a biphasic reaction with  $k_1 = 3.1 \pm 0.4 \text{ sec}^{-1}$  and  $k_2 = 0.76 \pm 0.08 \text{ sec}^{-1}$  ( $n = 6$ ) (solid line). The lower trace represents the final CD amplitude. [AUS]

## Interaction of NGF with its pro-peptide

with the fast phase  $\sim 20$  times faster than the overall process (Fig. 4A). These data clearly indicate that an intermediate (I) is populated during denaturation. Together with the very fast CD kinetics, these results can be explained by a folding/unfolding scheme  $N \leftrightarrow I1 \leftrightarrow I2 \leftrightarrow U$ . In this scheme, the reaction  $N \leftrightarrow I1$  is too fast to be quantified by stopped flow CD and is fluorescently silent, whereas the reactions  $I1 \leftrightarrow I2$  and  $I2 \leftrightarrow U$  represent the fast and slow phases, respectively, observed by fluorescence.

Upon denaturation of the native protein at 1.75 M GdmCl, I2 is accumulating during the first 1 sec of denaturation. Subsequently, I2 unfolds to the fully denatured state. The time-dependent population of I2 can be visualized directly by varying the time of denaturation in double-jump experiments (Fig. 4A). In the subsequent refolding reactions, the amplitudes of the fast and slow

kinetics correspond to the accumulation of I2 and U, respectively. Taking these amplitudes, the kinetics of accumulation and disappearance of I2 and the accumulation of U could be analyzed (Fig. 4B). The resulting rate constants of the two processes fit well to the constants obtained from the biphasic denaturation kinetics measured by stopped flow fluorescence (Fig. 3B).

A fluorescence spectrum of the intermediate I2 could not be recorded during the unfolding kinetics because the reaction  $I2 \rightarrow U$  was too fast. Therefore, denaturation kinetics at 1.8 M GdmCl were measured at different emission wavelengths between 330 and 360 nm. From these kinetic data, the specific fluorescence of the native, intermediate, and denatured state could be calculated and the spectra reconstituted (Fig. 5). The data revealed a wavelength shift of the maximum emission from 340 nm (native state) to 345–350 nm (denatured state) already in the intermediate I2. Thus, the solvent accessibility of the tryptophan that is responsible for the change of the fluorescence signal must be similar in I2 and U. It should be noted that the fluorescence intensities of the observed spectra are valid only under the given conditions (1.8 M GdmCl). Since the fluorescence intensity of the spectrum of the intermediate I2 decreases with increasing GdmCl concentrations while that of the native state does not (data not shown), the intermediate possesses a lower fluorescence than the native state at denaturing conditions but a slightly higher fluorescence in the absence of GdmCl. The fluorescence of isolated tryptophan molecules decreases with increasing GdmCl concentrations in a range of 0–3 M (Schmid 1997). Thus, the decrease in intrinsic fluorescence of the intermediate I2 with increasing GdmCl concentrations indicates the solvent exposure of a tryptophan residue in the intermediate structure. This result is confirmed by the red-shift of the fluorescence maximum of the corresponding spectrum (Fig. 5). Similar fluorescence characteristics of folding intermediates have been observed for other proteins such as antibody fragments (Lilie et al. 1995).

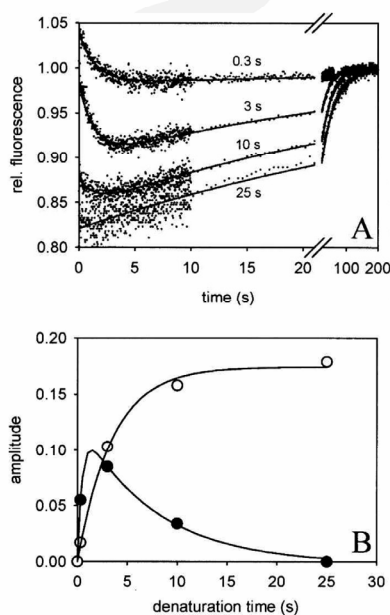


**Figure 4.** Time-dependent accumulation of a folding intermediate upon unfolding of the NGF-coupled pro-peptide. ProNGF was denatured in 1.7 M GdmCl for 0.3, 3, 10, and 25 sec. Subsequently, refolding was initiated by a 1:11 dilution in 50 mM Na-phosphate, pH 7, and the change in fluorescence was analyzed (280 nm excitation, 325 nm cut off for emission). (A) Refolding kinetics after different times of denaturation. The traces could be described by a biphasic reaction with rate constants of  $k_1 = 0.71 \text{ sec}^{-1}$  and  $k_2 = 0.03 \text{ sec}^{-1}$ . (B) Analyses of the amplitudes of the folding reactions. The amplitudes of the fast (●) and slow (○) phase correspond to the population of a folding intermediate and the denatured state, respectively. The time-dependent distribution of both species could be fitted by a serial first order reaction with  $k_1 = 2.2 \text{ sec}^{-1}$  and  $k_2 = 0.3 \text{ sec}^{-1}$ , values similar to those of the corresponding unfolding kinetic (see Fig. 3B).

## Thermodynamics of pro-peptide folding

In order to understand the kinetic and energetic relationship of the different states of the pro-peptide moiety folding, the microscopic rate constants of folding and unfolding were determined. To this end, the GdmCl-dependent folding and unfolding kinetics were analyzed by fluorescence spectroscopy. Whereas the change in tryptophan fluorescence upon denaturation permitted the observation of both the transient accumulation of the intermediate and the formation of the denatured state, the same method revealed just the reaction  $U \rightarrow I$  upon refolding. Folding of the intermediate to the native state was measured separately by double-jump experiments, in

Kliemann et al.

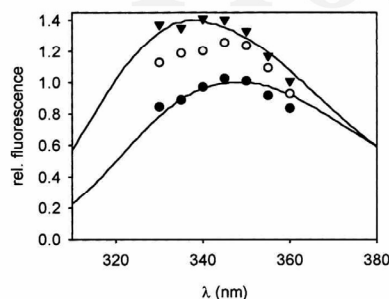


**Figure 5.** Fluorescence spectra of proNGF. The specific fluorescence of the native (▼), intermediate (○), and denatured state (●) of proNGF was calculated from biphasic denaturation kinetics, measured at different wavelengths. For comparison, spectra of native (—) and denatured (in 2 M GdmCl) proNGF (---) were taken from Kliemann et al. (2004).

AU6

which native proNGF was submitted to 1.8 M GdmCl for only 1 sec (or 1.2 M GdmCl for 4 sec) to populate the intermediate I2. In the following refolding reaction, the reaction  $I2 \rightarrow I1/N$  could be quantified. As mentioned before, the states I1 and N could not be discerned by fluorescence. Therefore, in the following section, the species I1 and N are not distinguished. The results of folding/unfolding are depicted in Figure 6. The global fit of the data yielded microscopic rates of folding and unfolding of N/I1, I2, and U under native conditions as well as the thermodynamic stability of the native and intermediate state I2 (Fig. 6). The overall stability of  $N/I1 \leftrightarrow U$  of the NGF-coupled pro-peptide is 20.9 kJ/mol, which is subdivided in the two transitions  $N/I1 \leftrightarrow I2$  (14.8 kJ/mol) and  $I2 \leftrightarrow U$  (6.1 kJ/mol). The microscopic unfolding rate of both N/I1 and I2 was identical ( $k_u = 0.0025 \text{ sec}^{-1}$ ); the activation energy was 86.3 kJ/mol. In contrast, the activation energy of folding showed a difference of 8.3 kJ/mol for folding of U and I2, respectively (Supplemental Fig. S2).

F6

It should be stressed that the Chevron plot does not describe the complete folding/unfolding process of the pro-peptide of NGF, since unfolding measured by far-UV CD spectroscopy was too fast to be quantified. Thus, only changes in the environment of the tryptophans could be monitored; changes on the secondary structural level are not considered in the interpretation of the Chevron plot.

## Discussion

Despite the increasing knowledge about the biological function(s) of pro-peptides, little information is available about the structural properties of pro-peptides and how they exert their roles on a structural basis. Only for some serine and cysteine proteases has the X-ray structure of the pro-form been solved (Gallagher et al. 1995; Podobnik

et al. 1997; Jain et al. 1998; LaLonde et al. 1999) and a molecular model predicted how the pro-peptide serves as an intramolecular chaperone (Gallagher et al. 1995). Here, we analyzed structure formation, stability, and intramolecular interaction of the NGF pro-peptide in the context of the mature part. Unexpectedly, kinetic and thermodynamic analyses revealed a loss of at least a major part of the secondary structures before disruption of tertiary contacts. These tertiary contacts reflect an intramolecular interaction of the pro-peptide with the mature part.

It has been shown previously that the pro-peptide acts as an intramolecular chaperone during oxidative folding of proNGF (Rattenholl et al. 2001a, b). This function suggests an interaction of the pro-peptide with folding intermediates of the NGF part based primarily on the properties of the solvent-exposed surface of these intermediates, such as hydrophobicity, rather than well defined structural features. The pro-peptide needs to be covalently attached to NGF in order to exhibit this folding-enhancing function, as the addition of the isolated pro-peptide to folding NGF molecules *in trans* does not promote folding. This finding indicates a very weak interaction of the pro-peptide with folding intermediates of the mature part (Rattenholl et al. 2001a). In contrast, the intramolecular interaction of the pro-peptide with native NGF is surprisingly stable: It is characterized by an overall energy of  $\Delta G = 20.9 \text{ kJ/mol}$ . Furthermore, one of the transitions reflecting this interaction is highly cooperative (cf. fast phases in Fig. 6), indicating a well defined structural interface between the pro-peptide and NGF. Thus, the intramolecular interaction of the pro-peptide and NGF seems to be quite different in the native state and during folding regarding both structural and thermodynamic parameters.

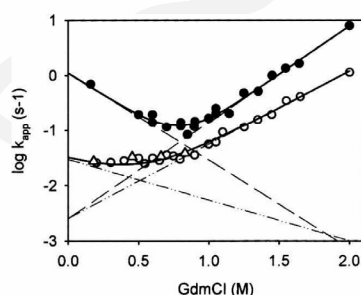


**Figure 6.** Unfolding/refolding kinetics of the NGF-coupled pro-peptide. Unfolding and refolding at different GdmCl concentrations of the NGF-coupled pro-peptide were measured as described in Figure 3. Unfolding and refolding were monitored by fluorescence (●, ○); CD measurements were used to observe refolding (△). (Solid lines) Fit of the complete data set, (dashed lines) GdmCl dependence of the microscopic rate constants of folding and unfolding.

AU7

The experimental data suggest that the interaction between NGF and its pro-peptide is mediated by a surface area of the mature NGF comprising a tryptophan residue and the peptide Trp<sup>-83</sup>-Ala<sup>-63</sup> of the pro-peptide. Unfortunately, currently no detailed structural data for the pro-peptide are available. Even the CD spectrum of the NGF-coupled pro-peptide hardly allows a prediction of the overall secondary structural content (Kliemann et al. 2004). A sequence analysis of the pro-peptide according to the hydrophobic moment method of Eisenberg (Eisenberg et al. 1984) shows that the peptide Trp<sup>-83</sup>-Ala<sup>-63</sup> possesses the highest hydrophobic moment of the whole pro-peptide. In a helical wheel representation, this peptide is highly amphiphilic with a perfect segregation of hydrophobic and polar/charged amino acids (not shown). However, without structural data of the pro-peptide at the atomic level, a structural interpretation of the pro-peptide region involved in the intramolecular interaction with NGF remains speculative.

As mentioned above, the intramolecular association of NGF with its pro-peptide is mainly of a hydrophobic nature and involves tryptophan residues. The fluorescence change obtained upon unfolding of the NGF-coupled pro-peptide is related to the environmental change of one or more tryptophans. Since a chimeric construct of NGF and the related heterologous pro-peptide of NT-3, which lacks tryptophans, also showed a change in tryptophan fluorescence upon unfolding (in prep.), at least part of the fluorescence signal must originate from an altered solvent accessibility of tryptophans of the NGF part. The NGF monomer contains three tryptophans, two of which are located in the dimer interface and thus are buried in the hydrophobic core. These tryptophan residues would presumably not change their spectroscopic properties upon unfolding of the pro-peptide. The third tryptophan of NGF, Trp<sup>21</sup>, has been identified as the most solvent-exposed and reactive tryptophan residue that is readily modified by N-bromosuccinimide (Cohen et al. 1980). Solvent exposure of this residue has been confirmed by X-ray structure analysis (McDonald et al. 1991; Fig. 7). Our fluorescence data suggest that the pro-peptide shields Trp<sup>21</sup> of NGF from solvent since unfolding of the NGF-coupled pro-peptide alters the solvent accessibility of Trp<sup>21</sup> of mature NGF. Assuming that the presence of the pro-peptide does not affect the structure of the mature part (especially the dimer interface where the other tryptophans are located), the spectroscopic properties of proNGF would indicate a direct interaction of the pro-peptide with Trp<sup>21</sup> of mature NGF.

Trp<sup>21</sup> of NGF is also part of the interface of the NGF-receptor complex in both the TrkA- and p75 receptors (Cohen et al. 1980; Drinkwater et al. 1991; Wiesmann et al. 1999; He and Garcia 2004). In case of TrkA, for example, seven amino acids of the receptor are <8 Å apart from Trp<sup>21</sup> of NGF (Fig. 7). Thus, from the structural

point of view it seems that the pro-peptide competes for the binding site of the mature part to both the TrkA and p75 receptors. This should result in a substantially decreased affinity of proNGF to its receptors compared with mature NGF, which indeed has been observed experimentally (Nykjaer et al. 2004). The spectroscopic and thermodynamic analyses of the NGF-coupled pro-peptide showed that Trp<sup>21</sup> of NGF, which is buried in native proNGF, becomes solvent-accessible in the reaction N/I1 → I2 as demonstrated by the fluorescence spectrum of the intermediate I2 (Fig. 5). This reaction and thus the loss of interaction of the pro-peptide with NGF via a region involving Trp<sup>21</sup> require an energy input of 14.8 kJ/mol under the given buffer conditions. Assuming a simple model of competition, this energy must be provided by the binding of the receptors to proNGF in order to form a proNGF-receptor complex. Another possibility would be a partial overlap of the binding sites for the pro-peptide and the receptors. In this case it would be conceivable that receptor binding may occur without displacing the pro-peptide. In this scheme the receptor affinity to proNGF would be decreased as well compared with mature NGF. However, depending on the size and the overlapping part of the contact sites for receptor and pro-peptide, the loss of energy in receptor binding due to the presence of the pro-peptide may be smaller than in the displacing model. Although a competition of the pro-peptide with NGF for binding to the receptors TrkA or p75 appears plausible, the precise mode of proNGF receptor interaction remains to be deduced by structural analysis at atomic resolution of proNGF and its receptor complex.

## Materials and methods

### *Preparation of recombinant human proNGF and the isolated pro-peptide*

All recombinant constructs were cloned in the vector pET11a. *Escherichia coli* BL21(DE3) was employed as a bacterial host. Recombinant expression of proNGF resulted in formation of inclusion bodies. Processing of inclusion bodies of proNGF and protein renaturation was performed as described previously (Rattenholl et al. 2001a). The isolated pro-peptide of NGF was expressed in soluble form. The fully folded protein was obtained as published previously (Kliemann et al. 2004).

### *Fluorescence spectroscopy*

Fluorescence measurements were carried out at a FluoroMax-2 (Jobin-Yvon). Slit widths for both excitation and emission wavelengths were 5 nm. Experiments were performed in 50 mM Na-phosphate, pH 7.0, and 1 mM EDTA at 20°C. Equilibrium transitions of the NGF-coupled pro-peptide (10 µg/mL) were monitored at an excitation wavelength of 280 nm and 325 nm emission. Fluorescence of the isolated pro-peptide (50 µg/mL) was analyzed using an excitation of phenylalanine at 250 nm and

Kliemann et al.

Proof Only

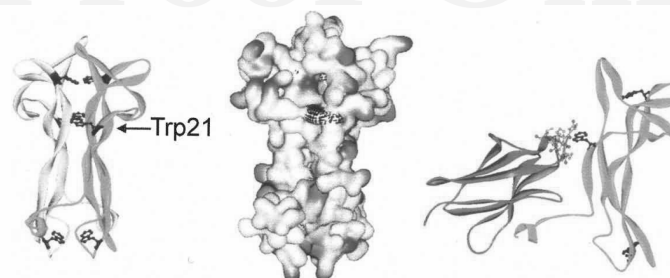


**Figure 7.** Structure of NGF and its complex with the extracellular domain 5 of the TrkA receptor (PDB file 1www.pdb [Wiesmann et al. 1999]). The panels show a scheme of dimeric NGF with the Trp residues marked (black, *left*), the surface of dimeric NGF with the surface of Trp residues marked (black, *middle*), and the complex of a monomeric subunit of NGF with TrkA (*right*), where Trp<sup>21</sup> of NGF and the surrounding residues of domain 5 of TrkA (8 Å distance) are shown in detail.

after an energy transfer to tryptophan an emission at 345 nm (Kliemann et al. 2004).

Fluorescence kinetics were carried out either on a FluoroMax 2 using conditions mentioned above or by stopped flow experiments on a SX.18MV spectrometer (Applied Photophysics). In the latter case, fluorescence was detected using a cut-off filter of 320 nm (cp = 0.4 mg/mL) or by single wavelength detection (cp = 1.5 mg/mL). Fluorescence spectra from denaturation kinetics at different emission wavelengths were reconstituted by calculating the specific fluorescence of the native, intermediate, and denatured state using an equation for a serial first-order reaction.

#### Circular dichroism (CD) spectroscopy

Far UV-CD spectra were recorded on a Jasco J710 spectropolarimeter. Equilibrium transitions of the NGF-coupled pro-peptide (100 µg/mL) were recorded at 220 nm in 50 mM Na-phosphate, pH 7.0 at 20°C in a 1-cm cuvette. Rapid structural changes were followed at 220 nm by stopped flow experiments on a π-star spectropolarimeter (Applied Photophysics). The final protein concentrations of both folding and unfolding reactions were 1 mg/mL.

#### H/D exchange-coupled MALDI-TOF mass spectrometry

Determination of the deuterium incorporation by exchange of the amide protons of peptide bonds was carried out by MALDI-TOF mass spectrometry using a BRUKER Reflex II mass spectrometer (BRUKER Daltonik GmbH). Experimental details are described in the Supplemental Material. In short, proNGF was incubated in D<sub>2</sub>O for 2 min. Subsequently, it was digested with pepsin, and the resulting fragments were analyzed by MALDI-ToF. For the alignments of the obtained proteolytic fragments, the program FindPept (<http://www.expasy.ch/tools/findpept.html>) was used.

#### Acknowledgments

We thank Renate Nitsch for technical assistance and Angelika Schierhorn for help in mass spectroscopy. This work was

supported by the Deutsche Forschungsgemeinschaft (grant SCHW 375/4 to E.S. and R.R.).

#### References

- Bai, Y., Milne, J.S., Mayne, L., and Englander, S.W. 1993. Primary structure effects on peptide group hydrogen exchange. *Proteins* **17**: 75–86.
- Barde, Y.A. 1990. The nerve growth factor family. *Prog. Growth Factor Res.* **2**: 237–248.
- Bothwell, M.A. and Shooter, E.M. 1977. Dissociation equilibrium constant of β nerve growth factor. *J. Biol. Chem.* **252**: 8532–8536.
- Böttinger, E.P., Factor, V.M., Tsang, M.L., Weatherbee, J.A., Kopp, J.B., Qian, S.W., Wakefield, L.M., Roberts, A.B., Thorgeirsson, S.S., and Sporn, M.B. 1996. The recombinant proregion of transforming growth factor β1 (latency-associated peptide) inhibits active transforming growth factor β1 in transgenic mice. *Proc. Natl. Acad. Sci.* **93**: 5877–5882.
- Bradshaw, R.A., Blundell, T.L., Lapatto, R., McDonald, N.Q., and Murray-Rust, J. 1993. Nerve growth factor revisited. *Trends Biochem. Sci.* **18**: 48–52.
- Buczek, O., Olivera, B.M., and Bulaj, G. 2004. Propeptide does not act as an intramolecular chaperone but facilitates protein disulfide isomerase-assisted folding of a conotoxin precursor. *Biochemistry* **43**: 1093–1101.
- Buevich, A.V., Shinde, U.P., Inouye, M., and Baum, J. 2001. Backbone dynamics of the natively unfolded pro-peptide of subtilisin by heteronuclear NMR relaxation studies. *J. Biomol. NMR* **20**: 233–249.
- Casaccia-Bonnel, P., Carter, B.D., Dobrowsky, R.T., and Chao, M.V. 1996. Death of oligodendrocytes mediated by the interaction of nerve growth factor with its receptor p75. *Nature* **383**: 716–719.
- Cohen, P., Sutter, A., Landreth, G., Zimmermann, A., and Shooter, E.M. 1980. Oxidation of tryptophan-21 alters the biological activity and receptor binding characteristics of mouse nerve growth factor. *J. Biol. Chem.* **255**: 2949–2954.
- De Young, L.R., Burton, L.E., Liu, J., Powell, M.F., Schmelzer, C.H., and Skelton, N.J. 1996. RhNGF slow unfolding is not due to proline isomerization: Possibility of a cystine knot loop-threading mechanism. *Protein Sci.* **5**: 1554–1566.
- Degnin, C., Jean, F., Thomas, G., and Christian, J.L. 2004. Cleavages within the prodomain direct intracellular trafficking and degradation of mature bone morphogenetic protein-4. *Mol. Biol. Cell* **15**: 5012–5020.
- Drinkwater, C.C., Suter, U., Angst, C., and Shooter, E.M. 1991. Mutation of tryptophan-21 in mouse nerve growth factor (NGF) affects binding to the fast NGF receptor but not induction of neurites on PC12 cells. *Proc. Biol. Sci.* **246**: 307–313.
- Eisenberg, D., Weiss, R.M., and Terwilliger, T.C. 1984. The hydrophobic moment detects periodicity in protein hydrophobicity. *Proc. Natl. Acad. Sci.* **81**: 140–144.
- Ermfors, P., Ibanez, C.F., Ebendal, T., Olson, L., and Persson, H. 1990. Molecular cloning and neurotrophic activities of a protein with structural similarities to nerve growth factor: Developmental and topographical expression in the brain. *Proc. Natl. Acad. Sci.* **87**: 5454–5458.

Proof Only

## Interaction of NGF with its pro-peptide

- Fahnestock, M., Yu, G., and Coughlin, M.D. 2004. ProNGF: A neurotrophic or an apoptotic molecule? *Prog. Brain Res.* **146**: 107–110.
- Fairlie, W.D., Zhang, H.P., Wu, W.M., Pankhurst, S.L., Bauskin, A.R., Russell, P.K., Brown, P.K., and Breit, S.N. 2001. The propeptide of the transforming growth factor- $\beta$  superfamily member, macrophage inhibitory cytokine-1 (MIC-1), is a multifunctional domain that can facilitate protein folding and secretion. *J. Biol. Chem.* **276**: 16911–16918.
- Feeney, B. and Clark, A.C. 2005. Reassembly of active caspase-3 is facilitated by the propeptide. *J. Biol. Chem.* **280**: 39772–39785.
- Frade, J.M., Rodriguez-Tebar, A., and Barde, Y.A. 1996. Induction of cell death by endogenous nerve growth factor through its p75 receptor. *Nature* **383**: 166–168.
- Gallagher, T., Gilliland, G., Wang, L., and Bryan, P. 1995. The prosegment-subtilisin BPN' complex: Crystal structure of a specific 'foldase.' *Structure* **3**: 907–914.
- Gray, A.M. and Mason, A.J. 1990. Requirement for activin A and transforming growth factor- $\beta$  1 pro-regions in homodimer assembly. *Science* **247**: 1328–1330.
- Hasan, W., Pedchenko, T., Krizan-Agbas, D., Baum, L., and Smith, P.G. 2003. Sympathetic neurons synthesize and secrete pro-nerve growth factor protein. *J. Neurobiol.* **57**: 38–53.
- He, X.L. and Garcia, K.C. 2004. Structure of nerve growth factor complexed with the shared neurotrophin receptor p75. *Science* **304**: 870–875.
- Hidaka, Y., Ohno, M., Hemmasi, B., Hill, O., Forssmann, W.G., and Shimonishi, Y. 1998. In vitro disulfide-coupled folding of guanylyl cyclase-activating peptide and its precursor protein. *Biochemistry* **37**: 8498–8507.
- Hillger, F., Herr, G., Rudolph, R., and Schwarz, E. 2005. Biophysical comparison of BMP-2, ProBMP-2, and the free pro-peptide reveals stabilization of the pro-peptide by the mature growth factor. *J. Biol. Chem.* **280**: 14974–14980.
- Hohn, A., Leibrock, J., Bailey, K., and Barde, Y.A. 1990. Identification and characterization of a novel member of the nerve growth factor/brain-derived neurotrophic factor family. *Nature* **344**: 339–341.
- Ikemura, H., Takagi, H., and Inouye, M. 1987. Requirement of pro-sequence for the production of active subtilisin E in *Escherichia coli*. *J. Biol. Chem.* **262**: 7859–7864.
- Jain, S.C., Shinde, U., Li, Y., Inouye, M., and Berman, H.M. 1998. The crystal structure of an autoprocessed Ser221Cys-subtilisin E-propeptide complex at 2.0 Å resolution. *J. Mol. Biol.* **284**: 137–144.
- Kliemann, M., Rattenholl, A., Golbik, R., Balbach, J., Lilie, H., Rudolph, R., and Schwarz, E. 2004. The mature part of proNGF induces the structure of its pro-peptide. *FEBS Lett.* **566**: 207–212.
- LaLonde, J.M., Zhao, B., Janson, C.A., D'Alessio, K.J., McQueney, M.S., Orsini, M.J., Debouck, C.M., and Smith, W.W. 1999. The crystal structure of human procathepsin K. *Biochemistry* **38**: 862–869.
- Lee, R., Kermani, P., Teng, K.K., and Hempstead, B.L. 2001. Regulation of cell survival by secreted proneurotrophins. *Science* **294**: 1945–1948.
- Lilie, H., Jaenicke, R., and Buchner, J. 1995. Characterization of a quaternary-structured folding intermediate of an antibody Fab-fragment. *Protein Sci.* **4**: 917–924.
- McDonald, N.O., Lapatto, R., Murray-Rust, J., Gunning, J., Wlodawer, A., and Blundell, T.L. 1991. New protein fold revealed by a 2.3-Å resolution crystal structure of nerve growth factor. *Nature* **354**: 411–414.
- Nykjaer, A., Lee, R., Teng, K.K., Jansen, P., Madsen, P., Nielsen, M.S., Jacobsen, C., Kliemann, M., Schwarz, E., Willnow, T.E., et al. 2004. Sortilin is essential for proNGF-induced neuronal cell death. *Nature* **427**: 843–848.
- Podobnik, M., Kuhelj, R., Turk, V., and Turk, D. 1997. Crystal structure of the wild-type human procathepsin B at 2.5 Å resolution reveals the native active site of a papain-like cysteine protease zymogen. *J. Mol. Biol.* **271**: 774–788.
- Rattenholl, A., Lilie, H., Grossmann, A., Stern, A., Schwarz, E., and Rudolph, R. 2001a. The pro-sequence facilitates folding of human nerve growth factor from *Escherichia coli* inclusion bodies. *Eur. J. Biochem.* **268**: 3296–3303.
- Rattenholl, A., Ruoppolo, M., Flagiello, A., Monti, M., Vinci, F., Marino, G., Lilie, H., Schwarz, E., and Rudolph, R. 2001b. Pro-sequence assisted folding and disulfide bond formation of human nerve growth factor. *J. Mol. Biol.* **305**: 523–533.
- Ruvinov, S., Wang, L., Ruan, B., Almog, O., Gilliland, G.L., Eisenstein, E., and Bryan, P.N. 1997. Engineering the independent folding of the subtilisin BPN' prodomain: Analysis of two-state folding versus protein stability. *Biochemistry* **36**: 10414–10421.
- Schmid, F.X. 1997. Spectral methods of characterizing protein conformation and conformational changes. In *Protein structure: A practical approach* (ed. T.E. Creighton), pp. 261–297. IRL-Press, Oxford, United Kingdom. **AU4**
- Seidah, N.G., Benjannet, S., Pareek, S., Savaria, D., Hamelin, J., Goulet, B., Laliberte, J., Lazure, C., Chretien, M., and Murphy, R.A. 1996. Cellular processing of the nerve growth factor precursor by the mammalian pro-protein convertases. *Biochem. J.* **314**: 951–960.
- Shinde, U. and Inouye, M. 2000. Intramolecular chaperones: Polypeptide extensions that modulate protein folding. *Semin. Cell Dev. Biol.* **11**: 35–44.
- Shinde, U., Li, Y., Chatterjee, S., and Inouye, M. 1993. Folding pathway mediated by an intramolecular chaperone. *Proc. Natl. Acad. Sci.* **90**: 6924–6928.
- Sorenson, P., Winther, J.R., Kaarsholm, N.C., and Poulsen, F.M. 1993. The pro region required for folding of carboxypeptidase Y is a partially folded domain with little regular structural core. *Biochemistry* **32**: 12160–12166.
- Timm, D.E. and Neet, K.E. 1992. Equilibrium denaturation studies of mouse  $\beta$ -nerve growth factor. *Protein Sci.* **1**: 236–244.
- Weissman, J.S. and Kim, P.S. 1992. The pro region of BPTI facilitates folding. *Cell* **71**: 841–851.
- Wiesmann, C., Ullsch, M.H., Bass, S.H., and de Vos, A.M. 1999. Crystal structure of nerve growth factor in complex with the ligand-binding domain of the TrkA receptor. *Nature* **401**: 184–188.
- Winther, J.R. and Sorensen, P. 1991. Propeptide of carboxypeptidase Y provides a chaperone-like function as well as inhibition of the enzymatic activity. *Proc. Natl. Acad. Sci.* **88**: 9330–9334.
- Wise, R.J., Pittman, D.D., Handin, R.I., Kaufman, R.J., and Orkin, S.H. 1988. The propeptide of von Willebrand factor independently mediates the assembly of von Willebrand multimers. *Cell* **52**: 229–236.
- Zhang, Z. and Smith, D.L. 1993. Determination of amide hydrogen exchange by mass spectrometry: a new tool for protein structure elucidation. *Protein Sci.* **2**: 522–531.

## Änderungen der Korrektur- zur Druckversion :

- In Abbildung 3A sind die Fluoreszenzdaten als dicke Line und die CD-Daten als Punkte dargestellt.
- Das obere Fluoreszenzspektrum in Abbildung 5 resultiert vom nativen proNGF und die untere vom partiell denaturiertem proNGF (2 M GdmCl).
- Die Kreise im Chevron-Plot in Abbildung 6 symbolisieren die Daten der *stopped-flow*-Fluoreszenzmessung während der De- und Renaturierung des Pro-Peptids im proNGF. Die schwarzen Kreise zeigen den Übergang zwischen nativen Zustand bzw. ersten Intermediatzustand und dem zweiten Intermediatzustand. Die weißen Kreise bilden den Übergang zwischen zweitem Intermediatzustand und dem entfalteten Zustand ab. Die Dreiecke resultieren aus der *stopped-flow*-CD-Messung.

by reaction  $j$  producing (consuming) metabolite  $i$  by:

$$\dot{v}_{ij} = |S_{ij}|v_j$$

#### Random uptake conditions

We choose randomly  $X\%$  (where  $X = 10, 50$  or  $80$ ) of the 89 potential input substrates that *E. coli* consumes in addition to the minimal uptake basis. For each of the transport reactions, we set the uptake rate to 20 mmol per gram of dry weight per hour. As there are a very large number of possible combinations of the selected input substrates, we repeat this process 5,000 times and average over each realization.

#### The hit-and-run method

We select a set of basis vectors spanning the solution space using singular-value decomposition. Because the reaction fluxes must be positive, the 'bouncer' is constrained to the part of the solution space that intersects the positive orthant. We constrain the bouncer within a hypersphere of radius  $R_{\max}$  and outside a hypersphere of radius  $R_{\min} < R_{\max}$ , where we find that the sampling results are independent of the choices of  $R_{\min}$  and  $R_{\max}$ . Starting from a random initial point inside the positive flux cone in a randomly chosen direction, the bouncer travels deterministically a distance  $d$  between sample points. Each sample point, corresponding to a solution vector where the components are the individual fluxes, is normalized by projection onto the unit sphere. After every  $l$ th bounce off the internal walls of the flux cone, the direction of the bouncer is randomized.

#### High-flux backbone

For each metabolite we keep only the reactions with the largest flux that produces and consumes the metabolite. Metabolites that are not produced (consumed) are discounted. Subsequently, a directed link is introduced between two metabolites A and B if (1) A is a substrate of the most active reaction producing B, and (2) B is a product of the maximal reaction consuming A. We consider only metabolites that are connected to at least one other metabolite after steps (1) and (2). For clarity, we remove P<sub>i</sub>, PP<sub>i</sub> and ADP. Further details and figures are provided in the Supplementary Information.

Received 29 August; accepted 12 December 2003; doi:10.1038/nature02289.

- Jeong, H., Tombor, B., Albert, R., Oltvai, Z. N. & Barabási, A.-L. The large-scale organization of metabolic networks. *Nature* **407**, 651–654 (2000).
- Wagner, A. & Fell, D. A. The small world inside large metabolic networks. *Proc. R. Soc. Lond. B* **268**, 1803–1810 (2001).
- Ravasz, E., Somera, A. L., Mongru, D. A., Oltvai, Z. N. & Barabási, A.-L. Hierarchical organization of modularity in metabolic networks. *Science* **297**, 1551–1555 (2002).
- Holme, P., Huss, M. & Jeong, H. Subnetwork hierarchies of biochemical pathways. *Bioinformatics* **19**, 532–538 (2003).
- Savageau, M. A. *Biochemical Systems Analysis: a Study of Function and Design in Molecular Biology* (Addison-Wesley, Reading, MA, 1976).
- Heinrich, R. & Schuster, S. *The Regulation of Cellular Systems* (Chapman & Hall, New York, 1996).
- Goldbeter, A. *Biochemical Oscillations and Cellular Rhythms: the Molecular Bases of Periodic and Chaotic Behavior* (Cambridge Univ. Press, Cambridge, UK, 1996).
- Edwards, J. S. & Palsson, B. O. The *Escherichia coli* MG1655 *in silico* metabolic genotype: its definition, characteristics, and capabilities. *Proc. Natl Acad. Sci. USA* **97**, 5528–5533 (2000).
- Edwards, J. S., Ibarra, R. U. & Palsson, B. O. *In silico* predictions of *Escherichia coli* metabolic capabilities are consistent with experimental data. *Nature Biotechnol.* **19**, 125–130 (2001).
- Ibarra, R. U., Edwards, J. S. & Palsson, B. O. *Escherichia coli* K-12 undergoes adaptive evolution to achieve *in silico* predicted optimal growth. *Nature* **420**, 186–189 (2002).
- Edwards, J. S., Ramakrishna, R. & Palsson, B. O. Characterizing the metabolic phenotype: a phenotype phase plane analysis. *Biotechnol. Bioeng.* **77**, 27–36 (2002).
- Segre, D., Vitkup, D. & Church, G. M. Analysis of optimality in natural and perturbed metabolic networks. *Proc. Natl Acad. Sci. USA* **99**, 15112–15117 (2002).
- Blattner, F. R. *et al.* The complete genome sequence of *Escherichia coli* K-12. *Science* **277**, 1453–1474 (1997).
- Gerdes, S. Y. *et al.* Experimental determination and system level analysis of essential genes in *Escherichia coli* MG1655. *J. Bacteriol.* **185**, 5673–5684 (2003).
- Emmerling, M. *et al.* Metabolic flux responses to pyruvate kinase knockout in *Escherichia coli*. *J. Bacteriol.* **184**, 152–164 (2002).
- Smith, R. L. Efficient Monte-Carlo procedures for generating points uniformly distributed over bounded regions. *Oper. Res.* **32**, 1296–1308 (1984).
- Lovász, L. Hit-and-run mixes fast. *Math. Program.* **86**, 443–461 (1999).
- Goh, K. L., Kahng, B. & Kim, D. Universal behavior of load distribution in scale-free networks. *Phys. Rev. Lett.* **87**, 278701 (2001).
- Barabási, A.-L. & Albert, R. Emergence of scaling in random networks. *Science* **286**, 509–512 (1999).
- Barthelemy, M., Gondran, B. & Guichard, E. Spatial structure of the Internet traffic. *Physica A* **319**, 633–642 (2003).
- Ma, H. W. & Zeng, A. P. The connectivity structure, giant strong component and centrality of metabolic networks. *Bioinformatics* **19**, 1423–1430 (2003).
- Dandekar, T., Schuster, S., Snel, B., Huynen, M. & Bork, P. Pathway alignment: application to the comparative analysis of glycolytic enzymes. *Biochem. J.* **343**, 115–124 (1999).
- Schuster, S., Fell, D. A. & Dandekar, T. A general definition of metabolic pathways useful for systematic organization and analysis of complex metabolic networks. *Nature Biotechnol.* **18**, 326–332 (2000).
- Stelling, J., Klamt, S., Bettenbrock, K., Schuster, S. & Gilles, E. D. Metabolic network structure determines key aspects of functionality and regulation. *Nature* **420**, 190–193 (2002).
- Sauer, U. *et al.* Metabolic flux ratio analysis of genetic and environmental modulations of *Escherichia coli* central carbon metabolism. *J. Bacteriol.* **181**, 6679–6688 (1999).
- Canonaco, F. *et al.* Metabolic flux response to phosphoglucose isomerase knock-out in *Escherichia coli* and impact of overexpression of the soluble transhydrogenase UdhA. *FEMS Microbiol. Lett.* **204**, 247–252 (2001).

- Fischer, E. & Sauer, U. Metabolic flux profiling of *Escherichia coli* mutants in central carbon metabolism using GC-MS. *Eur. J. Biochem.* **270**, 880–891 (2003).
- Hartwell, L. H., Hopfield, J. J., Leibler, S. & Murray, A. W. From molecular to modular cell biology. *Nature* **402**, C47–C52 (1999).
- Wolf, D. M. & Arkin, A. P. Motifs, modules and games in bacteria. *Curr. Opin. Microbiol.* **6**, 125–134 (2003).

Supplementary Information accompanies the paper on [www.nature.com/nature](http://www.nature.com/nature).

**Acknowledgements** We thank M. Bárász, J. Becker, E. Ravasz, A. Vazquez and S. Wuchty for discussions; and B. Palsson and S. Schuster for comments on the manuscript. Research at Eötvös University was supported by the Hungarian National Research Grant Foundation (OTKA), and work at the University of Notre Dame and at Northwestern University was supported by the US Department of Energy, the NIH and the NSF.

**Competing interests statement** The authors declare that they have no competing financial interests.

**Correspondence** and requests for materials should be addressed to A.-L.B. (alb@nd.edu).

## Sortilin is essential for proNGF-induced neuronal cell death

Anders Nykjaer<sup>1,2</sup>, Ramee Lee<sup>3</sup>, Kenneth K. Teng<sup>3</sup>, Pernille Jansen<sup>1,4</sup>, Peder Madsen<sup>1</sup>, Morten S. Nielsen<sup>1</sup>, Christian Jacobsen<sup>1</sup>, Marco Kliewmann<sup>3</sup>, Elisabeth Schwarz<sup>3</sup>, Thomas E. Willnow<sup>2,4</sup>, Barbara L. Hempstead<sup>3</sup> & Claus M. Petersen<sup>1</sup>

<sup>1</sup>Department of Medical Biochemistry, Ole Worms Allé 170, Aarhus University, and <sup>2</sup>ReceptIcon Aps, Gustav Wieds vej 10, DK-8000 Aarhus C, Denmark

<sup>3</sup>Weill Medical College of Cornell University, New York, New York 10021, USA

<sup>4</sup>Max-Delbrück-Center for Molecular Medicine, 13125 Berlin, Germany

<sup>5</sup>Institute for Biotechnology, Martin-Luther-Universität, Halle-Wittenberg, 06120 Halle, Germany

Sortilin<sup>1</sup> (~95 kDa) is a member of the recently discovered family of Vps10p-domain receptors<sup>2,3</sup>, and is expressed in a variety of tissues, notably brain, spinal cord and muscle. It acts as a receptor for neurotensin<sup>4,5</sup>, but predominates in regions of the nervous system that neither synthesize nor respond to this neuropeptide<sup>6</sup>, suggesting that sortilin has additional roles. Sortilin is expressed during embryogenesis<sup>7</sup> in areas where nerve growth factor (NGF) and its precursor, proNGF, have well-characterized effects<sup>6,7</sup>. These neurotrophins can be released by neuronal tissues<sup>8,9</sup>, and they regulate neuronal development through cell survival and cell death signalling. NGF regulates cell survival and cell death via binding to two different receptors, TrkA and p75<sup>NTR</sup> (ref. 10). In contrast, proNGF selectively induces apoptosis through p75<sup>NTR</sup> but not TrkA<sup>11</sup>. However, not all p75<sup>NTR</sup>-expressing cells respond to proNGF, suggesting that additional membrane proteins are required for the induction of cell death. Here we report that proNGF creates a signalling complex by simultaneously binding to p75<sup>NTR</sup> and sortilin. Thus sortilin acts as a co-receptor and molecular switch governing the p75<sup>NTR</sup>-mediated pro-apoptotic signal induced by proNGF.

Binding of NGF was examined by surface-plasmon resonance (SPR). As demonstrated in Fig. 1a, sortilin bound mature NGF with moderate affinity (dissociation constant ( $K_d$ ) ~90 nM). In contrast, the affinity of NGF for p75<sup>NTR</sup> and TrkA was high ( $K_d$  1–2 nM), in accordance with previous studies in cells<sup>11–13</sup>. As the NGF precursor (proNGF) may escape intracellular processing and be released extracellularly, we next examined binding of proNGF<sup>9,11,14,15</sup>. Whereas lack of processing reduces the affinity of proNGF for p75<sup>NTR</sup> and TrkA ( $K_d$  ~15–20 nM), it results in a much higher affinity ( $K_d$  ~5 nM) for sortilin (Fig. 1a). This is surprising because



## letters to nature

proNGF has been reported to interact with cellular p75<sup>NTR</sup>, but not TrkA, with a higher affinity ( $K_d \sim 0.2$  nM) than mature NGF, and to selectively induce p75<sup>NTR</sup>-dependent apoptosis in neurons, smooth muscle cells and oligodendrocytes<sup>8,11</sup>. Our data may reflect the participation of a p75<sup>NTR</sup> co-receptor, and this receptor might be sortilin (see below).

To examine the structural basis of proNGF binding, we produced the pro domain of proNGF as a glutathione *S*-transferase fusion protein (GST-pro) (Fig. 1b). The GST-pro protein bound to sortilin with an affinity very similar to that of proNGF ( $K_d \sim 8$  nM), but not to p75<sup>NTR</sup> or TrkA (Fig. 1a). Additional experiments further demonstrated that binding of proNGF to sortilin was inhibited markedly (>75%) by neurotensin, and was almost abolished in the presence of GST-pro (Fig. 1c). Thus, the pro domain constitutes the structural basis for the high-affinity binding between proNGF and sortilin.

We next assessed binding of proNGF to cellular sortilin. We transfected 293 cells without endogenous sortilin with the receptor constructs indicated in Fig. 2a, and evaluated binding of proNGF at 37 °C. Control cells demonstrated no binding or uptake of ligand, whereas cells expressing wild-type sortilin exhibited significant endocytosis of proNGF (Fig. 2b), but not of mature NGF (Fig. 2c). The observed uptake was hampered strongly in the presence of excess neurotensin or GST-pro (data not shown). Furthermore, transfectants expressing a mutant sortilin protein (sortilin(mut)) that accumulates on the plasma membrane owing to disrupted motifs for endocytosis<sup>16</sup>, displayed intense surface labelling with proNGF, but little uptake.

Binding and uptake of proNGF was also investigated in cells transfected with TrkA and p75<sup>NTR</sup>, and in cells expressing each of the two receptors in combination with sortilin (Fig. 2b). TrkA transfectants exhibited a very modest uptake of proNGF, and on co-transfection with sortilin, endocytosis of proNGF was comparable to that observed in cells expressing sortilin alone. In contrast, uptake of mature NGF was efficient in TrkA-expressing cells and was unaffected by co-transfection with sortilin (Fig. 2c). In p75<sup>NTR</sup> transfectants, proNGF as well as mature NGF was almost exclusively found on the plasma membrane, indicating a slow or insignificant endocytosis (Fig. 2b, c) consistent with prior observations<sup>17,18</sup>. However, coexpression of p75<sup>NTR</sup> with sortilin re-established uptake of proNGF, and coexpression with sortilin(mut), as well as with wild-type sortilin, induced a significant increase in surface-associated ligand, suggesting a synergistic rather than a simple

additive effect of sortilin and p75<sup>NTR</sup> coexpression.

The findings demonstrate that sortilin exhibits negligible binding of NGF, but also that it conveys a significantly higher capacity for uptake of proNGF than either of the two established receptors (that is, p75<sup>NTR</sup> and TrkA). Moreover, results in double transfectants suggest that sortilin and p75<sup>NTR</sup> cooperate to promote proNGF binding.

To characterize the molecular mechanisms underlying the putative cooperativity between p75<sup>NTR</sup> and sortilin, affinity crosslinking was performed. Crosslinking of <sup>125</sup>I-labelled proNGF to p75<sup>NTR</sup> and sortilin double transfectants produced labelled complexes of ~110, ~140 and ~240 kDa (Fig. 3a, lane 1), but was unproductive in single transfectants, suggesting that coexpression of sortilin and p75<sup>NTR</sup> is required for efficient binding at subnanomolar concentrations of proNGF (Fig. 3a, lanes 5–6). Furthermore, immunoprecipitation with receptor antisera established that both sortilin and p75<sup>NTR</sup> were components of the crosslinked adducts (Fig. 3a, lanes 7–8). Similar experiments performed on cells coexpressing p75<sup>NTR</sup> and sortilin(mut), which has a higher surface expression than wild-type sortilin<sup>16</sup>, resulted in a quantitative increase in crosslinked complexes (data not shown). Finally, generation of the crosslinking adducts was markedly reduced in the presence of unlabelled proNGF, neurotensin or GST-pro, implying that sortilin, as well as the NGF pro domain, is critical to complex formation (Fig. 3a, lanes 2–4).

We conclude that the ~240 kDa adduct probably represents a heterotrimeric complex comprising proNGF, sortilin and p75<sup>NTR</sup>, whereas the ~110 kDa and ~140 kDa species constitute proNGF in association with a single receptor. Expression of both receptors is required for efficient binding of proNGF, and our results support a model in which the pro domain and the 'mature' part of proNGF simultaneously engage sortilin and p75<sup>NTR</sup>, respectively.

Corresponding experiments established that proNGF does not form stable complexes with TrkA (Fig. 3b). In fact, crosslinking with proNGF using cells expressing all three receptors (TrkA, p75<sup>NTR</sup> and sortilin) resulted in ~110, ~140 and ~240 kDa adducts that could be precipitated with anti-sortilin (data not shown) and anti-p75<sup>NTR</sup> antibodies but not with TrkA-specific antiserum. Thus, proNGF discriminates between TrkA and p75<sup>NTR</sup> in cells that express both receptors in combination with sortilin.

In accordance with previous reports<sup>12,13</sup>, crosslinking using mature <sup>125</sup>I-labelled NGF yielded complexes with both p75<sup>NTR</sup> (~90 and ~180 kDa) and TrkA (~160 kDa) (Fig. 3c). However,

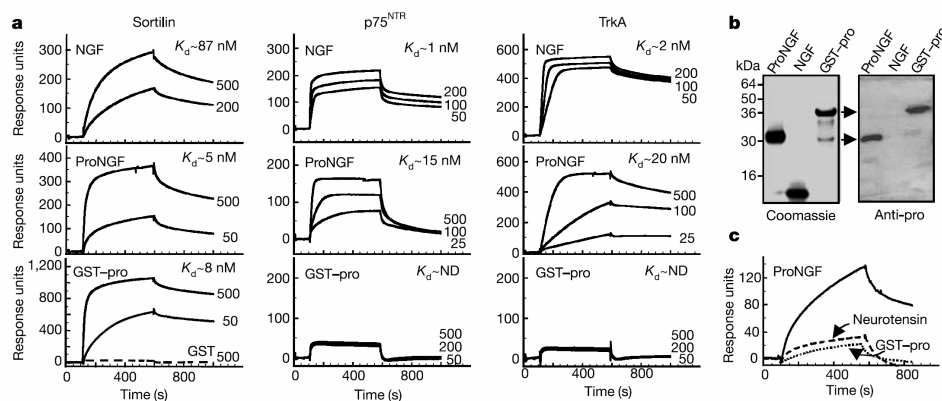


**Figure 1** SPR analysis of ligand binding. **a**, Binding of 20–1,000 nM NGF, proNGF and GST-pro to immobilized sortilin ( $51 \text{ fmol mm}^{-2}$ ), p75<sup>NTR</sup> ( $91 \text{ fmol mm}^{-2}$ ) and TrkA ( $66 \text{ fmol mm}^{-2}$ ). Calculated  $K_d$  values are indicated. **b**, SDS-PAGE analysis of ligands used in **a**. A Coomassie-stained gel (left panel) and a western blot (anti-pro domain

antibody; right panel) are shown. **c**, Binding of proNGF (25 nM) to sortilin ( $66 \text{ fmol mm}^{-2}$ ) in the absence or presence of 10  $\mu\text{M}$  neurotensin (dashed line) and 5  $\mu\text{M}$  GST-pro (dotted line). The SPR response obtained for the inhibitors alone has been subtracted.



letters to nature

no additional crosslinked complexes were observed when either of the two was coexpressed with sortilin, and sortilin single transfectants did not bind NGF. These results indicate that sortilin neither interacts with mature NGF nor is part of a complex formed on binding of mature NGF to p75<sup>NTR</sup> or TrkA.

We next examined whether sortilin and p75<sup>NTR</sup> physically associate on the cell membrane. Cells expressing both receptors were biolabelled and incubated in the absence or presence of proNGF, followed by treatment with a membrane-impermeable reducible crosslinker, lysis and immunoprecipitation using anti-p75<sup>NTR</sup> antibodies. Sortilin could be crosslinked directly to p75<sup>NTR</sup> (Fig. 3d). However, in the presence of proNGF, the relative amount of crosslinked and co-precipitated sortilin increased by about fivefold (3.9% to 18.4%). Equilibrium binding studies were then designed to determine whether p75<sup>NTR</sup> and sortilin coexpression might influence the specificity and affinity of ligand binding. As demonstrated in Fig. 3e, <sup>125</sup>I-labelled NGF bound to cells coexpressing sortilin and p75<sup>NTR</sup> with an estimated  $K_d$  of ~1.0 nM. This agrees with previous results<sup>12</sup> obtained in p75<sup>NTR</sup>-expressing cells, and as sortilin single transfectants did not bind mature NGF (data not shown), the data indicate that mature NGF binds strictly to p75<sup>NTR</sup>. In contrast, similar experiments with <sup>125</sup>I-labelled proNGF further indicated that sortilin and p75<sup>NTR</sup> cooperate in proNGF binding. Thus, cells expressing a single receptor type—either sortilin or p75<sup>NTR</sup>—did not bind <sup>125</sup>I-labelled proNGF (data not shown), whereas cells

coexpressing these receptors did. Scatchard analysis (Fig. 3e) suggested fewer binding sites for proNGF than for NGF in the double transfectants, but also a higher affinity for proNGF ( $K_d$  ~160 pM) that could not be accounted for by binding to any single receptor. Accordingly, A875 cells, which bind proNGF with high affinity<sup>11</sup>, express high levels of endogenous sortilin and p75<sup>NTR</sup>

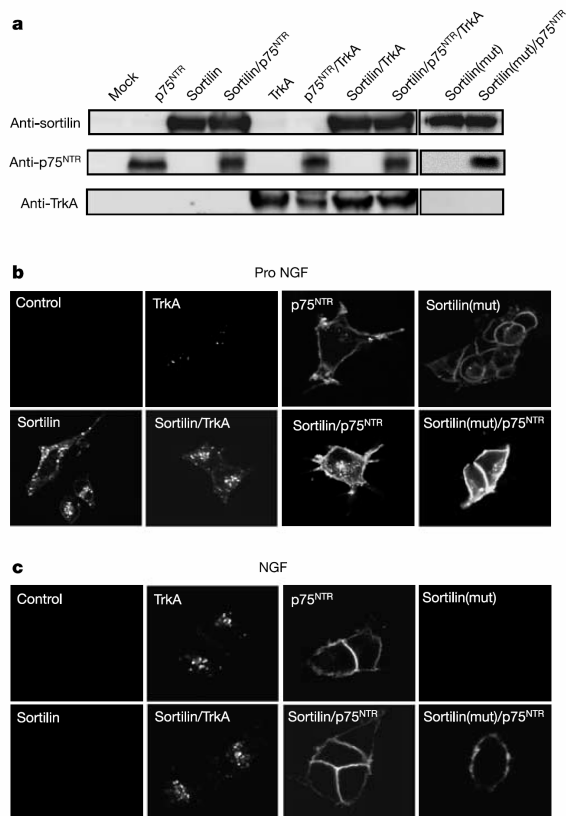


**Figure 2** Binding and uptake of proNGF and NGF in 293 cells. **a**, Western blot showing the level of receptor expression in the transfected 293 cells. **b, c**, Untransfected cells (control) and cells transfected with the indicated receptors were incubated (37 °C, 45 min) with 50 nM proNGF (**b**) or NGF (**c**) before fixation and staining with anti-NGF antibodies.

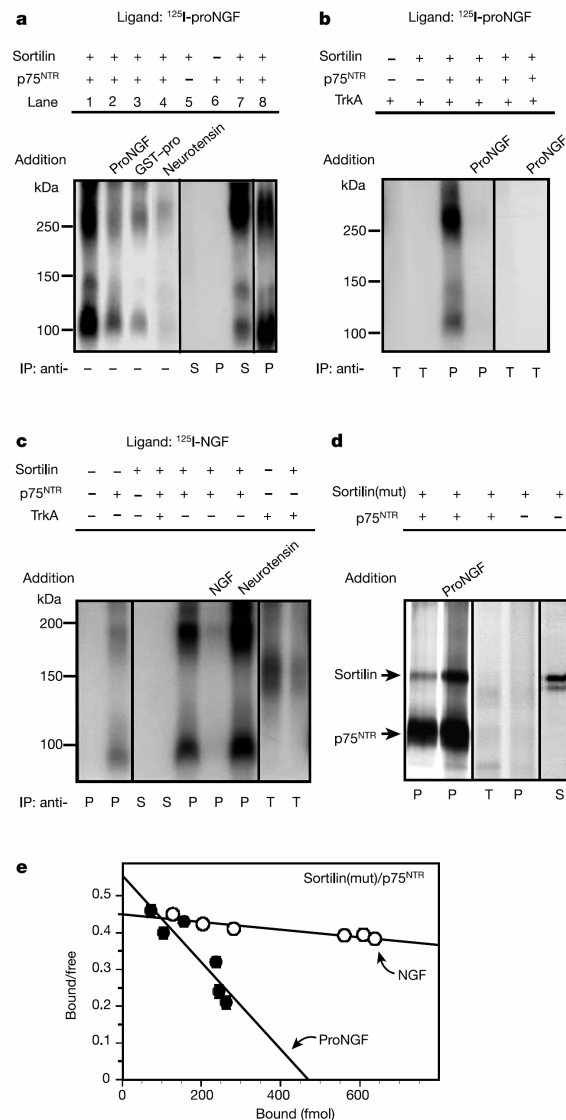


**Figure 3** ProNGF-induced formation of heterotrimeric complexes comprising sortilin and p75<sup>NTR</sup>. **a-c**, Crosslinking of <sup>125</sup>I-labelled proNGF (**a, b**) or <sup>125</sup>I-labelled NGF (**c**) to transfected 293 cells in the presence and absence of excess proNGF, NGF, GST-pro or neurotensin. Crude lysates (-) and immunoprecipitated proteins were subjected to SDS-PAGE and labelled bands were visualized by autoradiography. Antibodies used for immunoprecipitation (IP) of sortilin (S), p75<sup>NTR</sup> (P) and TrkA (T) are indicated. **d**, Biolabelled cells overexpressing sortilin(mut) and p75<sup>NTR</sup> were incubated with and without proNGF (25 nM) and treated with a reducible crosslinker. Autoradiographic bands resulting from reducing SDS-PAGE of immunoprecipitates are shown. **e**, Scatchard plot showing binding of radiolabelled NGF (open circles) and proNGF (closed circles) to cells expressing sortilin(mut) and p75<sup>NTR</sup>.

letters to nature

(Fig. 4a). The results support a model in which proNGF binds to and promotes the formation of a multi-component receptor complex comprising both sortilin and p75<sup>NTR</sup>.

ProNGF is more efficient than NGF in inducing apoptosis in superior cervical ganglion (SCG) neurons, vascular smooth muscle (SM-11) cells and oligodendrocytes, and in promoting chemotaxis and ligand binding in A875 melanoma cells<sup>8,11,19</sup>. These cell types all express significant levels of sortilin and p75<sup>NTR</sup> (Fig. 4a). We found that uptake of proNGF in dissociated SCG cultures was inhibited by the GST-pro protein (data not shown), which selectively inhibits binding to sortilin. Moreover, crosslinking of <sup>125</sup>I-labelled proNGF to SM-11 cells resulted in labelled adducts of ~110, ~140 and ~240 kDa, similar to those obtained in the p75<sup>NTR</sup> and sortilin double transfectants (Fig. 4b). These findings suggest that the biological effects of proNGF require coexpression of sortilin and p75<sup>NTR</sup>. To assess directly whether binding of proNGF to sortilin

regulates biological action, the ability of GST-pro and neurotensin to impair proNGF actions was evaluated. In order to minimize conversion of proNGF into mature NGF, which might introduce a bias by facilitating survival in TrkA-positive cells, a furin-resistant mutant of proNGF<sup>11</sup> was used in all subsequent experiments, unless otherwise stated. In SM-11 cells co-expressing p75<sup>NTR</sup> and sortilin, furin-resistant proNGF was more effective than mature NGF in inducing cell death as assessed by a TdT-mediated dUTP nick end labelling (TUNEL) assay (Fig. 4c). In addition, wild-type proNGF induced apoptosis as effectively as furin-resistant proNGF (data not shown). Co-incubation of proNGF with an excess of neurotensin, or with excess GST-pro, but not GST alone, impaired the induction of cell death and apoptosis by more than 90% (Fig. 4c). Similar findings were obtained in cultured SCG neurons expressing sortilin and p75<sup>NTR</sup> as well as TrkA. Thus, both GST-pro and neurotensin significantly reduced proNGF-induced apoptosis in SCG neurons,

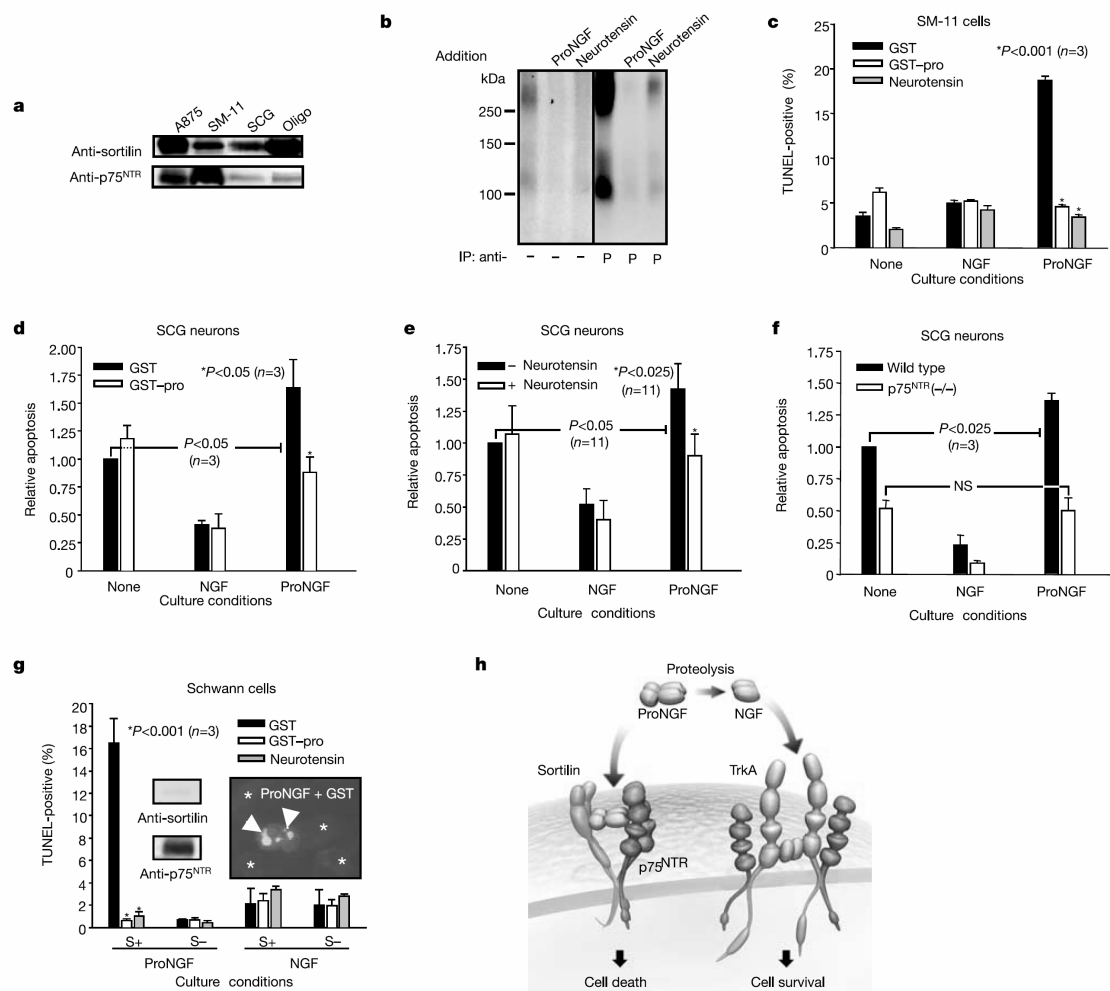


**Figure 4** Sortilin is required for the pro-apoptotic action of proNGF. **a**, Receptor expression in proNGF-responsive cell types. **b**, Crosslinking of <sup>125</sup>I-labelled proNGF to SM-11 cells and inhibition by unlabelled competitors. **c-e**, ProNGF-induced apoptosis (cell type indicated) and its inhibition by GST, GST-pro and neurotensin. The number of apoptotic and total cells counted per condition was 100/~300 (**d** and **f**) and 300/~1,100 (**e**). All values are normalized to apoptosis in the absence of any additions. **f**, Killing of SCG

neurons from wild-type and p75<sup>NTR</sup> knockout mice. **g**, ProNGF-induced apoptosis of Schwann cells transiently transfected with sortilin. Columns indicate per cent of TUNEL-positive cells among cells that express (S+) or lack (S-) sortilin. Left inset shows western blot of Schwann cell lysate; right inset shows apoptotic nuclei (TUNEL-positive, green) in transfectants expressing sortilin (red staining). Asterisk indicates an untransfected cell. **h**, Schematic model of receptor-complex formation.

whereas neither affected neuronal survival in response to mature NGF or on NGF withdrawal (Fig. 4d, e). As shown in Fig. 4f, p75<sup>NTR</sup>-deficient neurons from p75<sup>NTR</sup> knockout mice<sup>20</sup> that express sortilin in the absence of p75<sup>NTR</sup> (data not shown) exhibit NGF-dependent survival, but are resistant to proNGF-induced killing. A similar resistance to proNGF was seen in Schwann cells expressing p75<sup>NTR</sup> but not sortilin (Fig. 4g); however, after transfection with sortilin, Schwann cells became sensitive to proNGF-induced apoptosis. Approximately 95% of the cells that expressed sortilin (~18% of total) were TUNEL positive, and among all TUNEL-positive cells ~96% expressed both sortilin and p75<sup>NTR</sup>. This sensitivity to proNGF-induced killing was reversed by co-incubation with GST-pro (Fig. 4g) and neurotensin, which blocked binding of proNGF to sortilin. It follows that both receptors are obligate for the induction of proNGF-mediated cell death, whereas sortilin expression has no impact on NGF responsiveness under these circumstances.

We conclude that proNGF targets and promotes formation of a signalling complex comprising endogenous sortilin and p75<sup>NTR</sup>, and that both receptors are required for proNGF-mediated apoptosis. In contrast, mature NGF preferentially binds p75<sup>NTR</sup> and/or TrkA, with sortilin having little or no bearing on NGF-initiated signalling.

Our study indicates that the neurotrophins use not two but three distinct receptor classes to dictate and regulate opposing biological responses of survival and death. We identify sortilin as a biologically important neurotrophin receptor that targets the pro domain of proNGF with high affinity. The present data suggest that sortilin is a required component for transmitting proNGF-dependent death signals via p75<sup>NTR</sup>. Together with p75<sup>NTR</sup>, sortilin facilitates the formation of a composite high-affinity binding site for proNGF (Fig. 4h). Thus, sortilin serves as a co-receptor and molecular switch, enabling neurons expressing Trk and p75<sup>NTR</sup> to respond to a pro-neurotrophin and to initiate pro-apoptotic rather than pro-survival actions. In the absence of sortilin, regulated activity of extracellular proteases may cleave proNGF to mature NGF<sup>11</sup>, promoting Trk-mediated survival signals (Fig. 4h). In conclusion, NGF-induced neuronal survival and death is far more complicated than previously appreciated, as it depends on an intricate balance between proNGF and mature NGF, as well as on the spatial and temporal expression of three distinct receptors: TrkA, p75<sup>NTR</sup> and sortilin. As sortilin is but one member of the Vps10p-domain receptor family expressed in the nervous system, future studies should show whether other pro-neurotrophins use related Vps10p-containing receptors to switch biological responsiveness to neurotrophin isoforms. □

## Methods

### Recombinant proteins and radiolabelling

Human proNGF and mature NGF generated in *Escherichia coli*<sup>21</sup> were a gift from Scil Proteins GmbH. Radioiodinated ligands<sup>22,23</sup> (~3,000 d.p.m. fmol<sup>-1</sup>) were used within 48 h of iodination and their integrity and bioactivity was assayed by SDS-polyacrylamide gel electrophoresis (PAGE), PC12 cell neurogenesis (NGF) and apoptosis of p75<sup>NTR</sup>-expressing vascular smooth muscle cells (proNGF). Mature NGF and furin-resistant mouse proNGF were purified from media of transfected 293 cells<sup>11</sup>. The NGF pro domain (amino acids E19 to R121) was expressed in *E. coli* as a GST fusion protein and purified on glutathione-agarose beads. The luminal domain of sortilin was expressed and purified as described<sup>5</sup>. p75<sup>NTR</sup>-Fc and TrkA-Fc (fusion proteins) were from R&D Systems.

### SPR analysis, equilibrium binding and western blotting

The SPR analysis was performed essentially as described<sup>5,24</sup>. The receptors were immobilized (at 10–15 µg ml<sup>-1</sup>) on a CM5 chip and remaining coupling sites were blocked with 1 M ethanolamine. Sample and running buffer was 10 mM HEPES, 150 mM (NH<sub>4</sub>)<sub>2</sub>SO<sub>4</sub>, 1.5 mM CaCl<sub>2</sub>, 1 mM EGTA, 0.005% Tween-20 pH 7.4. After each analytic cycle the sensor chip was regenerated in a 10 mM glycine-HCl buffer. The SPR signal was expressed in relative response units (RU); that is, the response obtained in a control flow channel was subtracted. Kinetic parameters were determined using BIAevaluation 3.1 software. Equilibrium-binding studies were performed as described<sup>5</sup>. In brief, the cells (2 × 10<sup>6</sup> ml<sup>-1</sup>) were incubated (4°C, 40 min) with radioiodinated NGF or proNGF (2–20 × 10<sup>6</sup> M) in the presence or absence of a 500-fold molar excess of NGF or

neurotensin, respectively. Bound ligand was then separated from free ligand by centrifugation through calf serum. Mean values of triplicates (from two independent experiments) were evaluated using the PRISM program.

Western blotting, after reducing SDS-PAGE, was performed using a rabbit antibody (1:1,000) directed against the pro domain of NGF (amino acids 23–81) of human NGF<sup>8</sup> and horseradish-peroxidase-conjugated swine anti-rabbit immunoglobulin (Amersham Biosciences).

### Transfected cell lines

Parental 293 cells and transfectants expressing p75<sup>NTR</sup> or TrkA<sup>12</sup> were transfected with wild-type sortilin<sup>5</sup> or the sortilin(mut) variant impaired in endocytosis (alanine substituted for Y14, L17, L51 and L52 in the cytoplasmic tail)<sup>16</sup>, and selected using zeocin. Primary rat Schwann cells<sup>25</sup>, plated on polylysine-coated plates, were transfected with pcDNA wild-type sortilin<sup>5</sup> or pcDNA alone using calcium phosphate.

### Crosslinking, biolabelling and immunoprecipitation

Cells (2 × 10<sup>6</sup> ml<sup>-1</sup>) were incubated (4°C, 2 h) with radioiodinated proNGF or NGF (400 pM), in the absence or presence of 100 nM unlabelled proNGF, 40 µM neurotensin or 200 nM GST or GST-pro, followed by crosslinking (15 min) with 4 mM 1-ethyl-3-[3-dimethylaminopropyl]carbodiimide and 25 mM DSS (Pierce). Washed cells were subsequently lysed in 1% Nonidet P40 buffer containing protease inhibitors and precipitations were performed using anti-p75<sup>NTR</sup> and anti-TrkA antisera<sup>15</sup>, and anti-sortilin antibody<sup>5</sup>.

Transfected cells were biolabelled (3–4 h) with L-[<sup>35</sup>S]cysteine and L-[<sup>35</sup>S]methionine, then incubated (20°C, 2 h) with or without 25 nM proNGF and, finally, treated (30 min) with 5 mM of the reducible crosslinker DTSSP (Pierce) before lysis in 1% Triton-X100 buffer containing protease inhibitors<sup>26</sup>. Immunoprecipitation was performed using rabbit anti-p75<sup>NTR</sup> (number 9993), anti-Trk (Santa Cruz) and anti-sortilin<sup>5</sup>. All precipitated proteins were analysed by reducing SDS-PAGE and were detected by autoradiography.

### Induction of apoptosis in various cells

A vascular smooth muscle cell line expressing human p75<sup>NTR</sup> but not TrkA<sup>27</sup> was incubated (16 h) with 2 ng ml<sup>-1</sup> of mature NGF or furin-resistant proNGF<sup>11</sup> in the presence of 50 nM GST or GST-pro, or 40 µM neurotensin. After fixation, cells were fixed, incubated with 4,6-diamidino-2-phenylindole (DAPI) and subjected to TUNEL analysis (Roche Molecular Biochemicals). Results represent the mean value of three independent experiments performed in triplicate. At least 300 cells per condition were counted.

Dissociated P0–P1 rat SCG neurons<sup>28</sup> or mouse SCG neurons obtained from p75<sup>NTR</sup> knockout mice<sup>29</sup> or wild-type littermates were plated on collagen-coated slides and maintained for 5 days in 50 ng ml<sup>-1</sup> NGF before use. Replicate cultures were rinsed five times with NGF-free medium and treated with or without the given additives, as indicated. After 36 h SCG cultures were processed for TUNEL analysis and counterstained with anti-neuronal-specific β-tubulin (Tuj1, Covance)<sup>11</sup>. TUNEL-positive neurons were scored blindly by the observer and at least 100 cells were counted for each culture condition.

Transfected Schwann cells were replated on 8-well slides (NUNC) at 20,000 cells per well. At 48 h after transfection, cells were treated (18 h) with 5 ng ml<sup>-1</sup> mature NGF, purified recombinant cleavage-resistant proNGF or diluent alone. After fixation, the cells were stained using mouse anti-sortilin antibody (Transduction Biolabs, anti-NTR3 612101) and rhodamine goat anti-mouse IgG followed by DAPI incubation, and then subjected to TUNEL analysis (Roche Molecular Biochemicals). At least 1,000 cells per condition were counted in a blinded manner, and results are representative of three independent experiments. Where appropriate, statistical significance was determined by Student's *t*-test.

Received 3 November; accepted 23 December 2003; doi:10.1038/nature02319.

- Petersen, C. M. *et al.* Molecular identification of a novel candidate sorting receptor purified from human brain by receptor-associated protein affinity chromatography. *J. Biol. Chem.* **272**, 3599–3605 (1997).
- Hermey, G. *et al.* Characterization of sorCS1, an alternatively spliced receptor with completely different cytoplasmic domains that mediate different trafficking in cells. *J. Biol. Chem.* **278**, 7390–7396 (2003).
- Jacobsen, L. *et al.* Activation and functional characterization of the mosaic receptor SorLA/LR11. *J. Biol. Chem.* **276**, 22788–22796 (2001).
- Mazella, J. *et al.* The 100-kDa neurotensin receptor is gp95/sortilin, a non-G-protein-coupled receptor. *J. Biol. Chem.* **273**, 26273–26276 (1998).
- Munck, P. C. *et al.* Propeptide cleavage conditions sortilin/neurotensin receptor-3 for ligand binding. *EMBO J.* **18**, 595–604 (1999).
- Sarret, P. *et al.* Distribution of NTS3 receptor/sortilin mRNA and protein in the rat central nervous system. *J. Comp. Neurol.* **461**, 483–505 (2003).
- Hermans-Borgmeyer, L., Hermey, G., Nykjaer, A. & Schaller, C. Expression of the 100-kDa neurotensin receptor sortilin during mouse embryonal development. *Brain Res. Mol. Brain Res.* **65**, 216–219 (1999).
- Beattie, M. S. *et al.* ProNGF induces p75-mediated death of oligodendrocytes following spinal cord injury. *Neuron* **36**, 375–386 (2002).
- Hasan, W., Pedchenko, T., Krizsan-Agbas, D., Baum, L. & Smith, P. G. Sympathetic neurons synthesize and secrete pro-nerve growth factor protein. *J. Neurobiol.* **57**, 38–53 (2003).
- Chao, M. V. Neurotrophins and their receptors: a convergence point for many signalling pathways. *Nature Rev. Neurosci.* **4**, 299–309 (2003).
- Lee, R., Kermani, P., Teng, K. K. & Hempstead, B. L. Regulation of cell survival by secreted pro-neurotrophins. *Science* **294**, 1945–1948 (2001).
- Esposito, D. *et al.* The cytoplasmic and transmembrane domains of the p75 and TrkA receptors regulate high affinity binding to nerve growth factor. *J. Biol. Chem.* **276**, 32687–32695 (2001).

## letters to nature

13. Mahadeo, D., Kaplan, L., Chao, M. V. & Hempstead, B. L. High affinity nerve growth factor binding displays a faster rate of association than p140trk binding. Implications for multi-subunit polypeptide receptors. *J. Biol. Chem.* **269**, 6884–6891 (1994).
14. Fahnestock, M., Michalski, B., Xu, B. & Coughlin, M. D. The precursor pro-nerve growth factor is the predominant form of nerve growth factor in brain and is increased in Alzheimer's disease. *Mol. Cell. Neurosci.* **18**, 210–220 (2001).
15. Heymach, J. V. Jr & Shooter, E. M. The biosynthesis of neurotrophin heterodimers by transfected mammalian cells. *J. Biol. Chem.* **270**, 12297–12304 (1995).
16. Nielsen, M. S. *et al.* The sortilin cytoplasmic tail conveys Golgi-endosome transport and binds the VHS domain of the GGA2 sorting protein. *EMBO J.* **20**, 2180–2190 (2001).
17. Gargano, N., Levi, A. & Alema, S. Modulation of nerve growth factor internalization by direct interaction between p75 and TrkA receptors. *J. Neurosci. Res.* **50**, 1–12 (1997).
18. Bronfman, F. C., Tcherpakov, M., Jovin, T. M. & Fainzilber, M. Ligand-induced internalization of the p75 neurotrophin receptor: a slow route to the signaling endosome. *J. Neurosci.* **23**, 3209–3220 (2003).
19. Shonukan, O., Bagayogo, I., McCreary, P., Chao, M. & Hempstead, B. Neurotrophin-induced melanoma cell migration is mediated through the actin-bundling protein fascin. *Oncogene* **22**, 3616–3623 (2003).
20. Lee, K. F. *et al.* Targeted mutation of the gene encoding the low affinity NGF receptor p75 leads to deficits in the peripheral sensory nervous system. *Cell* **69**, 737–749 (1992).
21. Rattenholl, A. *et al.* The pro-sequence facilitates folding of human nerve growth factor from *Escherichia coli* inclusion bodies. *Eur. J. Biochem.* **268**, 3296–3303 (2001).
22. Hempstead, B. L., Schleifer, L. S. & Chao, M. V. Expression of functional nerve growth factor receptors after gene transfer. *Science* **243**, 373–375 (1989).
23. Hempstead, B. L., Martin-Zanca, D., Kaplan, D. R., Parada, L. F. & Chao, M. V. High-affinity NGF binding requires coexpression of the trk proto-oncogene and the low-affinity NGF receptor. *Nature* **350**, 678–683 (1991).
24. Nykjaer, A. *et al.* Cubilin dysfunction causes abnormal metabolism of the steroid hormone 25(OH) vitamin D(3). *Proc. Natl. Acad. Sci. USA* **98**, 13895–13900 (2001).
25. Einheber, S., Milner, T. A., Giancotti, F. & Salzer, J. L. Axonal regulation of Schwann cell integrin expression suggests a role for  $\alpha 6 \beta 4$  in myelination. *J. Cell Biol.* **123**, 1223–1236 (1993).
26. Nykjaer, A. *et al.* Mannose 6-phosphate/insulin-like growth factor-II receptor targets the urokinase receptor to lysosomes via a novel binding interaction. *J. Cell Biol.* **141**, 815–828 (1998).
27. Wang, S. *et al.* p75(NTR) mediates neurotrophin-induced apoptosis of vascular smooth muscle cells. *Am. J. Pathol.* **157**, 1247–1258 (2000).
28. Mitsui, C., Sakai, K., Ninomiya, T. & Koike, T. Involvement of TLCK-sensitive serine protease in colchicine-induced cell death of sympathetic neurons in culture. *J. Neurosci. Res.* **66**, 601–611 (2001).
29. Bamji, S. X. *et al.* The p75 neurotrophin receptor mediates neuronal apoptosis and is essential for naturally occurring sympathetic neuron death. *J. Cell Biol.* **140**, 911–923 (1998).

**Acknowledgements** We thank M. V. Chao and G. R. Lewin for valuable discussions. J. Salzer, R. Kraemer and P. Fischer are acknowledged for reagents and advice, and S. Tevar for assistance in p75<sup>NTR</sup> mice genotyping. This work was supported by the Novo Nordisk Foundation, The Danish Medical Research Council, The Carlsberg Foundation (A.N. and C.M.P.) and the NIH (B.L.H. and R.L.).

**Competing interests statement** The authors declare that they have no competing financial interests.

**Correspondence** and requests for materials should be addressed to A.N. (an@biokemi.au.dk).

## The cytoplasmic body component TRIM5 $\alpha$ restricts HIV-1 infection in Old World monkeys

Matthew Stremlau<sup>1</sup>, Christopher M. Owens<sup>1</sup>, Michel J. Perron<sup>1</sup>, Michael Kiessling<sup>1</sup>, Patrick Autissier<sup>2</sup> & Joseph Sodroski<sup>1,3</sup>

<sup>1</sup>Department of Cancer Immunology and AIDS, Dana-Farber Cancer Institute, Department of Pathology, Division of AIDS, and <sup>2</sup>Division of Viral Pathogenesis, Beth Israel Deaconess Medical Center, Department of Medicine, Division of AIDS, Harvard Medical School, Boston, Massachusetts 02115, USA

<sup>3</sup>Department of Immunology and Infectious Diseases, Harvard School of Public Health, Boston, Massachusetts 02115, USA

Host cell barriers to the early phase of immunodeficiency virus replication explain the current distribution of these viruses among human and non-human primate species<sup>1–4</sup>. Human immunodeficiency virus type 1 (HIV-1), the cause of acquired immunodeficiency syndrome (AIDS) in humans, efficiently enters the cells of Old World monkeys but encounters a block before reverse transcription<sup>2–4</sup>. This species-specific restriction acts on the incoming HIV-1 capsid<sup>5–7</sup> and is mediated by a

dominant repressive factor<sup>7–9</sup>. Here we identify TRIM5 $\alpha$ , a component of cytoplasmic bodies, as the blocking factor. HIV-1 infection is restricted more efficiently by rhesus monkey TRIM5 $\alpha$  than by human TRIM5 $\alpha$ . The simian immunodeficiency virus, which naturally infects Old World monkeys<sup>10</sup>, is less susceptible to the TRIM5 $\alpha$ -mediated block than is HIV-1, and this difference in susceptibility is due to the viral capsid. The early block to HIV-1 infection in monkey cells is relieved by interference with TRIM5 $\alpha$  expression. Our studies identify TRIM5 $\alpha$  as a species-specific mediator of innate cellular resistance to HIV-1 and reveal host cell components that modulate the uncoating of a retroviral capsid.

Recombinant HIV-1 expressing green fluorescent protein and pseudotyped with the vesicular stomatitis virus (VSV) G glycoprotein (denoted HIV-1-GFP) can efficiently infect the cells of many mammalian species including humans, but not those of Old World monkeys<sup>4–9</sup>. Here we used a murine leukaemia virus vector to transduce human HeLa cells, which are susceptible to HIV-1-GFP infection, with a complementary DNA library prepared from primary rhesus monkey lung fibroblasts (PRL cells). Two independent HeLa clones resistant to HIV-1-GFP infection, but susceptible to infection with recombinant simian immunodeficiency virus (SIV-GFP) or murine leukaemia virus (MLV-GFP), were identified in a screen (Methods).

The only monkey cDNA insert common to both HIV-1-GFP-resistant clones was predicted to encode TRIM5 $\alpha$ , a member of the tripartite motif (TRIM) family of proteins containing RING domains, B-boxes and coiled coils<sup>11–13</sup>. TRIM5 $\alpha$  also contains a carboxy-terminal B30.2 (SPRY) domain not found in the other TRIM5 isoforms (ref. 13 and Fig. 1a). The natural functions of TRIM5 $\alpha$ , or of the cytoplasmic bodies in which the TRIM5 proteins localize<sup>13,14</sup>, are unknown. One TRIM5 isoform has been shown to have ubiquitin ligase activity typical of RING-containing proteins<sup>14</sup>. TRIM5 proteins are expressed constitutively in many tissues<sup>13</sup>, consistent with the pattern of expression expected for the HIV-1-blocking factor in monkeys<sup>4</sup>.

HeLa cells stably expressing rhesus monkey TRIM5 $\alpha$  (TRIM5 $\alpha_{rh}$ ) and control HeLa cells containing empty vector were incubated with different amounts of recombinant HIV-1-GFP, SIV-GFP and MLV-GFP. Expression of TRIM5 $\alpha_{rh}$  resulted in a marked inhibition of infection by HIV-1-GFP, whereas MLV-GFP infected control and TRIM5 $\alpha_{rh}$ -expressing HeLa cells equivalently (Fig. 1b, c). TRIM5 $\alpha_{rh}$  inhibited infection by SIV-GFP less efficiently than that by HIV-1-GFP (Fig. 1c). Stable TRIM5 $\alpha_{rh}$  expression also inhibited the replication of infectious HIV-1 in HeLa-CD4 cells, which express the receptors for HIV-1 (ref. 15 and Fig. 1d). The replication of a simian-human immunodeficiency virus (SHIV) chimaera, which contains core proteins (including the capsid protein) of SIV<sub>mac</sub> (ref. 16), was not inhibited in these TRIM5 $\alpha_{rh}$ -expressing cells. When the infections were done with eightfold more HIV-1 and SHIV, similar results were obtained (Supplementary Information). We conclude that expression of TRIM5 $\alpha_{rh}$  specifically and efficiently blocks infection by HIV-1, and exerts a slight inhibitory effect on infection by SIV<sub>mac</sub>.

To investigate the viral target of the TRIM5 $\alpha_{rh}$ -mediated restriction, HeLa cells expressing TRIM5 $\alpha_{rh}$  or control HeLa cells were incubated with recombinant HIV-1-GFP, SIV-GFP, SIV(HCA-p2)-GFP or HIV(SCA)-GFP. SIV(HCA-p2)-GFP is identical to SIV-GFP, except that the SIV capsid and adjacent p2 sequences have been replaced by those of HIV-1 (ref. 17), and SIV(HCA-p2)-GFP has been shown to be susceptible to the block in Old World monkey cells<sup>5,7</sup>. HIV(SCA)-GFP is identical to HIV-1-GFP, except that most of the capsid protein has been replaced by that of SIV<sup>5</sup>, and HIV(SCA)-GFP has been shown to be less susceptible than HIV-1 to the block in Old World monkey cells<sup>5</sup>. We found that HIV-1-GFP and SIV(HCA-p2)-GFP infections were restricted to the same extent in TRIM5 $\alpha_{rh}$ -expressing HeLa cells, whereas infec-

## Anhang

### Literaturverzeichnis

- Aloyz, R. S., Bamji, S. X., Pozniak, C. D., Toma, J. G., Atwal, J., Kaplan, D. R., and Miller, F. D. (1998). p53 is essential for developmental neuron death as regulated by the TrkA and p75 neurotrophin receptors. *J. Cell Biol.*, **143**:1691-1703.
- Anfinsen, C. B. (1973). Principles that govern the folding of protein chains. *Science*, **181**:223-230.
- Angeletti, R. H. and Bradshaw, R. A. (1971). Nerve growth factor from mouse submaxillary gland: amino acid sequence. *Proc. Natl. Acad. Sci. U. S. A.*, **68**:2417-2420.
- Apfel, S. C., Arezzo, J. C., Lipson, L., and Kessler, J. A. (1992). Nerve growth factor prevents experimental cisplatin neuropathy. *Ann. Neurol.*, **31**:76-80.
- Apfel, S. C. and Kessler, J. A. (1996). Neurotrophic factors in the treatment of peripheral neuropathy. *Ciba Found. Symp.*, **196**:98-108.
- Aurikko, J. P., Ruotolo, B. T., Grossmann, J. G., Moncrieffe, M. C., Stephens, E., Leppanen, V. M., Robinson, C. V., Saarma, M., Bradshaw, R. A., and Blundell, T. L. (2005). Characterization of symmetric complexes of nerve growth factor and the ectodomain of the pan-neurotrophin receptor, p75NTR. *J. Biol. Chem.*, **280**:33453-33460.
- Bai, Y., Milne, J. S., Mayne, L., and Englander, S. W. (1993). Primary structure effects on peptide group hydrogen exchange. *Proteins*, **17**:75-86.
- Baker, D., Sohl, J. L., and Agard, D. A. (1992). A protein-folding reaction under kinetic control. *Nature*, **356**:263-265.
- Bamji, S. X., Majdan, M., Pozniak, C. D., Belliveau, D. J., Aloyz, R., Kohn, J., Causing, C. G., and Miller, F. D. (1998). The p75 neurotrophin receptor mediates neuronal apoptosis and is essential for naturally occurring sympathetic neuron death. *J. Cell Biol.*, **140**:911-923.
- Barbacid, M. (1995). Neurotrophic factors and their receptors. *Curr. Opin. Cell Biol.*, **7**:148-155.
- Barde, Y. A. (1990). The nerve growth factor family. *Prog. Growth Factor Res.*, **2**:237-248.
- Bauskin, A. R., Zhang, H. P., Fairlie, W. D., He, X. Y., Russell, P. K., Moore, A. G., Brown, D. A., Stanley, K. K., and Breit, S. N. (2000). The propeptide of macrophage inhibitory cytokine (MIC-1), a TGF-beta superfamily member, acts as a quality control determinant for correctly folded MIC-1. *EMBO J.*, **19**:2212-2220.

- Bax, B., Blundell, T. L., Murray-Rust, J., and McDonald, N. Q. (1997). Structure of mouse 7S NGF: a complex of nerve growth factor with four binding proteins. *Structure*, **5**:1275-1285.
- Beattie, M. S., Harrington, A. W., Lee, R., Kim, J. Y., Boyce, S. L., Longo, F. M., Bresnahan, J. C., Hempstead, B. L., and Yoon, S. O. (2002). ProNGF induces p75-mediated death of oligodendrocytes following spinal cord injury. *Neuron*, **36**:375-386.
- Belliveau, D. J., Krivko, I., Kohn, J., Lachance, C., Pozniak, C., Rusakov, D., Kaplan, D., and Miller, F. D. (1997). NGF and neurotrophin-3 both activate TrkA on sympathetic neurons but differentially regulate survival and neuritogenesis. *J. Cell Biol.*, **136**:375-388.
- Berger, E. A. and Shooter, E. M. (1977). Evidence for pro-beta-nerve growth factor, a biosynthetic precursor to beta-nerve growth factor. *Proc. Natl. Acad. Sci. USA*, **74**:3647-3651.
- Bibel, M., Hoppe, E., and Barde, Y. A. (1999). Biochemical and functional interactions between the neurotrophin receptors trk and p75NTR. *EMBO J.*, **18**:616-622.
- Bohm, G., Muhr, R., and Jaenicke, R. (1992). Quantitative analysis of protein far UV circular dichroism spectra by neural networks. *Protein Eng*, **5**:191-195.
- Bothwell, M. A. and Shooter, E. M. (1977). Dissociation equilibrium constant of  $\beta$  nerve growth factor. *J. Biol. Chem.*, **252**:8532-8536.
- Böttinger, E. P., Factor, V. M., Tsang, M. L., Weatherbee, J. A., Kopp, J. B., Qian, S. W., Wakefield, L. M., Roberts, A. B., Thorgeirsson, S. S., and Sporn, M. B. (1996). The recombinant proregion of transforming growth factor beta1 (latency-associated peptide) inhibits active transforming growth factor beta1 in transgenic mice. *Proc. Natl. Acad. Sci. USA*, **93**:5877-5882.
- Bowie, J. U. and Sauer, R. T. (1989). Equilibrium dissociation and unfolding of the Arc repressor dimer. *Biochemistry*, **28**:7139-7143.
- Bradshaw, R. A., Blundell, T. L., Lapatto, R., McDonald, N. Q., and Murray-Rust, J. (1993). Nerve growth factor revisited. *Trends Biochem. Sci.*, **18**:48-52.
- Brann, A. B., Tcherpakov, M., Williams, I. M., Futerman, A. H., and Fainzilber, M. (2002). Nerve growth factor-induced p75-mediated death of cultured hippocampal neurons is age-dependent and transduced through ceramide generated by neutral sphingomyelinase. *J. Biol. Chem.*, **277**:9812-9818.
- Bresnahan, P. A., Leduc, R., Thomas, L., Thorner, J., Gibson, H. L., Brake, A. J., Barr, P. J., and Thomas, G. (1990). Human fur gene encodes a yeast KEX2-like endoprotease that cleaves pro-beta-NGF in vivo. *J. Cell Biol.*, **111**:2851-2859.
- Bryan, P. N. (2002). Prodomains and protein folding catalysis. *Chem. Rev.*, **102**:4805-4816.
- Buczek, O., Olivera, B. M., and Bulaj, G. (2004). Propeptide does not act as an intramolecular chaperone but facilitates protein disulfide isomerase-assisted folding of a conotoxin precursor. *Biochemistry*, **43**:1093-1101.

- Buevich, A. V., Shinde, U. P., Inouye, M., and Baum, J. (2001). Backbone dynamics of the natively unfolded pro-peptide of subtilisin by heteronuclear NMR relaxation studies. *J. Biomol. NMR*, **20**:233-249.
- Casaccia-Bonnet, P., Carter, B. D., Dobrowsky, R. T., and Chao, M. V. (1996). Death of oligodendrocytes mediated by the interaction of nerve growth factor with its receptor p75. *Nature*, **383**:716-719.
- Casademunt, E., Carter, B. D., Benzel, I., Frade, J. M., Dechant, G., and Barde, Y. A. (1999). The zinc finger protein NRIF interacts with the neurotrophin receptor p75(NTR) and participates in programmed cell death. *EMBO J.*, **18**:6050-6061.
- Chakrabarti, S., Sima, A. A., Lee, J., Brachet, P., and Dicou, E. (1990). Nerve growth factor (NGF), proNGF and NGF receptor-like immunoreactivity in BB rat retina. *Brain Res.*, **523**:11-15.
- Chao, M. V. (2003). Neurotrophins and their receptors: a convergence point for many signalling pathways. *Nat. Rev. Neurosci.*, **4**:299-309.
- Chao, M. V. and Hempstead, B. L. (1995). p75 and Trk: a two-receptor system. *Trends Neurosci.*, **18**:321-326.
- Chen, Y., Dicou, E., and Djakiew, D. (1997). Characterization of nerve growth factor precursor protein expression in rat round spermatids and the trophic effects of nerve growth factor in the maintenance of Sertoli cell viability. *Mol. Cell Endocrinol.*, **127**:129-136.
- Cohen, P., Sutter, A., Landreth, G., Zimmermann, A., and Shooter, E. M. (1980). Oxidation of tryptophan-21 alters the biological activity and receptor binding characteristics of mouse nerve growth factor. *J. Biol. Chem.*, **255**:2949-2954.
- Cohen, S. (1960). Purification of a nerve-growth promoting protein from the mouse salivary gland and its neuro-cytotoxic antiserum. *Proc. Natl. Acad. Sci. USA*, **46**:302-311.
- Creighton, T. E. (1991). Molecular chaperones. Unfolding protein folding. *Nature*, **352**:17-18.
- Daopin, S., Piez, K. A., Ogawa, Y., and Davies, D. R. (1992). Crystal structure of transforming growth factor-beta 2: an unusual fold for the superfamily. *Science*, **257**:369-373.
- Darling, T. L., Petrides, P. E., Beguin, P., Frey, P., Shooter, E. M., Selby, M., and Rutter, W. J. (1983). The biosynthesis and processing of proteins in the mouse 7S nerve growth factor complex. *Cold Spring Harb. Symp. Quant. Biol.*, **48 Pt 1**:427-434.
- Davey, F. and Davies, A. M. (1998). TrkB signalling inhibits p75-mediated apoptosis induced by nerve growth factor in embryonic proprioceptive neurons. *Curr. Biol.*, **8**:915-918.
- De Bernardes, Clark E., Schwarz, E., and Rudolph, R. (1999). Inhibition of aggregation side reactions during in vitro protein folding. *Methods Enzymol.*, **309**:217-236.
- De Young, L. R., Burton, L. E., Liu, J., Powell, M. F., Schmelzer, C. H., and Skelton, N. J. (1996). RhNGF slow unfolding is not due to proline isomerization: possibility of a cystine knot loop-threading mechanism. *Protein Sci.*, **5**:1554-1566.

- De Young, L. R., Schmelzer, C. H., and Burton, L. E. (1999). A common mechanism for recombinant human NGF, BDNF, NT-3, and murine NGF slow unfolding. *Protein Sci.*, **8**:2513-2518.
- Dechant, G. (2001). Molecular interactions between neurotrophin receptors. *Cell Tissue Res.*, **305**:229-238.
- Degnin, C., Jean, F., Thomas, G., and Christian, J. L. (2004). Cleavages within the prodomain direct intracellular trafficking and degradation of mature bone morphogenetic protein-4. *Mol. Biol. Cell*, **15**:5012-5020.
- Delsite, R. and Djakiew, D. (1999). Characterization of nerve growth factor precursor protein expression by human prostate stromal cells: a role in selective neurotrophin stimulation of prostate epithelial cell growth. *Prostate*, **41**:39-48.
- Dicou, E., Pflug, B., Magazin, M., Lehy, T., Djakiew, D., Ferrara, P., Nerriere, V., and Harvie, D. (1997). Two peptides derived from the nerve growth factor precursor are biologically active. *J Cell Biol*, **136**:389-398.
- Drinkwater, C. C., Suter, U., Angst, C., and Shooter, E. M. (1991). Mutation of tryptophan-21 in mouse nerve growth factor (NGF) affects binding to the fast NGF receptor but not induction of neurites on PC12 cells. *Proc. Biol. Sci.*, **246**:307-313.
- Eder, J., Rheinnecker, M., and Fersht, A. R. (1993). Folding of subtilisin BPN': role of the pro-sequence. *J. Mol. Biol.*, **233**:293-304.
- Edwards, R. H., Selby, M. J., Mobley, W. C., Weinrich, S. L., Hruby, D. E., and Rutter, W. J. (1988). Processing and secretion of nerve growth factor: expression in mammalian cells with a vaccinia virus vector. *Mol. Cell Biol.*, **8**:2456-2464.
- Edwards, R. H., Selby, M. J., and Rutter, W. J. (1986). Differential RNA splicing predicts two distinct nerve growth factor precursors. *Nature*, **319**:784-787.
- Eisenberg, D., Weiss, R. M., and Terwilliger, T. C. (1984). The hydrophobic moment detects periodicity in protein hydrophobicity. *Proc. Natl. Acad. Sci. USA*, **81**:140-144.
- Ernfors, P., Ibanez, C. F., Ebendal, T., Olson, L., and Persson, H. (1990). Molecular cloning and neurotrophic activities of a protein with structural similarities to nerve growth factor: developmental and topographical expression in the brain. *Proc. Natl. Acad. Sci. USA*, **87**:5454-5458.
- Esposito, D., Patel, P., Stephens, R. M., Perez, P., Chao, M. V., Kaplan, D. R., and Hempstead, B. L. (2001). The cytoplasmic and transmembrane domains of the p75 and Trk A receptors regulate high affinity binding to nerve growth factor. *J. Biol. Chem.*, **276**:32687-32695.
- Fahnestock, M., Michalski, B., Xu, B., and Coughlin, M. D. (2001). The precursor pro-nerve growth factor is the predominant form of nerve growth factor in brain and is increased in Alzheimer's disease. *Mol. Cell Neurosci.*, **18**:210-220.
- Fahnestock, M., Yu, G., and Coughlin, M. D. (2004a). ProNGF: a neurotrophic or an apoptotic molecule? *Prog. Brain Res.*, **146**:107-110.



- Fahnestock, M., Yu, G., Michalski, B., Mathew, S., Colquhoun, A., Ross, G. M., and Coughlin, M. D. (2004b). The nerve growth factor precursor proNGF exhibits neurotrophic activity but is less active than mature nerve growth factor. *J. Neurochem.*, **89**:581-592.
- Fairlie, W. D., Zhang, H. P., Wu, W. M., Pankhurst, S. L., Bauskin, A. R., Russell, P. K., Brown, P. K., and Breit, S. N. (2001). The propeptide of the transforming growth factor-beta superfamily member, macrophage inhibitory cytokine-1 (MIC-1), is a multifunctional domain that can facilitate protein folding and secretion. *J. Biol. Chem.*, **276**:16911-16918.
- Farhadi, H., Pareek, S., Day, R., Dong, W., Chretien, M., Bergeron, J. J., Seidah, N. G., and Murphy, R. A. (1997). Prohormone convertases in mouse submandibular gland: colocalization of furin and nerve growth factor. *J. Histochem. Cytochem.*, **45**:795-804.
- Fayard, B., Loeffler, S., Weis, J., Vogelín, E., and Kruttgen, A. (2005). The secreted brain-derived neurotrophic factor precursor pro-BDNF binds to TrkB and p75NTR but not to TrkA or TrkC. *J. Neurosci. Res.*, **80**:18-28.
- Feeney, B. and Clark, A. C. (2005). Reassembly of active caspase-3 is facilitated by the propeptide. *J. Biol. Chem.*, **280**:39772-39785.
- Fischer, G., Tradler, T., and Zarnt, T. (1998). The mode of action of peptidyl prolyl cis/trans isomerases in vivo: binding vs. catalysis. *FEBS Lett.*, **426**:17-20.
- Fox, T., de Miguel E., Mort, J. S., and Storer, A. C. (1992). Potent slow-binding inhibition of cathepsin B by its propeptide. *Biochemistry*, **31**:12571-12576.
- Frade, J. M., Rodriguez-Tebar, A., and Barde, Y. A. (1996). Induction of cell death by endogenous nerve growth factor through its p75 receptor. *Nature*, **383**:166-168.
- Freedman, R. B., Hirst, T. R., and Tuite, M. F. (1994). Protein disulphide isomerase: building bridges in protein folding. *Trends Biochem. Sci.*, **19**:331-336.
- Friedman, W. J. (2000). Neurotrophins induce death of hippocampal neurons via the p75 receptor. *J. Neurosci.*, **20**:6340-6346.
- Gallagher, T., Gilliland, G., Wang, L., and Bryan, P. (1995). The prosegment-subtilisin BPN' complex: crystal structure of a specific 'foldase'. *Structure*, **3**:907-914.
- Gentry, L. E. and Nash, B. W. (1990). The pro domain of pre-pro-transforming growth factor beta 1 when independently expressed is a functional binding protein for the mature growth factor. *Biochemistry*, **29**:6851-6857.
- Gray, A. M. and Mason, A. J. (1990). Requirement for activin A and transforming growth factor--beta 1 pro- regions in homodimer assembly. *Science*, **247**:1328-1330.
- Greene, L. A., Shooter, E. M., and Varon, S. (1969). Subunit interaction and enzymatic activity of mouse 7S nerve growth factor. *Biochemistry*, **8**:3735-3741.
- Grewal, S. S., York, R. D., and Stork, P. J. (1999). Extracellular-signal-regulated kinase signalling in neurons. *Curr. Opin. Neurobiol.*, **9**:544-553.

- Hasan, W., Pedchenko, T., Krizsan-Agbas, D., Baum, L., and Smith, P. G. (2003). Sympathetic neurons synthesize and secrete pro-nerve growth factor protein. *J. Neurobiol.*, **57**:38-53.
- He, X. L. and Garcia, K. C. (2004). Structure of nerve growth factor complexed with the shared neurotrophin receptor p75. *Science*, **304**:870-875.
- Hempstead, B. L. (2002). The many faces of p75NTR. *Curr. Opin. Neurobiol.*, **12**:260-267.
- Hempstead, B. L., Martin-Zanca, D., Kaplan, D. R., Parada, L. F., and Chao, M. V. (1991). High-affinity NGF binding requires coexpression of the trk proto-oncogene and the low-affinity NGF receptor. *Nature*, **350**:678-683.
- Hermey, G., Keat, S. J., Madsen, P., Jacobsen, C., Petersen, C. M., and Gliemann, J. (2003). Characterization of sorCS1, an alternatively spliced receptor with completely different cytoplasmic domains that mediate different trafficking in cells. *J. Biol. Chem.*, **278**:7390-7396.
- Hidaka, Y., Ohno, M., Hemmasi, B., Hill, O., Forssmann, W. G., and Shimonishi, Y. (1998). In vitro disulfide-coupled folding of guanylyl cyclase-activating peptide and its precursor protein. *Biochemistry*, **37**:8498-8507.
- Hillger, F., Herr, G., Rudolph, R., and Schwarz, E. (2005). Biophysical comparison of BMP-2, ProBMP-2, and the free pro-peptide reveals stabilization of the pro-peptide by the mature growth factor. *J. Biol. Chem.*, **280**:14974-14980.
- Hohn, A., Leibrock, J., Bailey, K., and Barde, Y. A. (1990). Identification and characterization of a novel member of the nerve growth factor/brain-derived neurotrophic factor family. *Nature*, **344**:339-341.
- Ibanez, C. F., Ebendal, T., Barbany, G., Murray-Rust, J., Blundell, T. L., and Persson, H. (1992). Disruption of the low affinity receptor-binding site in NGF allows neuronal survival and differentiation by binding to the trk gene product. *Cell*, **69**:329-341.
- Ibanez, C. F., Ilag, L. L., Murray-Rust, J., and Persson, H. (1993). An extended surface of binding to Trk tyrosine kinase receptors in NGF and BDNF allows the engineering of a multifunctional pan-neurotrophin. *EMBO J.*, **12**:2281-2293.
- Ikemura, H., Takagi, H., and Inouye, M. (1987). Requirement of pro-sequence for the production of active subtilisin E in *Escherichia coli*. *J. Biol. Chem.*, **262**:7859-7864.
- Inouye, M. (1991). Intramolecular chaperone: the role of the pro-peptide in protein folding. *Enzyme*, **45**:314-321.
- Ip, N. Y., Ibanez, C. F., Nye, S. H., McClain, J., Jones, P. F., Gies, D. R., Belluscio, L., Le Beau, M. M., Espinosa, R., III, Squinto, S. P., Persson, H., and Yancopoulos, G. D. (1992). Mammalian neurotrophin-4: structure, chromosomal localization, tissue distribution, and receptor specificity. *Proc Natl Acad Sci USA*, **89**:3060-3064.
- Isackson, P. J. and Bradshaw, R. A. (1984). The alpha-subunit of mouse 7 S nerve growth factor is an inactive serine protease. *J. Biol. Chem.*, **259**:5380-5383.

- Jain, S. C., Shinde, U., Li, Y., Inouye, M., and Berman, H. M. (1998). The crystal structure of an autoprocessed Ser221Cys-subtilisin E-propeptide complex at 2.0 Å resolution. *J. Mol. Biol.*, **284**:137-144.
- Kahle, P., Burton, L. E., Schmelzer, C. H., and Hertel, C. (1992). The amino terminus of nerve growth factor is involved in the interaction with the receptor tyrosine kinase p140trkA. *J. Biol. Chem.*, **267**:22707-22710.
- Kaplan, D. R. and Miller, F. D. (1997). Signal transduction by the neurotrophin receptors. *Curr. Opin. Cell Biol.*, **9**:213-221.
- Kaplan, D. R. and Miller, F. D. (2000). Neurotrophin signal transduction in the nervous system. *Curr. Opin. Neurobiol.*, **10**:381-391.
- Klein, R., Jing, S. Q., Nanduri, V., O'Rourke, E., and Barbacid, M. (1991a). The trk proto-oncogene encodes a receptor for nerve growth factor. *Cell*, **65**:189-197.
- Klein, R., Nanduri, V., Jing, S. A., Lamballe, F., Tapley, P., Bryant, S., Cordon-Cardo, C., Jones, K. R., Reichardt, L. F., and Barbacid, M. (1991b). The trkB tyrosine protein kinase is a receptor for brain-derived neurotrophic factor and neurotrophin-3. *Cell*, **66**:395-403.
- Kliemann, M. (2001). Untersuchung zur Funktion der beiden C-terminalen Aminosäuren des NGF-Vorläuferproteins bei der in vitro Strukturbildung des Wachstumsfaktors. *Diplomarbeit* Martin-Luther-Universität Halle-Wittenberg.
- Kliemann, M., Rattenholl, A., Golbik, R., Balbach, J., Lilie, H., Rudolph, R., and Schwarz, E. (2004). The mature part of proNGF induces the structure of its pro-peptide. *FEBS Lett.*, **566**:207-212.
- Kullander, K., Kaplan, D., and Ebendal, T. (1997). Two restricted sites on the surface of the nerve growth factor molecule independently determine specific TrkA receptor binding and activation. *J Biol Chem*, **272**:9300-9307.
- LaLonde, J. M., Zhao, B., Janson, C. A., D'Alessio, K. J., McQueney, M. S., Orsini, M. J., Debouck, C. M., and Smith, W. W. (1999). The crystal structure of human procathepsin K. *Biochemistry*, **38**:862-869.
- Lamballe, F., Klein, R., and Barbacid, M. (1991). trkC, a new member of the trk family of tyrosine protein kinases, is a receptor for neurotrophin-3. *Cell*, **66**:967-979.
- Large, T. H., Bodary, S. C., Clegg, D. O., Weskamp, G., Otten, U., and Reichardt, L. F. (1986). Nerve growth factor gene expression in the developing rat brain. *Science*, **234**:352-355.
- Larsen, T. A., Olson, A. J., and Goodsell, D. S. (1998). Morphology of protein-protein interfaces. *Structure*, **6**:421-427.
- Le-Niculescu, H., Bonfoco, E., Kasuya, Y., Claret, F. X., Green, D. R., and Karin, M. (1999). Withdrawal of survival factors results in activation of the JNK pathway in neuronal cells leading to Fas ligand induction and cell death. *Mol. Cell Biol.*, **19**:751-763.

- Lee, R., Kermani, P., Teng, K. K., and Hempstead, B. L. (2001). Regulation of cell survival by secreted proneurotrophins. *Science*, **294**:1945-1948.
- Leibrock, J., Lottspeich, F., Hohn, A., Hofer, M., Hengerer, B., Masiakowski, P., Thoenen, H., and Barde, Y. A. (1989). Molecular cloning and expression of brain-derived neurotrophic factor. *Nature*, **341**:149-152.
- Levi-Montalcini, R. (1987). The nerve growth factor 35 years later. *Science*, **237**:1154-1162.
- Linggi, M. S., Burke, T. L., Williams, B. B., Harrington, A., Kraemer, R., Hempstead, B. L., Yoon, S. O., and Carter, B. D. (2005). Neurotrophin receptor interacting factor (NRIF) is an essential mediator of apoptotic signaling by the p75 neurotrophin receptor. *J. Biol. Chem.*, **280**:13801-13808.
- Lobos, E., Gebhardt, C., Kluge, A., and Spanel-Borowski, K. (2005). Expression of nerve growth factor isoforms in the rat uterus during pregnancy: accumulation of precursor proNGF. *Endocrinology*
- Lonze, B. E. and Ginty, D. D. (2002). Function and regulation of CREB family transcription factors in the nervous system. *Neuron*, **35**:605-623.
- Mahadeo, D., Kaplan, L., Chao, M. V., and Hempstead, B. L. (1994). High affinity nerve growth factor binding displays a faster rate of association than p140trk binding. Implications for multi-subunit polypeptide receptors. *J. Biol. Chem.*, **269**:6884-6891.
- Maisonpierre, P. C., Belluscio, L., Squinto, S., Ip, N. Y., Furth, M. E., Lindsay, R. M., and Yancopoulos, G. D. (1990). Neurotrophin-3: a neurotrophic factor related to NGF and BDNF. *Science*, **247**:1446-1451.
- Majdan, M., Walsh, G. S., Aloyz, R., and Miller, F. D. (2001). TrkA mediates developmental sympathetic neuron survival in vivo by silencing an ongoing p75NTR-mediated death signal. *J. Cell Biol.*, **155**:1275-1285.
- Mason, A. J., Evans, B. A., Cox, D. R., Shine, J., and Richards, R. I. (1983). Structure of mouse kallikrein gene family suggests a role in specific processing of biologically active peptides. *Nature*, **303**:300-307.
- McDonald, N. Q. and Hendrickson, W. A. (1993). A structural superfamily of growth factors containing a cystine knot motif. *Cell*, **73**:421-424.
- McDonald, N. Q., Lapatto, R., Murray-Rust, J., Gunning, J., Wlodawer, A., and Blundell, T. L. (1991). New protein fold revealed by a 2.3-Å resolution crystal structure of nerve growth factor. *Nature*, **354**:411-414.
- Miller, F. D. and Kaplan, D. R. (2001). Neurotrophin signalling pathways regulating neuronal apoptosis. *Cell Mol. Life Sci.*, **58**:1045-1053.
- Mobley, W. C., Schenker, A., and Shooter, E. M. (1976). Characterization and isolation of proteolytically modified nerve growth factor. *Biochemistry*, **15**:5543-5552.
- Moore, J. B., Jr., Mobley, W. C., and Shooter, E. M. (1974). Proteolytic modification of the beta nerve growth factor protein. *Biochemistry*, **13**:833-840.

- Mowla, S. J., Pareek, S., Farhadi, H. F., Petrecca, K., Fawcett, J. P., Seidah, N. G., Morris, S. J., Sossin, W. S., and Murphy, R. A. (1999). Differential sorting of nerve growth factor and brain-derived neurotrophic factor in hippocampal neurons. *J. Neurosci.*, **19**:2069-2080.
- Murphy, R. A., Chlumecky, V., Smillie, L. B., Carpenter, M., Nattriss, M., Anderson, J. K., Rhodes, J. A., Barker, P. A., Siminoski, K., Campenot, R. B., and Haskins, J. (1989). Isolation and characterization of a glycosylated form of beta nerve growth factor in mouse submandibular glands. *J. Biol. Chem.*, **264**:12502-12509.
- Narhi, L. O., Rosenfeld, R., Talvenheimo, J., Prestrelski, S. J., Arakawa, T., Lary, J. W., Kolvenbach, C. G., Hecht, R., Boone, T., Miller, J. A., and Yphantis, D. A. (1993). Comparison of the biophysical characteristics of human brain-derived neurotrophic factor, neurotrophin-3, and nerve growth factor. *J. Biol. Chem.*, **268**:13309-13317.
- Neri, D., Billeter, M., Wider, G., and Wuthrich, K. (1992). NMR determination of residual structure in a urea-denatured protein, the 434-repressor. *Science*, **257**:1559-1563.
- Nilsson, A. S., Fainzilber, M., Falck, P., and Ibanez, C. F. (1998). Neurotrophin-7: a novel member of the neurotrophin family from the zebrafish. *FEBS Lett.*, **424**:285-290.
- Nykjaer, A., Lee, R., Teng, K. K., Jansen, P., Madsen, P., Nielsen, M. S., Jacobsen, C., Kliemannel, M., Schwarz, E., Willnow, T. E., Hempstead, B. L., and Petersen, C. M. (2004). Sortilin is essential for proNGF-induced neuronal cell death. *Nature*, **427**:843-848.
- O'Connell, L., Hongo, J. A., Presta, L. G., and Tsoulfas, P. (2000). TrkA amino acids controlling specificity for nerve growth factor. *J. Biol. Chem.*, **275**:7870-7877.
- Oefner, C., D'Arcy, A., Winkler, F. K., Eggimann, B., and Hosang, M. (1992). Crystal structure of human platelet-derived growth factor BB. *EMBO J.*, **11**:3921-3926.
- Ohta, Y., Hojo, H., Aimoto, S., Kobayashi, T., Zhu, X., Jordan, F., and Inouye, M. (1991). Pro-peptide as an intramolecular chaperone: renaturation of denatured subtilisin E with a synthetic pro-peptide [corrected]. *Mol. Microbiol.*, **5**:1507-1510.
- Pallaghy, P. K., Nielsen, K. J., Craik, D. J., and Norton, R. S. (1994). A common structural motif incorporating a cystine knot and a triple-stranded beta-sheet in toxic and inhibitory polypeptides. *Protein Sci.*, **3**:1833-1839.
- Pantazis, N. J. (1983). Nerve growth factor synthesized by mouse fibroblast cells in culture: absence of alpha and gamma subunits. *Biochemistry*, **22**:4264-4271.
- Petersen, C. M., Nielsen, M. S., Nykjaer, A., Jacobsen, L., Tommerup, N., Rasmussen, H. H., Roigaard, H., Gliemann, J., Madsen, P., and Moestrup, S. K. (1997). Molecular identification of a novel candidate sorting receptor purified from human brain by receptor-associated protein affinity chromatography. *J. Biol. Chem.*, **272**:3599-3605.
- Philo, J., Talvenheimo, J., Wen, J., Rosenfeld, R., Welcher, A., and Arakawa, T. (1994). Interactions of Neurotrophin-3 (Nt-3), Brain-Derived Neurotrophic Factor (Bdnf), and the Nt-3 Bdnf Heterodimer with the Extracellular Domains of the Trkb and Trkc Receptors. *J. Biol. Chem.*, **269**:27840-27846.

- Philo, J. S., Rosenfeld, R., Arakawa, T., Wen, J., and Narhi, L. O. (1993). Refolding of Brain-Derived Neurotrophic Factor from Guanidine-Hydrochloride - Kinetic Trapping in A Collapsed Form Which Is Incompetent for Dimerization. *Biochemistry*, **32**:10812-10818.
- Podobnik, M., Kuhelj, R., Turk, V., and Turk, D. (1997). Crystal structure of the wild-type human procathepsin B at 2.5 Å resolution reveals the native active site of a papain-like cysteine protease zymogen. *J. Mol. Biol.*, **271**:774-788.
- Price-Carter, M., Gray, W. R., and Goldenberg, D. P. (1996a). Folding of omega-conotoxins. 1. Efficient disulfide-coupled folding of mature sequences in vitro. *Biochemistry*, **35**:15537-15546.
- Price-Carter, M., Gray, W. R., and Goldenberg, D. P. (1996b). Folding of omega-conotoxins. 2. Influence of precursor sequences and protein disulfide isomerase. *Biochemistry*, **35**:15547-15557.
- Radziejewski, C., Robinson, R. C., DiStefano, P. S., and Taylor, J. W. (1992). Dimeric structure and conformational stability of brain-derived neurotrophic factor and neurotrophin-3. *Biochemistry*, **31**:4431-4436.
- Ramer, M. S., Priestley, J. V., and McMahon, S. B. (2000). Functional regeneration of sensory axons into the adult spinal cord. *Nature*, **403**:312-316.
- Rattenholl, A. (2001). Untersuchung zur Pro-Sequenz-vermittelten Faltung von rekombinanten, humanen Nervenwachstumsfaktor. *Dissertation* Martin-Luther-Universität Halle-Wittenberg.
- Rattenholl, A., Lilie, H., Grossmann, A., Stern, A., Schwarz, E., and Rudolph, R. (2001a). The pro-sequence facilitates folding of human nerve growth factor from *Escherichia coli* inclusion bodies. *Eur. J. Biochem.*, **268**:3296-3303.
- Rattenholl, A., Ruoppolo, M., Flagiello, A., Monti, M., Vinci, F., Marino, G., Lilie, H., Schwarz, E., and Rudolph, R. (2001b). Pro-sequence assisted folding and disulfide bond formation of human nerve growth factor. *J. Mol. Biol.*, **305**:523-533.
- Reinshagen, M., Geerling, I., Eysselein, V. E., Adler, G., Huff, K. R., Moore, G. P., and Lakshmanan, J. (2000). Commercial recombinant human beta-nerve growth factor and adult rat dorsal root ganglia contain an identical molecular species of nerve growth factor prohormone. *J. Neurochem.*, **74**:2127-2133.
- Rosenthal, A., Goeddel, D. V., Nguyen, T., Lewis, M., Shih, A., Laramee, G. R., Nikolics, K., and Winslow, J. W. (1990). Primary structure and biological activity of a novel human neurotrophic factor. *Neuron*, **4**:767-773.
- Roux, P. P. and Barker, P. A. (2002). Neurotrophin signaling through the p75 neurotrophin receptor. *Prog. Neurobiol.*, **67**:203-233.
- Rudolph, R. and Lilie, H. (1996). In vitro folding of inclusion body proteins. *FASEB J.*, **10**:49-56.

- Ruvinov, S., Wang, L., Ruan, B., Almog, O., Gilliland, G. L., Eisenstein, E., and Bryan, P. N. (1997). Engineering the independent folding of the subtilisin BPN' prodomain: analysis of two-state folding versus protein stability. *Biochemistry*, **36**:10414-10421.
- Ryden, M., Hempstead, B., and Ibanez, C. F. (1997). Differential modulation of neuron survival during development by nerve growth factor binding to the p75 neurotrophin receptor. *J. Biol. Chem.*, **272**:16322-16328.
- Saab-Rincon, G., Gualfetti, P. J., and Matthews, C. R. (1996). Mutagenic and thermodynamic analyses of residual structure in the alpha subunit of tryptophan synthase. *Biochemistry*, **35**:1988-1994.
- Schlunegger, M. P. and Grutter, M. G. (1992). An unusual feature revealed by the crystal structure at 2.2 Å resolution of human transforming growth factor-beta 2. *Nature*, **358**:430-434.
- Schmid, F. X. and Baldwin, R. L. (1979). The rate of interconversion between the two unfolded forms of ribonuclease A does not depend on guanidinium chloride concentration. *J. Mol. Biol.*, **133**:285-287.
- Seidah, N. G., Benjannet, S., Pareek, S., Savaria, D., Hamelin, J., Goulet, B., Laliberte, J., Lazure, C., Chretien, M., and Murphy, R. A. (1996). Cellular processing of the nerve growth factor precursor by the mammalian pro-protein convertases. *Biochem. J.*, **314** (Pt 3):951-960.
- Selby, M. J., Edwards, R., Sharp, F., and Rutter, W. J. (1987). Mouse nerve growth factor gene: structure and expression. *Mol. Cell Biol.*, **7**:3057-3064.
- Shinde, U. and Inouye, M. (2000). Intramolecular chaperones: polypeptide extensions that modulate protein folding. *Semin. Cell Dev. Biol.*, **11**:35-44.
- Shinde, U., Li, Y., Chatterjee, S., and Inouye, M. (1993). Folding pathway mediated by an intramolecular chaperone. *Proc. Natl. Acad. Sci. USA*, **90**:6924-6928.
- Silen, J. L. and Agard, D. A. (1989). The alpha-lytic protease pro-region does not require a physical linkage to activate the protease domain in vivo. *Nature*, **341**:462-464.
- Silverman, R. E. and Bradshaw, R. A. (1982). Nerve growth factor: subunit interactions in the mouse submaxillary gland 7S complex. *J. Neurosci. Res.*, **8**:127-136.
- Sorenson, P., Winther, J. R., Kaarsholm, N. C., and Poulsen, F. M. (1993). The pro region required for folding of carboxypeptidase Y is a partially folded domain with little regular structural core. *Biochemistry*, **32**:12160-12166.
- Steiner, D. F. and Clark, J. L. (1968). The spontaneous reoxidation of reduced beef and rat proinsulins. *Proc. Natl. Acad. Sci. USA*, **60**:622-629.
- Taylor, J. M., Cohen, S., and Mitchell, W. M. (1970). Epidermal growth factor: high and low molecular weight forms. *Proc. Natl. Acad. Sci. USA*, **67**:164-171.
- Teng, H. K., Teng, K. K., Lee, R., Wright, S., Tevar, S., Almeida, R. D., Kermani, P., Torkin, R., Chen, Z. Y., Lee, F. S., Kraemer, R. T., Nykjaer, A., and Hempstead, B. L. (2005).

- ProBDNF induces neuronal apoptosis via activation of a receptor complex of p75<sup>NTR</sup> and sortilin. *J. Neurosci.*, **25**:5455-5463.
- Timm, D. E., de Haset, P. L., and Neet, K. E. (1994). Comparative equilibrium denaturation studies of the neurotrophins: nerve growth factor, brain-derived neurotrophic factor, neurotrophin 3, and neurotrophin 4/5. *Biochemistry*, **33**:4667-4676.
- Timm, D. E. and Neet, K. E. (1992). Equilibrium denaturation studies of mouse  $\beta$ -nerve growth factor. *Protein Sci.*, **1**:236-244.
- Tuszynski, M. H. (2002). Growth-factor gene therapy for neurodegenerative disorders. *Lancet Neurol.*, **1**:51-57.
- Tuszynski, M. H., Thal, L., Pay, M., Salmon, D. P., HS, U., Bakay, R., Patel, P., Blesch, A., Vahlsing, H. L., Ho, G., Tong, G., Potkin, S. G., Fallon, J., Hansen, L., Mufson, E. J., Kordower, J. H., Gall, C., and Conner, J. (2005). A phase 1 clinical trial of nerve growth factor gene therapy for Alzheimer disease. *Nat. Med.*, **11**:551-555.
- Ullrich, A., Gray, A., Berman, C., and Dull, T. J. (1983). Human  $\beta$ -nerve growth factor gene sequence highly homologous to that of mouse. *Nature*, **303**:821-825.
- Urfer, R., Tsoulfas, P., Soppet, D., Escandon, E., Parada, L. F., and Presta, L. G. (1994). The binding epitopes of neurotrophin-3 to its receptors trkC and gp75 and the design of a multifunctional human neurotrophin. *EMBO J.*, **13**:5896-5909.
- Varon, S., Nomura, J., and Shooter, E. M. (1967). Subunit structure of a high-molecular-weight form of the nerve growth factor from mouse submaxillary gland. *Proc. Natl. Acad. Sci. USA*, **57**:1782-1789.
- Varon, S., Normura, J., and Shooter, E. M. (1968). Reversible dissociation of the mouse nerve growth factor protein into different subunits. *Biochemistry*, **7**:1296-1303.
- Voorberg, J., Fontijn, R., van Mourik, J. A., and Pannekoek, H. (1990). Domains involved in multimer assembly of von willebrand factor (vWF): multimerization is independent of dimerization. *EMBO J.*, **9**:797-803.
- Weissman, J. S. and Kim, P. S. (1992). The pro region of BPTI facilitates folding. *Cell*, **71**:841-851.
- Wentzel, A., Christmann, A., Kratzner, R., and Kolmar, H. (1999). Sequence requirements of the GPNG beta-turn of the Ecballium elaterium trypsin inhibitor II explored by combinatorial library screening. *J. Biol. Chem.*, **274**:21037-21043.
- Whittemore, S. R., Ebendal, T., Larkfors, L., Olson, L., Seiger, A., Stromberg, I., and Persson, H. (1986). Development and regional expression of beta nerve growth factor messenger RNA and protein in the rat central nervous system. *Proc. Natl. Acad. Sci. USA*, **83**:817-821.
- Wiesmann, C., Ultsch, M. H., Bass, S. H., and de Vos, A. M. (1999). Crystal structure of nerve growth factor in complex with the ligand-binding domain of the TrkA receptor. *Nature*, **401**:184-188.



- Winther, J. R. and Sorensen, P. (1991). Propeptide of carboxypeptidase Y provides a chaperone-like function as well as inhibition of the enzymatic activity. *Proc. Natl. Acad. Sci. USA*, **88**:9330-9334.
- Winther, J. R., Sorensen, P., and Kielland-Brandt, M. C. (1994). Refolding of a carboxypeptidase Y folding intermediate in vitro by low-affinity binding of the proregion. *J. Biol. Chem.*, **269**:22007-22013.
- Wise, R. J., Pittman, D. D., Handin, R. I., Kaufman, R. J., and Orkin, S. H. (1988). The propeptide of von Willebrand factor independently mediates the assembly of von Willebrand multimers. *Cell*, **52**:229-236.
- Woo, S. B. and Neet, K. E. (1996). Characterization of histidine residues essential for receptor binding and activity of nerve growth factor. *J. Biol. Chem.*, **271**:24433-24441.
- Woo, S. B., Timm, D. E., and Neet, K. E. (1995). Alteration of NH<sub>2</sub>-terminal residues of nerve growth factor affects activity and Trk binding without affecting stability or conformation. *J. Biol. Chem.*, **270**:6278-6285.
- Yamashita, T., Fujitani, M., Hata, K., Mimura, F., and Yamagishi, S. (2005). Diverse functions of the p75 neurotrophin receptor. *Anat. Sci. Int.*, **80**:37-41.
- Yardley, G., Relf, B., Lakshmanan, J., Reinshagen, M., and Moore, G. P. (2000). Expression of nerve growth factor mRNA and its translation products in the anagen hair follicle. *Exp. Dermatol.*, **9**:283-289.
- Yoon, S. O., Casaccia-Bonofil, P., Carter, B., and Chao, M. V. (1998). Competitive signaling between TrkA and p75 nerve growth factor receptors determines cell survival. *J. Neurosci.*, **18**:3273-3281.
- Zhang, Z. and Smith, D. L. (1993). Determination of amide hydrogen exchange by mass spectrometry: a new tool for protein structure elucidation. *Protein Sci.*, **2**:522-531.

**Abkürzungen**

Å	Angström
CD	Cirkulardichroismus
Cys	Cystein
Da	Dalton
<i>E. coli</i>	<i>Escherichia coli</i>
GdnHCl/GdmCl	Guanidin Hydrochlorid
GSH	reduziertes Glutathion
GSSG	oxidiertes Glutathion
HSQC	<i>heteronuclear single-quantum correlation</i>
IB	<i>inclusion body</i>
IPTG	Isopropyl-β-thiogalactopyranosid
K <sub>D</sub>	Gleichgewichts-Dissoziationskonstante
M	Molar
MALDI-TOF	<i>matrix assisted laser desorption ionization-time of flight</i>
NMR	<i>nuclear magnetic resonance</i>
NGF	Nervenwachstumsfaktor; <i>nerve growth factor</i>
NT	Neurotrophin
pdb	Proteindatenbank (www.pdb.org)
RP-HPLC	<i>reverse phase-HPLC</i>
Trk	Tyrosinkinase
UV	Ultraviolett

## **Danksagung**

*Die vorliegende Arbeit wurde im Zeitraum von November 2001 bis Dezember 2005 am Institut für Biotechnologie am Fachbereich Biochemie/Biotechnologie der Martin-Luther-Universität Halle-Wittenberg unter Einleitung von Frau PD Dr. Elisabeth Schwarz angefertigt.*

*Ich danke herzlich Herrn Prof. Dr. Rainer Rudolph für die Möglichkeit, diese Arbeit in der AG Proteinchemie anfertigen zu können, für die konstante Unterstützung und dem Interesse an meiner Arbeit.*

*Frau PD Dr. Elisabeth Schwarz möchte ich besonders für die angenehme Betreuung, ihre stete Diskussionsbereitschaft und Unterstützung bei der Anfertigung der Arbeit danken.*

*Bei Herrn PD Dr. Hauke Lilie bedanke ich mich für die unzähligen fruchtbaren Diskussionen und Anregungen sowie der praktischen Unterstützung bei der Laborarbeit.*

*Herrn PD. Dr. Ralph Golbik danke ich ebenfalls für die Unterstützung und die unzähligen gemeinsamen Stunden vor dem stopped-flow-Gerät.*

*Frau Dr. Anke Rattenholl danke ich für die Überlassung der Plasmide sowie der Einarbeitung in das Thema NGF.*

*Ich danke Herrn Prof. Dr. Jochen Balbach und seinem Mitarbeiter Herrn Ulrich Weininger für die Durchführung der NMR-Untersuchungen sowie deren Interpretation.*

*Frau Dr. Angelika Schirrhorn von der Forschungsstelle "Enzymologie der Proteinfaltung" der Max-Planck-Gesellschaft Halle danke ich für die massenspektroskopischen Untersuchungen und der Einarbeitung in die Bedienung des MALDI-TOF Massenspektrometers.*

*Bei Dr. Frank Hillger, Dr. Anke Rattenholl, Dr. Till Scheuermann sowie allen Mitarbeitern des Labors 262 und 264 möchte ich danken für die angenehme Arbeitsatmosphäre.*

*Besonderer Dank gilt meiner Familie und meiner Freundin auf deren Unterstützung ich stets vertrauen konnte.*

### **Eidesstattliche Erklärung**

Hiermit erkläre ich an Eides statt, dass ich mich bisher mit dieser Arbeit weder an der Martin-Luther-Universität Halle-Wittenberg, noch an einer anderen Einrichtung um die Erlangung eines akademischen Grades beworben habe. Ich versichere weiterhin, dass die vorliegende Arbeit selbständig und nur unter Benutzung der angegebenen Quellen und Hilfsmittel erstellt wurde. Den benutzten Werken wörtlich oder inhaltlich entnommenen Stellen sind als solche gekennzeichnet.

## Lebenslauf

Rennweg 17c  
79106 Freiburg  
Tel.: 0761 5039526  
kliemannel@yahoo.de

### Persönliche Daten

---

Geburtsdatum	6. November 1975
Geburtsort	Leipzig
Familienstand	ledig
Nationalität	deutsch

### Beruflicher Werdegang

---

Seit Januar 2006

Wissenschaftlicher Mitarbeiter der CellGenix Technologie Transfer GmbH

November 2001-Denzember 2005

Wissenschaftlicher Angestellter und Promotionsstudent am Institut für Biotechnologie der Martin-Luther-Universität Halle-Wittenberg

Oktober 1996 – September 2001

Biochemiestudium am Fachbereich Biochemie/Biotechnologie der Martin-Luther-Universität Halle-Wittenberg

**Abschluss: Diplom-Biochemiker**

### Schulische Ausbildung

---

August 1992 – Mai 1995

Hölty-Gymnasium, Wunstorf

**Abschluss: Abitur, Allgemeine Hochschulreife**

September 1982 – August 1992

Polytechnische Oberschule, Magdeburg

### Wehrdienst

---

Juli 1995 – August 1996